

UNCLASSIFIED

AD NUMBER

AD805241

LIMITATION CHANGES

TO:

Approved for public release; distribution is unlimited.

FROM:

Distribution authorized to U.S. Gov't. agencies and their contractors;  
Administrative/Operational Use; NOV 1966. Other requests shall be referred to Air Force Materiel Lab., Wright-Patterson AFB, OH 45433.

AUTHORITY

AFML ltr 26 May 1972

THIS PAGE IS UNCLASSIFIED

B067041

067041

AD-805241

**DEVELOPMENT  
OF  
ULTRASONIC WELDING EQUIPMENT  
FOR  
REFRACTORY METALS**

by  
Nicholas Maropis

**AEROPROJECTS INCORPORATED**  
West Chester, Pennsylvania

Contract: AF 33(600)-43026  
MMP Project No. 7-888

**FINAL REPORT**  
November 1966

This document is subject to special export controls and each transmittal to foreign governments or foreign nationals may be made only with prior approval of the Manufacturing Technology Division.

ADVANCED FABRICATION TECHNIQUES BRANCH  
MANUFACTURING TECHNOLOGY DIVISION  
AIR FORCE MATERIALS LABORATORY  
AIR FORCE SYSTEMS COMMAND  
WRIGHT-PATTERSON AIR FORCE BASE, OHIO



Distribution Change Order refer to Change Authority Field  
**Private STINET**

[Home](#) | [Collections](#)[View Saved Searches](#) | [View Shopping Cart](#) | [View Orders](#)[Add to Shopping Cart](#)

Other items on page 1 of your [search results](#): 1

[View XML](#)

Citation Format: Full Citation (1F)

**Accession Number:**

AD0805241

**Citation Status:**

Active

**Citation Classification:**

Unclassified

**Fields and Groups:**

110602 - Fabrication Metallurgy

**Corporate Author:**

AEROPROJECTS INC WEST CHESTER PA

**Unclassified Title:**

(U) DEVELOPMENT OF ULTRASONIC WELDING EQUIPMENT FOR REFRACTORY METALS.

**Title Classification:**

Unclassified

**Descriptive Note:**

Final technical engineering rept. 15 Feb 62-31 Aug 66,

**Personal Author(s):**

Maropis, Nicholas

**Report Date:**

Nov 1966

**Media Count:**

140 Page(s)

**Cost:**

\$14.60

**Contract Number:**

AF 33(600)-43026

**Report Number(s):**

RR-66-78

AFML-TR-66-351

**Project Number:**

MMP-7-888

**Monitor Acronym:**

AFML

**Monitor Series:**

TR-66-351

**Report Classification:**

Unclassified

**Descriptors:**

(U) \*INSTRUMENTATION), (\*ULTRASONIC WELDING, (\*REFRACTORY METALS, ULTRASONIC WELDING), METALLURGY, NIOBIUM ALLOYS, MOLYBDENUM ALLOYS, TUNGSTEN, STAINLESS STEEL, TRANSDUCERS, FREQUENCY CONVERTERS, ALUMINUM ALLOYS, WELDABILITY, TEMPERATURE, POWDER METALLURGY, HEAT TREATMENT, POWER, THICKNESS, STABILITY, ELECTRICAL IMPEDANCE

**Identifiers:**

(U) NICKEL ALLOY RENE 41, NICKEL ALLOY INCONEL, STEEL 1050, STEEL PH15-7MO,

SUPER ALLOYS.

Distribution Change Order refer to Change Authority Field

**Identifier Classification:**

Unclassified

**Abstract:**

(U) Ultrasonic welding equipment consisting of a highly stable and precisely adjustable motor-alternator frequency converter, new cartridge-type ceramic transducers exhibiting overall efficiencies in the range of 75 to 85 percent, and heavy-duty, force-insensitive acoustic coupling systems were developed and/or designed, built, and successfully utilized with the view to spot welding such refractory metals and superalloys as Rene 41, Mo-0.5Ti alloy, columbium, PH15-7Mo stainless steel, and tungsten. The equipment provides for programming the electrical power delivered to the transducers and the clamping force applied to the weldment so that improved impedance matching and better control of the welding process can be effected. Ultrasonic spot-type welds were made with this equipment in materials and thicknesses not heretofore achievable. (Author)

**Abstract Classification:**

Unclassified

**Distribution Limitation(s):**

01 - APPROVED FOR PUBLIC RELEASE

**Source Serial:**

F

**Source Code:**

009350

**Document Location:**

DTIC AND NTIS

**Change Authority:**

ST-A USAFSC LTR, 26 MAY 72



---

[Privacy & Security Notice](#) | [Web Accessibility](#)

[private-stinet@dtic.mil](mailto:private-stinet@dtic.mil)



## NOTICES

When Government drawings, specifications, or other data are used for any purpose other than in connection with a definitely related Government procurement operation, the United States Government thereby incurs no responsibility nor any obligation whatsoever; and the fact that the Government may have formulated, furnished, or in any way supplied the said drawings, specifications, or other data, is not to be regarded by implication or otherwise as in any manner licensing the holder or any other person or corporation, or conveying any rights or permission to manufacture, use, or sell any patented invention that may in any way be related thereto.

Qualified requesters may obtain copies from DDC, Defense Documentation Center, Cameron Station, Alexandria, Virginia. Orders will be expedited if placed through the Librarian or other person designated to request documents from DDC.

Reproduction in whole or in part is prohibited except with the permission of the Manufacturing Technology Division. However, DDC is authorized to reproduce the document for "U. S. Governmental Purposes".

Copies of this report should not be returned to the Research and Technology Division unless return is required by security considerations, contractual obligations, or notice on a specific document.

**DEVELOPMENT  
OF  
ULTRASONIC WELDING EQUIPMENT  
FOR  
REFRACTORY METALS**

by

Nicholas Maropis

**AEROPROJECTS INCORPORATED**

West Chester, Pennsylvania

November 1966

This document is subject to special export controls and each transmittal to foreign governments or foreign nationals may be made only with prior approval of the Manufacturing Technology Division.

ADVANCED FABRICATION TECHNIQUES BRANCH  
MANUFACTURING TECHNOLOGY DIVISION  
AIR FORCE MATERIALS LABORATORY  
AIR FORCE SYSTEMS COMMAND  
WRIGHT-PATTERSON AIR FORCE BASE, OHIO

## FOREWORD

This Final Technical Engineering Report covers the work performed under Contract AF33(600)-43026 from February 15, 1962 through August 31, 1966.

This contract with Aeroprojects Incorporated of West Chester, Pennsylvania was initiated under Manufacturing Methods Project 7-888, "Development of Ultrasonic Welding Equipment for Refractory Metals." It was administered under the direction of Mr. Frederick R. Miller of the Manufacturing Technology Division, AF Materials Laboratory, Wright-Patterson Air Force Base, Ohio.

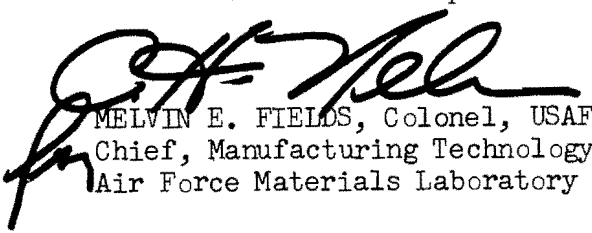
This project is under the direction of Mr. J. Byron Jones, with Nicholas Maropis serving as Project Engineer. Others associated with the program are Carmine F. DePrisco, Chief Electronics Engineer; John G. Thomas, Metallurgist; Janet Devine, Physicist; and W.C. Elmore, Consultant. This document has been given the Aeroprojects internal report number of RR-66-78 and is a final report.

This project has been accomplished as a part of the Air Force Manufacturing Methods Program, the primary objective of which is to develop, on a timely basis, manufacturing processes, techniques and equipment for use in economical production of USAF materials and components. The program encompasses the following technical areas:

Metallurgy - Rolling, Forging, Extruding, Casting, Fiber, Powder  
Chemical - Propellant, Coating, Ceramic, Graphite, Nonmetallics  
Electronic - Solid State, Materials and Special Techniques, Thermionics  
Fabrication - Forming, Material Removal, Joining, Components

Suggestions concerning additional manufacturing methods development required on this or other subjects will be appreciated.

This technical Report has been reviewed and is approved.



MELVIN E. FIELDS, Colonel, USAF  
Chief, Manufacturing Technology Division  
Air Force Materials Laboratory

ABSTRACT

*Start*  
[ Ultrasonic welding equipment consisting of a highly stable and precisely adjustable motor-alternator frequency converter, new cartridge-type ceramic transducers exhibiting overall efficiencies in the range of 75 to 85 percent, and heavy-duty, force-insensitive acoustic coupling systems were developed and/or designed, built, and successfully utilized with the view to spot welding such refractory metals and superalloys as Rene'41, Mo-0.5Ti alloy, columbium, PH15-7Mo stainless steel, and tungsten. The equipment provides for programming the electrical power delivered to the transducers and the clamping force applied to the weldment so that improved impedance matching and better control of the welding process can be effected. Ultrasonic spot-type welds were made with this equipment in materials and thicknesses not heretofore achieved. ~~sent~~ ]



## TABLE OF CONTENTS

SECTION	PAGE
I INTRODUCTION . . . . .	1
II WELDMENT MATERIALS . . . . .	6
A. Materials and Physical Properties . . . . .	6
B. Metallurgical Characteristics . . . . .	6
C. Ultrasonic Weldability . . . . .	11
D. Power Requirements for Welding . . . . .	13
III ULTRASONIC TRANSDUCER DEVELOPMENT . . . . .	20
A. Ceramic Elements . . . . .	20
B. Transducer Design . . . . .	22
C. Transducer Evaluation Technique . . . . .	22
D. Early 2-Kilowatt and 3.3-Kilowatt Assemblies . . . . .	23
E. Final 4.2-Kilowatt Assemblies . . . . .	26
IV COUPLER SYSTEM DEVELOPMENT . . . . .	30
A. Wedge-Reed System . . . . .	33
B. Lateral-Drive System . . . . .	34
C. Coupler Materials . . . . .	38
D. Final Coupler Design and Fabrication . . . . .	41
V WELDING TIPS . . . . .	45
A. Tip Materials . . . . .	45
B. Tip Geometry . . . . .	52
C. Final Tip Design and Fabrication . . . . .	54
VI FORCE APPLICATION SYSTEM . . . . .	58
VII POWER-FORCE PROGRAMMING . . . . .	64
VIII FREQUENCY CONVERTER . . . . .	69
A. Types of Frequency Converters . . . . .	69
B. Design and Specifications for Motor Alternator . . . . .	71
C. Switching . . . . .	73
D. Evaluation . . . . .	74

## TABLE OF CONTENTS (Concluded)

SECTION		PAGE
IX	ASSEMBLY AND CHECKOUT OF EQUIPMENT . . . . .	79
	A. Machine Structure . . . . .	79
	B. Instrumentation and Controls . . . . .	79
	C. Equipment Operation . . . . .	85
	D. Checkout of Equipment . . . . .	86
	E. Preliminary Welding . . . . .	87
X	EVALUATION OF WELDING PERFORMANCE . . . . .	89
	A. Weldment Characteristics . . . . .	94
	B. Metallographic Examination of Welds . . . . .	96
XI	CONCLUSIONS . . . . .	106
APPENDIX A -	THE TRANSMISSION OF ULTRASONIC POWER BY FLEXURAL WAVES ON A SLENDER BAR . . . . .	109
APPENDIX B -	CONTACT AREA BETWEEN TWO BODIES HAVING TWO PRINCIPAL RADII . . . . .	119
APPENDIX C -	WELDING DATA OBTAINED DURING EQUIPMENT CHECKOUT . . . . .	125
	REFERENCES . . . . .	133

## ILLUSTRATIONS

FIGURE		PAGE
1	25-kw Ultrasonic Welding Machine Developed on the Program . .	4
2	25-kw Motor-Alternator Frequency Converter for 15-kc Ultrasonic Welder . . . . .	5
3	Acoustical Energy Requirements as a Function of Sheet Thickness for Welding Selected Materials . . . . .	14
4	Electrical Energy Input to Nickel Transducers Required to Weld Selected Materials . . . . .	16
5	Electrical Energy Input to Nickel Transducers Required to Weld Selected Materials . . . . .	17
6	Acoustical Calorimeter . . . . .	24
7	Thread Configurations Used for the Ceramic Transducer Assembly	27
8	Schematic Diagram of Wedge-Reed Opposition-Drive System . . .	31
9	Schematic Diagram of Lateral-Type Opposition-Drive System . .	32
10	Curved and Sculptured Welding System . . . . .	35
11	Ultrasonic Welding Array . . . . .	37
12	Ultrasonic Welding Setup Used for Evaluation of Double Opposed Welding System . . . . .	39
13	Power Loss vs. Strain Characteristics of Candidate Coupler Materials . . . . .	42
14	High-Power Welding Transducer-Coupling System . . . . .	43
15	Lateral-Drive Transducer-Coupling Systems Mounted on Welding Machine . . . . .	44
16	Metallographic Structure of Candidate Tip Materials . . . . .	46
17	Photomicrographs of Heat-Treated Astroloy and Udimet 700 . . .	50
18	Mechanically Attached Welding Tips . . . . .	55
19	Close-up View of Sonotrode Tips on Double Opposed Ultrasonic Welding Test System . . . . .	57

# ILLUSTRATIONS (Continued)

FIGURE		PAGE
20	Clamping Force as a Function of Material Thickness . . . . .	59
21	Basic Air-Hydraulic Booster System . . . . .	61
22	Air-Hydraulic Force System . . . . .	62
23	Air-Hydraulic Force System Installed on Welding Machine . . .	63
24	Power-Force Programming System . . . . .	65
25	Timing Circuit for Power-Force Programming Unit . . . . .	66
26	Power-Force Program Circuit Detail . . . . .	68
27	Components of 25-Kilowatt, 15-Kilocycle Frequency Converter .	72
28	Equipment Array for Frequency Converter Acceptance Tests . . .	75
29	Instrument and Cabinet Arrangement for 25-Kilowatt Welding Unit . . . . .	80
30	Framework for 25-Kilowatt Spot-Type Welding Machine . . . . .	81
31	Instrument and Control Panels . . . . .	82
32	Estimated and Actual Input Energy Required for Welding with Ceramic Transducers . . . . .	90
33	Estimated and Actual Input Energy Required for Welding with Ceramic Transducers . . . . .	91
34	Oscillograph of Power Programming Command Signal for Peg-Board Schedule for Welding Refractory Metals . . . . .	92
35	Strength of Ultrasonic Welds in 2024-T3 and 2014-T6 Aluminum Alloys . . . . .	95
36	Edge of Ultrasonic Weld Between 0.060-Inch Sheets of 2024-T3 Aluminum Alloy . . . . .	98
37	Edge of Ultrasonic Weld Between 0.080-Inch Sheets of 2014-T6 Aluminum Alloy . . . . .	98
38	Surface Liquation in 0.040-Inch 2024-T3 Aluminum Alloy . . . .	98

# ILLUSTRATIONS (Concluded)

FIGURE		PAGE
39	Ultrasonic Weld Between Sheets of 0.040-Inch PH15-7Mo Stainless Steel . . . . .	99
40	Ultrasonic Weld Between Sheets of 0.040-Inch Rene'41 . . . . .	100
41	Ultrasonic Weld Between Sheets of 0.060-Inch Rene'41 . . . . .	100
42	Ultrasonic Weld Between Sheets of 0.040-Inch Inconel X-750 . . . . .	101
43	Ultrasonic Weld Between Sheets of 0.060-Inch Inconel X-750 . . . . .	101
44	Ultrasonic Weld Between Sheets of C-103 Columbium Alloy . . . . .	102
45	Ultrasonic Weld Between Sheets of TZM Alloy . . . . .	102
46	Ultrasonic Weld Between Sheets of 0.020-Inch Mo-0.5Ti Alloy . . . . .	103
47	Ultrasonic Weld Between Sheets of Rene'41 . . . . .	103
48	Area of Contact as a Function of the Larger Radius . . . . .	123

# TABLES

TABLE		PAGE
I	Gages and Metallurgical Condition of Weldment Materials . . . . .	7
II	Typical Mechanical Properties of Weldment Materials . . . . .	8
III	Density and Thermal Properties of Weldment Materials . . . . .	9
IV	Metallurgical Properties and Anticipated Weld Zone Temperatures for Weldment Materials . . . . .	10
V	Prior Experience in Welding Materials of Interest . . . . .	12
VI	Estimated Acoustical Energy and Power Required to Weld 0.10-Inch-Thick Material . . . . .	15
VII	Estimated Electrical Power Required to Weld 0.060-Inch Material at Various Weld Intervals . . . . .	18
VIII	Estimated Electrical Power Required to Weld 0.10-Inch Material at Various Weld Intervals . . . . .	19

# TABLES (Continued)

TABLE		PAGE
IX	Summary of Acoustical Energy Absorber Data for a Nickel and a Ceramic (PZT-4) Transducer Unit of 2-Kilowatt Power-Handling Capacity . . . . .	25
X	Test Data for 4.2-Kilowatt Ceramic Transducer . . . . .	29
XI	Evaluation of 4-Kilowatt Curved and Sculptured System Welding 2024-T3 Bare Aluminum Alloy . . . . .	36
XII	Evaluation of Double Opposed Transducer-Coupling Welding System . . . . .	40
XIII	Candidate Tip Materials: Source and Composition . . . . .	47
XIV	Candidate Tip Materials: Mechanical Properties in Fully Heat-Treated Condition . . . . .	48
XV	Heat Treatment of Udimet 700 and Astroloy Tip Materials . . . . .	49
XVI	Performance Comparison of Udimet 700 and Astroloy Tips . . . . .	51
XVII	Tip Radii Associated with Welding Various Sheet Thickness . . . . .	53
XVIII	Estimated Clamping Force Values for Welding 0.10-Inch Materials . . . . .	58
XIX	Frequency Output Data for 7.5-Kilowatt Motor Alternator . . . . .	70
XX	25-kw Alternator High-Frequency Tests . . . . .	76
XXI	25-kw Alternator Frequency Converter Tests . . . . .	77
XXII	30-kw Alternator Test Data . . . . .	78
XXIII	Summary Data of Welds Made with 25-Kilowatt Ultrasonic Welder . . . . .	93
XXIV	Microscopic Examination of Welds . . . . .	97
XXV	Preliminary Welding Checkout Data for 25-kw Ultrasonic Welder . . . . .	126
XXVI	Ultrasonic Welding of Superalloys Interspersed with Qualification Data for 25-kw Welder . . . . .	127
XXVII	Welding of Aluminum Alloys and Stainless Steel . . . . .	128

## TABLES (Concluded)

TABLES		PAGE
XXVIII	Welding of Aluminum Alloys and Stainless Steel After Extensive Rework of Lower Coupler . . . . .	129
XXIX	Welding of Refractory Metals and Alloys . . . . .	130
XXX	Welding Refractory Metals and Alloys with Modified Welding Tips and with Power-Force Programming . . . . .	131

## I. INTRODUCTION

The objective of this program was to investigate the mechanics and techniques of ultrasonic joining necessary to obtain reliable joints in high-temperature metals up to and including 0.100 inch thick, and to develop ultrasonic welding equipment to accomplish such joints.

The newer superalloys and refractory metals have become increasingly important in missile, space vehicle, and atomic applications because of their properties of strength, temperature-stability, and corrosion resistance. These properties, however, have introduced metal joining problems not yet solved by conventional methods.

Ultrasonic welding offers a potentially effective means for joining such metallic materials. The joint is effected by the combined action of a static normal force and oscillating shear forces, which disperse surface films and effect nascent metal-to-metal contact across the interface. A modest localized temperature rise occurs in the weld metal, but this is usually below the recrystallization temperature, within the range of about 35 to 50 percent of the absolute melting point of the material. At the same time the metal is transiently plasticized, facilitating atomic bonding across the interface.

Development of ultrasonic welding began with successful joining of thin gages of aluminum and its alloys. Since then, the process has been extended to heavier and harder materials, equipment and techniques have been refined, and equipment of increasing power capabilities has been evolved. Prior to initiation of this work, only in some of the softer aluminum alloys has welding been possible in the heavier gages (up to about 0.12 inch). The then-weldable gages for most other materials were limited to about 0.040 inch and thinner.

Prior work (1, 2, 3)\* had established the weldability of thin gages of some of the refractory metals and superalloys, including molybdenum, tungsten, tantalum, columbium and beryllium, as well as certain alloys of these metals, but available equipment had insufficient power for welding gages above about 0.010-0.015 inch. It was apparent that a substantial increase in net vibratory power would be necessary to extend the ultrasonic welding process to heavier gages of these materials.

Phase I of this program (4) confirmed the feasibility of ultrasonically welding selected refractory metals and superalloys in thin gages and delineated the requirements for ultrasonic welding equipment capable of welding the heavier gages of these materials.

---

\* Numbers in parentheses refer to references at the end of report.



The metals and alloys selected for this study were columbium-10Mo-10Ti, Inconel X-750, molybdenum-0.5Ti, PH15-7Mo stainless steel, Rene' 41, and tungsten. Using an 8-kilowatt laboratory spot-type welder, ultrasonic welds were made in these materials in gages up to about 0.030 inch. From the data thus obtained, extrapolations of the energy requirements for welding these materials in gages up to 0.100 inch (see Section II) indicated the necessity for an ultrasonic welder with a nominal electrical power input to efficient ceramic transducers of 25 kilowatts.

Phase I further delineated the basic requirements for such a welding machine and explored some of the problem areas. The primary avenues toward achieving the required greatly increased vibratory energy consisted of providing increased electrical power to the transducer-coupling system, and developing transducer-coupling systems of greater efficiency and greater power-handling capacity. These were the areas in which pioneering effort was expected to be required. The design of the machine structure, force application system, and instrumentation appeared to be straightforward.

The objective of the Phase II effort described in this report was to develop the techniques and equipment required to accomplish welds in the selected materials in gages up to 0.100 inch, or more specifically to:

1. Develop the necessary methods, techniques, and equipment to ultrasonically join the selected materials.
2. Design and construct an ultrasonic joining unit in accordance with the approach outlined in Phase I.
3. Develop methods and techniques to demonstrate the capability of the equipment to join the selected materials.

As the work progressed, a number of unanticipated problems arose which interrupted the scheduled effort and caused unforeseen delays in completion of the equipment.

The design, assembly, and test of ultrasonic transducers capable of efficiently providing the required high vibratory power levels proved to be a formidable task. A ceramic transducer, which offers high electromechanical conversion efficiency, had previously never been developed for such high power levels, and much theoretical and experimental effort was necessary to evolve practical assemblies.

Problems also arose in the development of a satisfactory coupling system that would withstand the static forces involved and that would transmit the vibratory power efficiently without undesirable mode conversion.

It was recognized early in the program that welding tips capable of handling the requisite levels of vibratory power presented a crucial problem, and the matter was discussed with the Air Force. It was decided to forego such work until the equipment became operable.

It was originally anticipated that available frequency converters would be used in combination to drive the high-power welding equipment. It became evident, however, from concurrent experience on other work, that such an arrangement would be unsatisfactory because of the difficulties of achieving precise synchronization of multiple driving units. It therefore became necessary to design and assemble a single high-power frequency converter that would provide the entire 25 kilowatts of power input to the transducer-coupling systems.

During the course of the program the various components--transducers, transducer-coupling systems, force application system, and the various instruments including power-force programming--were designed, fabricated, and tested individually to insure satisfactory performance, then were assembled on the machine structure. Figure 1 shows the assembled 25-kilowatt welding machine. In addition, a 25-kilowatt motor-alternator-type frequency converter was assembled from custom-designed components; this unit is shown in Figure 2.

The unforeseen difficulties encountered in component design necessitated a reorientation of the Phase II effort. The requirement for complete demonstration of the capability of the equipment was deleted, and the following items were substituted:

- "2. Make ultrasonic welds in aluminum alloys, such as 2024-T3 bare and/or 304 stainless steel to indicate the level of vibratory energy that is delivered to the weld zone as a function of applied r-f energy to the transducer, including one (1) specimen group of at least one hundred (100) welds. No effort will be expended to optimize machine performance, although the data collected may be useful to provide modification requirements to either the electrical circuitry or vibratory systems. No requisite level of welder performance is established to constitute the completed welding machine."
- "3a. Based upon the welding machine settings from the Phase I and Phase II work which preceded this task, ultrasonic spot welds will be made in selected sheet thicknesses, possibly up to the projected maximum capability of the machine. Maximum capability of this machine may be evaluated if this preliminary work indicates the absence of difficulties to achieve maximum performance. Ultrasonic welding will be attempted in several gages of each of the candidate materials."
- "3b. Weld quality determinations for this task will be based upon tensile-shear tests, macroscopic surface inspection and metallographic surface inspection, and metallographic cross sections in not more than two gages of each alloy."

The above provided the plan for evaluating the performance of the 25-kilowatt ultrasonic welding equipment.

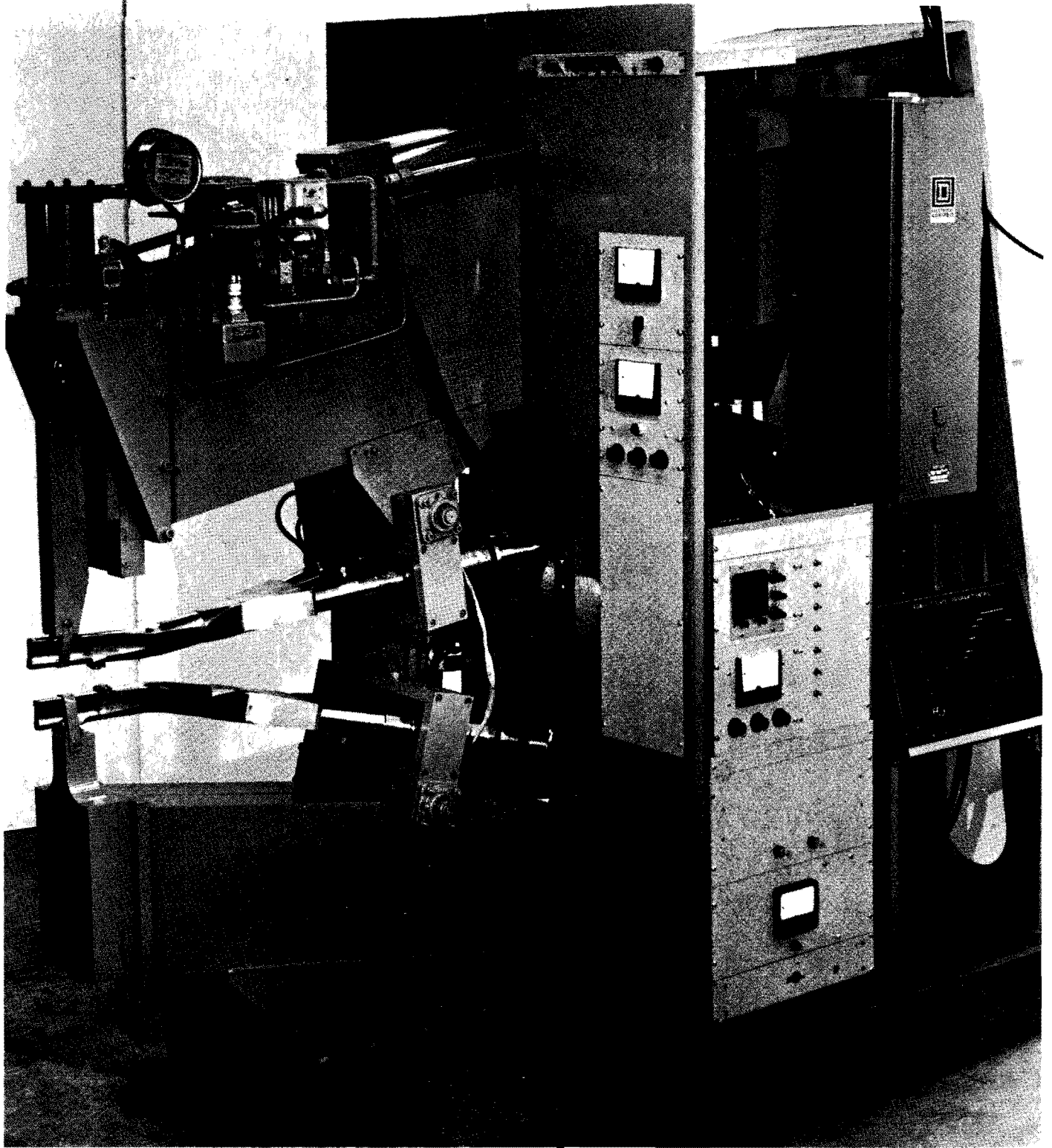


Figure 1: 25-kw Ultrasonic Welding Machine Developed on the Program

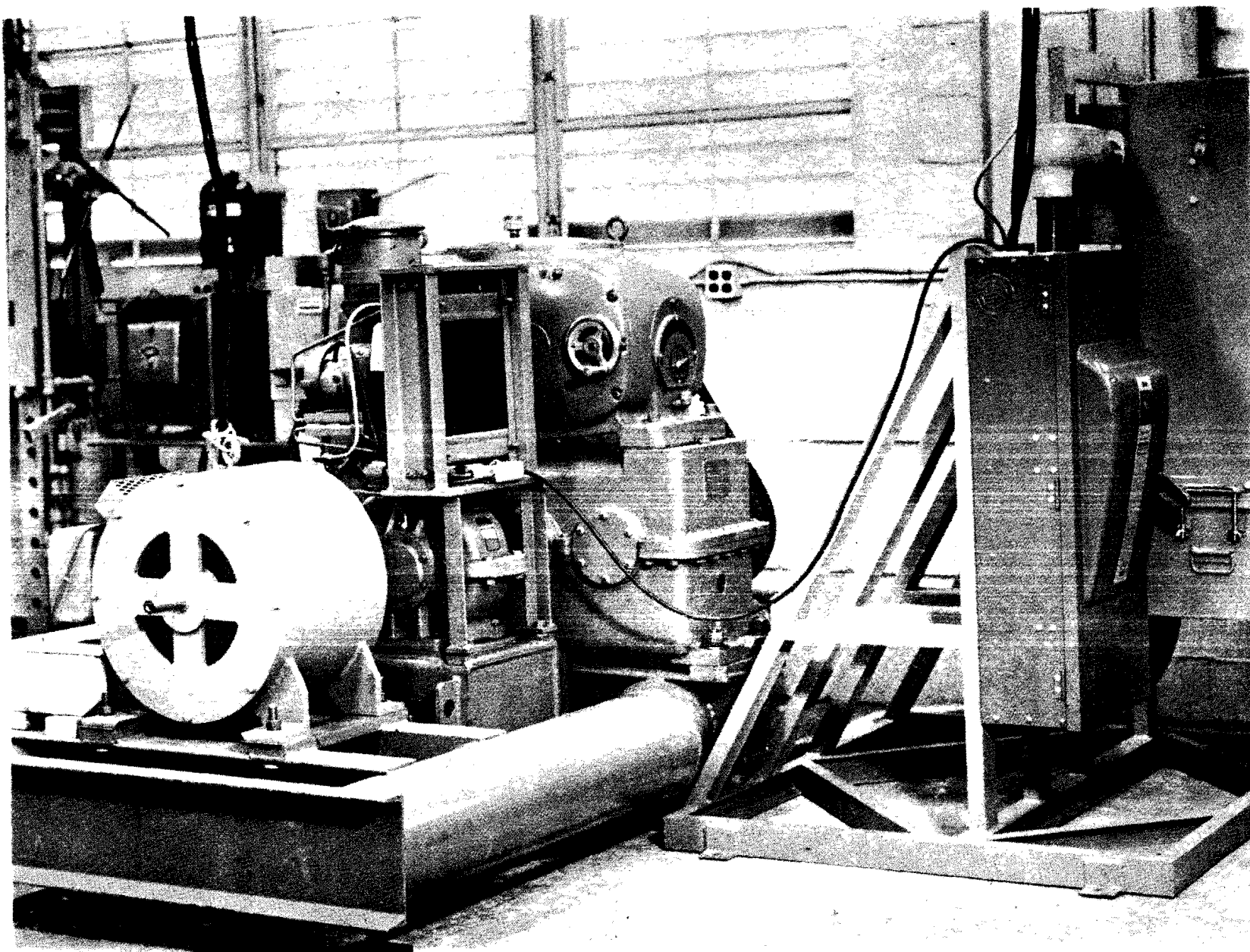


Figure 2: 25-kw Motor-Alternator Frequency Converter for 15-kc Ultrasonic Welder

## II. WELDMENT MATERIALS

Basic to the design of the welding equipment was consideration of the materials to be welded, properties of these materials that could influence weldability, and the anticipated energy requirements for welding.

### A. Materials and Physical Properties

Table I lists the materials and gages obtained for welding, together with the sources and the metallurgical condition for each. Insofar as possible, all materials were obtained in the annealed or stress-relieved condition.

Experience had indicated that the weldability of materials such as these is markedly affected by their quality, and effort was made to obtain high-quality materials. Efforts to obtain the latest materials produced under the Department of Defense Refractory Metals Sheet Rolling Program were only partially successful; the TZM alloy was thus obtained to supplement the supply of molybdenum-10% titanium, since the two materials have similar properties except that the TZM is somewhat more ductile.

Manufacturers' certifications of the compositions, processing specifications, and physical properties were not forthcoming for all materials, since some of them were still in the experimental stage and since proprietary information was involved in some instances. Typical mechanical properties, obtained from available information, are provided in Table II, while Table III provides densities and thermal properties.

### B. Metallurgical Characteristics

Prior studies in ultrasonic welding of refractory metals and alloys (2) had indicated that joining of these materials by ultrasonic or other metallurgical techniques is influenced by their metallurgical characteristics, particularly by their contamination, surface condition, grain structure, and brittle/ductile transition temperature. Data previously obtained was supplemented by further review of available literature and consultations with knowledgeable personnel, including manufacturers, Defense Metals Information Center personnel, and others having experience in the field.

Fabrication of the alloys Inconel X-750, René 41, and PH15-7Mo, which are generally face-centered-cubic metals (Table IV), apparently is relatively standardized to produce uniform products. Malleability and methods of joining have been studied. Solution annealed René 41, for example, is known (5) to be susceptible to embrittlement from grain-boundary carbide precipitation in the range of 1400°-1500°F. Fabrication, brazing, or fusion welding in this temperature range are therefore precluded. Ultrasonic welding, which does not involve external heating, does not induce heating to this temperature range, and experience (4) has revealed no embrittlement from this joining technique.

Table I

## GAGES AND METALLURGICAL CONDITION OF WELDMENT MATERIALS

Weldment Material	Procurement Source	Gage (inch)	Metallurgical Condition
Columbium- 10% Molybdenum- 10% Titanium (D-31)	E. I. du Pont de Nemours & Co.	0.040 0.060 0.100	Vacuum arc cast; stress- relieved
Inconel X-750	Huntington Alloy Products Division	0.040 0.100	Deoxidized and annealed
Molybdenum- 0.5% Titanium	Universal-Cyclops Steel Corp.	0.040 0.060 0.100	Arc cast; cross-rolled and stress-relieved
Molybdenum- 0.5% Titanium- 0.08% Zirconium (TZM)	Climax Molybdenum Company	0.012 0.020	Annealed
PH15-7Mo Stainless Steel	Hamilton Watch Co.	0.005 0.010 0.020 0.040	Annealed
	Peter A. Frasse & Co.	0.032 0.040	Annealed
	Armco Steel Corp.	0.090	Hot-rolled, annealed, and pickled
Rene 41	Alloy Metal Co.	0.020 0.060 0.096	
Tungsten	Fansteel Metal- lurgical Corp.	0.020 0.040 0.060 0.100	Powder metallurgy material; cross-rolled and stress- relieved

Table II

## TYPICAL MECHANICAL PROPERTIES OF WELDMENT MATERIALS

Weldment Material		Temperature (°F)	Elongation (%)	Strength		Modulus of Elasticity (10 <sup>6</sup> psi)	Shear Modulus (10 <sup>6</sup> psi)	Poisson's Ratio
Designation	Condition*			Ultimate Tensile (10 <sup>3</sup> psi)	Yield (0.2% offset) (10 <sup>3</sup> psi)			
Cb (D-31)	SR	70	15	100	90	16.5	6.0	0.380
		1000	5	68	68	12.8	--	--
Inconel X-750	SHT-A	70	49	115	47	31.0	12.0	0.290
		1000	25	95	--	25.0	--	--
Mo-0.5Ti	VAC-SR	70	14	130	120	45.5	17.4	0.324
		1000	--	110	100	--	--	--
PH15-7Mo	A	70	35	130	55	29.0	10.5	--
		1000	--	--	--	--	--	--
Rene' 41	A	70	20	185	140	31.6	12.1	0.310
		1000	13	178	134	27.3	10.2	0.325
Tungsten	A	70	0	120	--	50.0	21.8	0.284
		1000	--	75	18	55.0	--	--

\* A: annealed; SR: stress relieved; SHT: solution heat-treated; VAC: vacuum arc cast.

Table III

## DENSITY AND THERMAL PROPERTIES OF WELDMENT MATERIALS

Weldment Material		Temperature (°F)	Density ( $\rho$ ) (lb/in <sup>3</sup> )	Linear Coefficient of Thermal Expansion $10^6$ (in/in-°F)	Thermal Conductivity (k) (Btu/in-ft <sup>2</sup> -hr-°F)	Thermal Diffusivity $\alpha = k/\rho c$ (ft <sup>2</sup> -hr)	Specific Heat (c) (Btu/lb-°F)
Designation	Condition*						
Cb (D-31)	SR	70	0.292	4.1	--	--	0.074
		1000	--	--	--	--	--
Inconel X-750	SHT-A	70	0.298	6.9	83	0.132	0.103
		1000	--	8.1	131	0.169	0.130
Mo-0.5Ti	VAC-SR	70	0.368	3.1	936	2.01	0.061
		1000	--	3.2	840	1.75	0.063
PH15-7Mo	A	70	0.282	8.0	--	--	--
		1000	--	9.4	--	--	--
Rene'41	A	70	0.296	6.5	63	0.095	0.108
		1000	--	7.5	105	0.158	--
Tungsten	A	70	0.697	2.6	1150	0.249	0.032
		1000	--	2.7	900	--	--

\* See Table II.



Table IV  
METALLURGICAL PROPERTIES AND ANTICIPATED WELD ZONE  
TEMPERATURES FOR WELDMENT MATERIALS

Weldment Material		Crystal Structure	Recrystal- lization Temperature (°F)	Melting Temper- ature (°F)	Estimated Weld Zone Temperature	
Designation	Condition*				Minimum (°F)	Maximum (°F)
Cb (D-31)	SR	bcc	1800-2100	4100	1135	1820
Inconel X-750	SHT-A	fcc	1320	2540-2600	640	1070
Mo-0.5Ti	VAC-SR	bcc	2100	4730	1360	2135
PH15-7Mo	A	fcc (10%) bcc (90%)	1300	2500	610	1030
Rene 41	A	fcc	--	2385-2450	540	995
Tungsten	SR	bcc	2650	6170	1860	2855

\* See Table II.

The tungsten, columbium alloy, and molybdenum alloy, all of which have body-centered-cubic structures, are still under extensive investigation; fabricating procedures are constantly being modified, and standard commercial products have not yet evolved (6-11). These materials undergo recrystallization embrittlement and must be worked below recrystallization temperatures. Low-temperature working results in a fibrous grain structure, and the properties are sensitive to the rolling direction unless cross-rolling is utilized (12). Their ductile/brittle behavior and embrittlement sensitivity to small interstitial contaminant levels contribute to difficulties in achieving sound joints by conventional welding methods.

Embrittlement in tungsten has been attributed (13) to interstitial impurities, such as oxygen, nitrogen, and carbon, which diffuse toward the grain boundaries and become potential sites for cracking. Surface irregularities, such as the presence of mechanical notches or asperities, also apparently contribute to the brittle behavior of this material. It has been reported (14, 15) that by electropolishing tungsten wire, its strength is increased by as much as 30 percent and that its bend ductility is increased as much as sevenfold. Our prior experience demonstrated that the removal of about 0.005 inch from the diameter of fine tungsten wire and about 0.002 inch from the surface of thin tungsten sheet considerably improved ductility and ultrasonic weldability (16).

The ductility and transition temperature of molybdenum-10% titanium are likewise influenced by the presence of contaminants (8). Interstitial oxygen, for example, is particularly detrimental to welding molybdenum by conventional processes. Sensitivity to cracking is enhanced by the fibrous structure of the material, which leads to delamination during both conventional and ultrasonic welding (17). Our prior experience in ultrasonically welding thin gages of this alloy (1, 2, 16) revealed substantial variation in material quality among different lots and thus differences in its response to ultrasonic welding.

The D-31 columbium alloy, in the cold-worked and stress-relieved condition, is reportedly (18) ductile to about -275°F, whereas recrystallization increases its transition temperature to about 600°F. Its ductility is also influenced by interstitial elements such as hydrogen, oxygen, and nitrogen, and particularly by carbide precipitates at the grain boundaries. Embrittlement and cracking have been repeatedly observed in fusion welding this material (8, 18, 19, 20). Our prior experience (1) has shown substantial variation in ultrasonic weldability of the D-31 alloy with different lots of material.

Thus the metallurgical and physical quality of these materials is very significant to their ultrasonic weldability because the process involves a requirement for ductility at low temperatures as well as metallurgical involvement. As fabrication techniques are improved and higher quality materials are produced, some of the present joining difficulties should be obviated.

It is important that the temperature achieved during welding should not exceed the recrystallization temperature of the materials. Considering that weld zone temperatures during ultrasonic welding usually fall within the range of 35-50 percent of the absolute melting point (21), the data in Table IV indicate the unlikelihood of recrystallization during this joining process.

#### C. Ultrasonic Weldability

Prior to initiation of Phase I, welding of the above materials had been accomplished in very thin gages (generally 0.005-0.010 inch). Under the Phase I effort, welding had been attempted in heavier gages (up to about 0.030) using an 8-kilowatt laboratory spot-type welder. Representative data on welding conditions and tensile-shear strengths obtained are summarized in Table V. The differences in spot strength obtained are not significant since the work was concerned merely with establishing feasibility and not with optimizing welding conditions or developing joints of optimum weld quality.

Metallographic examination of selected weldments in each material (but not in every gage) indicated generally good bonds with no evidence of recrystallization or grain growth. In the case of Inconel X-750 there was actually

Table V

PRIOR EXPERIENCE IN WELDING MATERIALS OF INTEREST\*  
 Input Power: Up to 8 Kilowatts

Weldment Material		No. of Measurements	Clamping Force (lb)	Weld Energy (kw-sec)	Tensile-Shear Strength (lb)
Designation	Gage (inch)				
Cb (D-31)	0.006	--	350	1.2	38
	0.010	11	600-700	1.0	220
	0.015	9	800-1000	2.25	205
	0.025	3	900-1100	3.5	330
Inconel X-750	0.012	--	100	0.5-1.0	207
	0.020	--	150	1.5	290
	0.033	6	400-900	4.0	725
	0.040	11	1100	6.8	1100
Mo-0.5Ti	0.008	15	350-550	1.2	145
	0.015	--	400	2.0	220
	0.017	--	600	3.0	250
	0.020	15	650-1050	3.6	235
	0.032	9	1000-1100	8.2	300
PH15-7 Mo	0.008	--	350	1.5	280
	0.020	25	700-1000	2.0	1265
	0.030	18	800-1000	3.9	1975
Rene 41	0.010	--	800	1.0	350
	0.020	10	600-800	6.0	380
	0.030	3	1000	6.4	491
Tungsten	0.005	--	150	0.7	18
	0.010	--	900	2.6	75
	0.015	12	500-900	6.4	130
	0.020	7	700-900	8.3	150
	0.030	18	700-1100	13.2	450

\* From Reference 4.

grain refinement in the vicinity of the weld interface. Hairline cracks were observed in the molybdenum-0.5 Ti alloy, and delamination occurred in the tungsten welds. In some instances, particularly in the steel, a thin sliver of extruded, plasticized material was observed at the edge of the weld. With some of the materials, the bond was of such quality that the original interface was completely obliterated in discrete areas of the weld zone; in others, substantial plastic turbulence was evident within the confines of the weld zone.

This work thus established that ultrasonic welding of these refractory metals and superalloys is possible without the problem of grain growth due to temperature effects and recrystallization associated with fusion welding.

#### D. Power Requirements for Welding

The data obtained in the Phase I and other investigations were used to approximate the energy requirements for welding each of these materials to itself in gages up to approximately 0.10 inch. Calculations were made from a first-approximation equation previously derived from observations with a wide variety of materials (21):

$$E = K H^{3/2} t^{3/2}$$

where E = energy in joules (watt-seconds),  
H = Vickers microindentation hardness number,  
t = thickness of one sheet of the material (inches),  
K = a constant which incorporates other contributing factors.

By proper selection of "K" the following can be computed:

1. Acoustical energy into the weldment, or
2. Electrical energy into a specific magnetostrictive transducer, or
3. Electrical energy into a specific electrostrictive transducer.

This equation is based upon the simplest type of welding situation in which two sheets of equal thickness are joined by means of a single spot-type ultrasonic weld.

On the basis of available experimental data, the value of "K" for acoustical energy was estimated to be 63. Calculations from the energy equation of the acoustical energy required to weld each material as a function of sheet thickness produced the curves in Figure 3. The estimated acoustical power demanded of welding equipment to produce such welds is shown in Table VI.

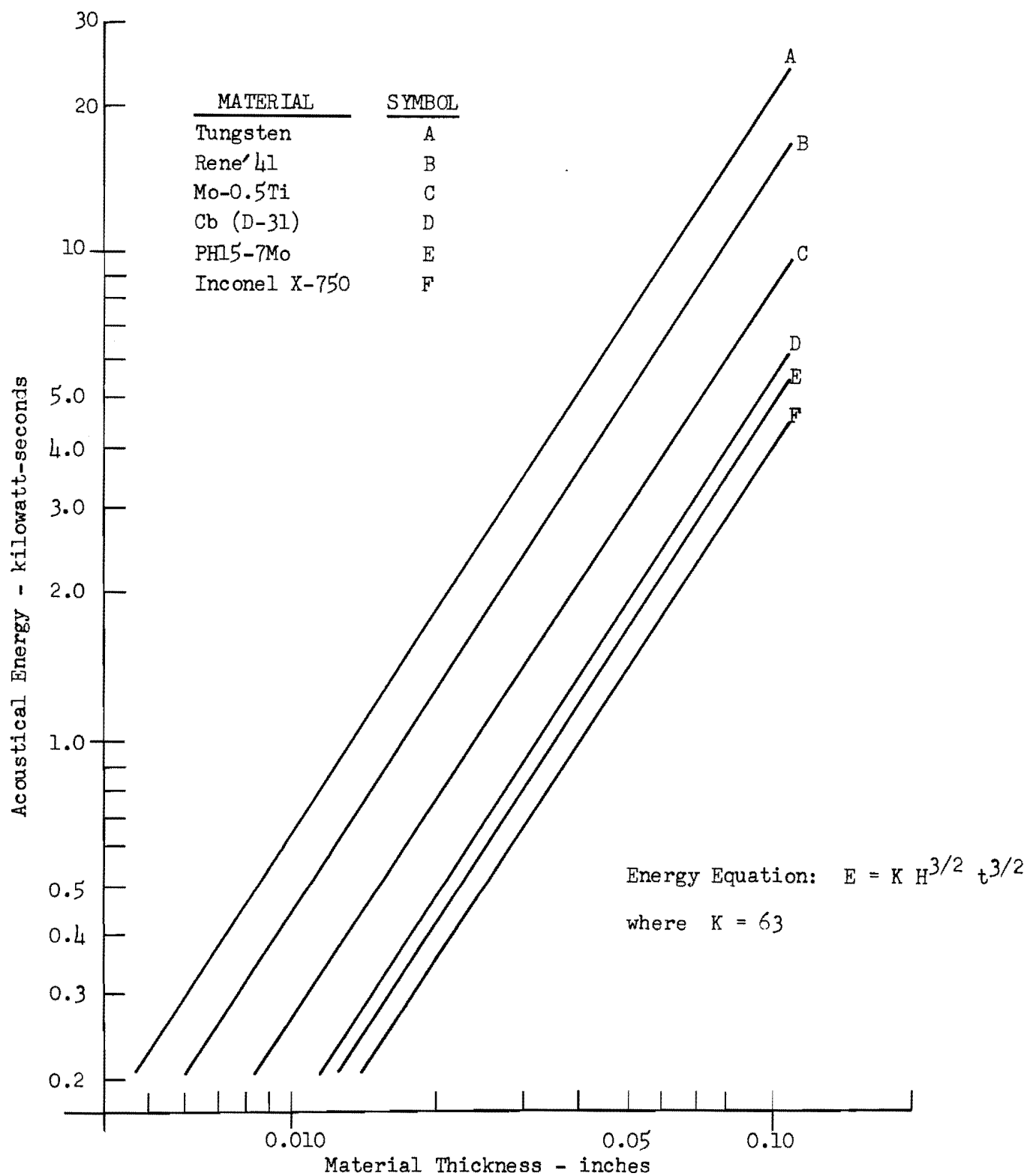


Figure 3: Acoustical Energy Requirements as a Function of Sheet Thickness for Welding Selected Materials

Table VI

ESTIMATED ACOUSTICAL ENERGY AND POWER REQUIRED  
TO WELD 0.10-INCH-THICK MATERIAL

Weldment Material		Estimated Acoustical Energy (kw-sec)	Power Required (kw) for Weld Time of		
Designation	Hardness (VHN*)		0.1 sec	0.5 sec	1.0 sec
Cb (D-31)	195	5.4	54	11	5
Inconel X-750	165	4.2	42	8	4
Mo-0.5Ti	265	9.2	92	18	9
PH15-7 Mo	180	4.8	48	10	5
Rene 41	380	14.8	148	30	15
Tungsten	490	22.4	224	45	22

\* Vickers hardness number as measured for the materials in the as-received and used condition.

Experimental data also indicate the "K" value for electrical energy input to nickel transducers to be 315, or approximately five times the acoustical "K". This corresponds to an electroacoustic conversion efficiency for nickel transducers of about 20 percent, which is generally in accordance with experience. Curves of calculated electrical energy vs. sheet thickness for each of the materials are shown in Figures 4 and 5; experimentally determined data, also recorded on these plots, show close agreement with the calculated data.

The curves of Figures 4 and 5 indicate that the electrical energy requirements for welding 0.10-inch thickness of the specified materials, assuming nickel transducers of 20-percent conversion efficiency, range from about 25 to 100 kilowatt-seconds. These requirements, however, can be markedly reduced with the use of more efficient transducers and coupling systems. Electrostrictive ceramic transducers, for example, are reported to be more than twice as efficient as magnetostrictive nickel stacks. As noted later, the ceramic transducers assembled on this program had efficiencies up to about 80 percent, although this value may be reduced by impedance mismatch from the welding system into the weld material.

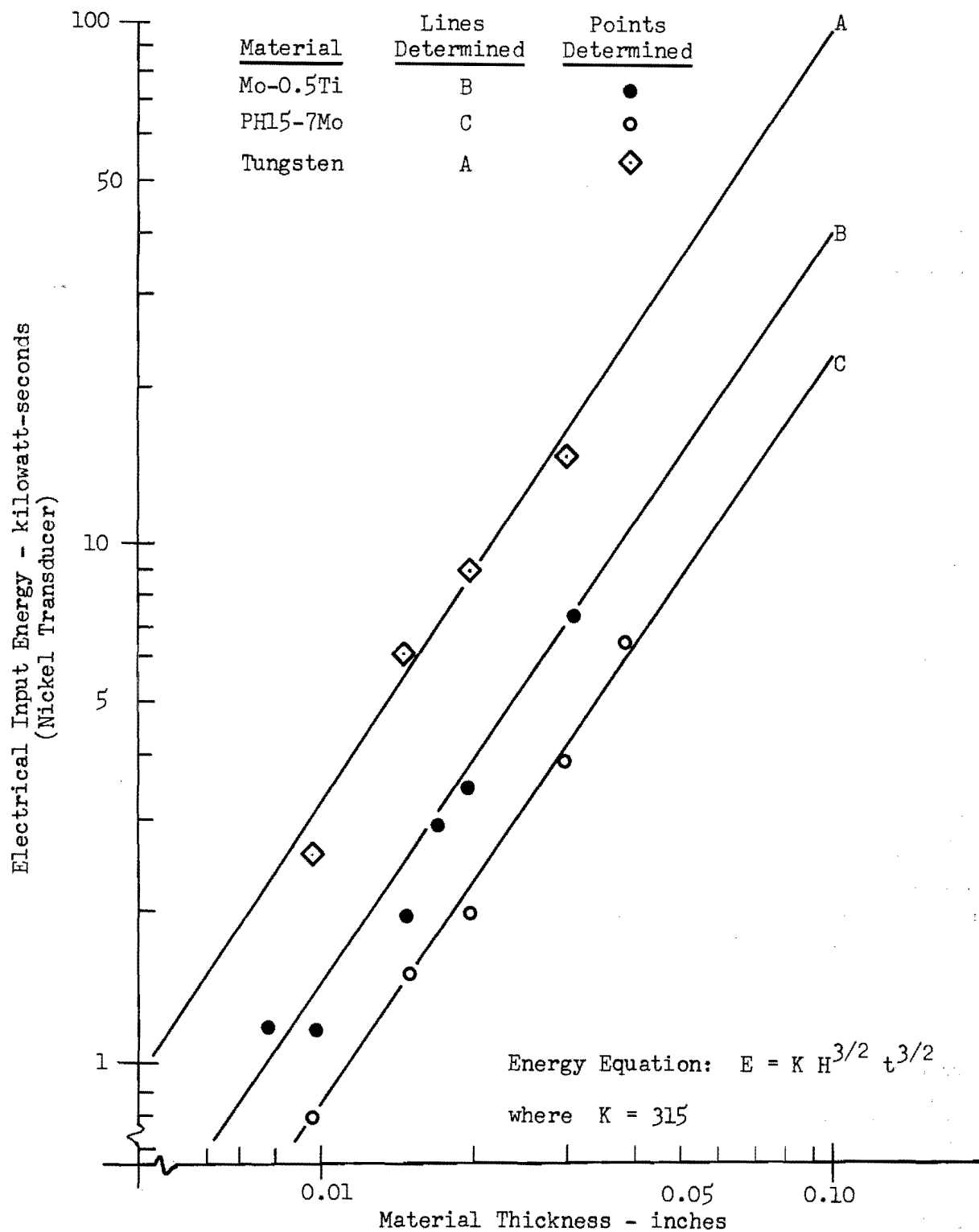


Figure 4: Electrical Energy Input to Nickel Transducers  
Required to Weld Selected Materials  
(Calculated and Experimentally Determined Values)

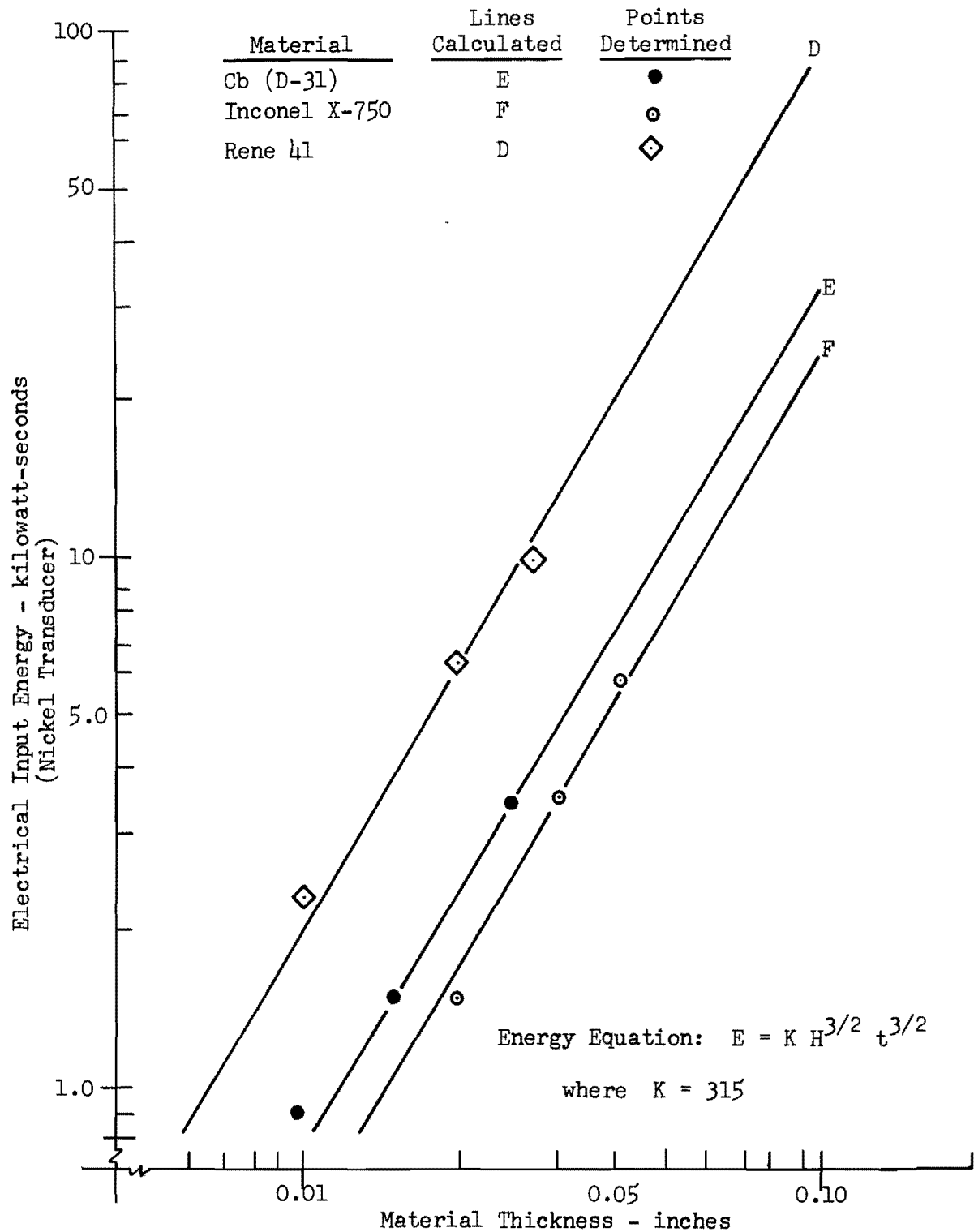


Figure 5: Electrical Energy Input to Nickel Transducers Required to Weld Selected Materials  
(Calculated and Experimentally Determined Values)



Assuming a realistic value of 50 percent conversion efficiency, the energy requirements for welding 0.060-inch and 0.10-inch gages of each material are presented in Tables VII and VIII in terms of estimated powers over a range of weld intervals up to 1.5 seconds, which represents a practical limit. These data indicate that 25 kilowatts of electrical power will suffice to weld 0.10-inch thickness of all the selected materials except tungsten. However, several avenues are available by which even this material may be weldable in 1.5 seconds with 25 kilowatts input power: (a) by achieving higher transducer conversion efficiencies, (b) by the use of power-force programming, (c) by the insertion of a foil interleaf between the components being joined, and/or (d) by modifying the tip radius or geometry.

With these augmentation factors, there appeared few doubts that a 25-kilowatt welding machine should join the selected materials in the desired thicknesses.

Table VII

ESTIMATED ELECTRICAL POWER REQUIRED TO WELD 0.060-INCH MATERIAL  
AT VARIOUS WELD INTERVALS  
(System Efficiency: 50 percent)

Weldment Material	Weld Interval (seconds)												
	0.3	0.4	0.5	0.6	0.7	0.8	0.9	1.0	1.1	1.2	1.3	1.4	1.5
	Estimated Electrical Power (kilowatts)												
Inconel X-750	13	10	7.6	6.3	5.4	4.7	4.2	3.8	3.4	3.1	2.9	2.7	2.5
PH15-7 Mo	14	11	8.6	7.2	6.2	5.4	4.8	4.3	3.9	3.6	3.3	3.1	2.9
Cb (D-31)	16	12	10	8.1	7.0	6.1	5.4	4.9	4.4	4.1	3.8	3.5	3.3
Mo-0.5Ti		20	16	13	11	10	8.9	8.0	7.3	6.7	6.2	5.7	5.3
Rene'41				23	20	17	15	14	13	12	11	10	9.2
Tungsten							22	20	18	16	15	14	13

Table VIII

ESTIMATED ELECTRICAL POWER REQUIRED TO WELD 0.10-INCH MATERIAL  
AT VARIOUS WELD INTERVALS  
(System Efficiency: 50 percent)

Weldment Material	Weld Interval (seconds)												
	0.3	0.4	0.5	0.6	0.7	0.8	0.9	1.0	1.1	1.2	1.3	1.4	1.5
	Estimated Electrical Power (kilowatts)												
Inconel X-750		21	17	14	12	11	9.4	8.4	7.6	7.0	6.4	6.0	5.6
PH15-7 Mo			21	17	15	13	12	10	10	8.7	8.0	7.4	6.9
Cb (D-31)			22	18	15	14	12	11	10	9.0	8.3	7.7	7.2
Mo-0.5Ti						22	19	17	16	14	13	12	12
Rene 41											23	21	20
Tungsten													

### III. ULTRASONIC TRANSDUCER DEVELOPMENT

Consideration of the various transducer materials under Phase I had indicated that possibly the most efficient electroacoustic energy conversion could be obtained with electrostrictive ceramic materials, of which lead zirconate titanate is one of the most promising presently available. Magnetostrictive nickel transducers, heretofore used in rugged ultrasonic welding equipment, have conversion efficiencies of about 30-35 percent under good loading conditions; thus the generation of acoustic power in the range of 12-15 kilowatts would require electrical input power in the vicinity of 45 kilowatts. Preliminary experiments with lead zirconate titanate transducer assemblies had indicated theoretical possibilities of achieving conversion efficiencies up to 80+ percent. The use of this material reduces the input power requirement and accordingly reduces the size and complexity of both the transducer assemblies and the frequency converting equipment.

The design input capacity of 25 kilowatts (with a maximum output for a reasonably well-loaded system of 15-20 acoustical kilowatts) could be achieved with eight transducers of 3.3 kilowatts input capacity or six transducers of 4.2 kilowatts capacity. The final choice of six 4.2-kilowatt transducers was based upon projected mechanical transformer requirements and the complexity of the transducer-coupling array.

Prior to this work, practical designs for high-power ceramic transducer assemblies, to insure axial radiation into metal coupling members and to achieve predictable performance, had not been evolved. Consequently design studies and evaluation were carried out on smaller 2.0- and 3.3-kilowatt units.

The final transducer assemblies utilized lead zirconate titanate disks (PZT-4) manufactured by the Clevite Corporation. (Ceramic disks of similar composition obtained from other manufacturers were also evaluated, and no significant difference in performance was detectable.)

#### A. Ceramic Elements

The design requirements for ceramic elements are based on the operational characteristics specified by the manufacturer (22, 23), the expected driving voltage for the volume of ceramic material being stressed, the heat power that will be generated internally in the ceramic, and practical means for removing this heat (since overheating reduces transduction efficiency).

The internal heat is caused primarily by hysteresis-type losses associated with domain reversals in the dielectric of the ceramic. This factor, generally designated  $\tan \delta$ , represents the series-loss resistance of the ceramic as a clamped capacitance. As the temperature of the ceramic increases, the electromechanical coupling efficiency decreases, and more of

the applied power is lost as internal heat, thus creating a catastrophic cycle. The temperature rise must therefore be limited to a safe value. The manufacturer recommends that these elements be operated at a loss tangent of less than 0.04, a determination which in turn establishes the maximum driving field.

The thermal conductivity of PZT-4 is low, and to assure minimum heating the ceramic should be wafer thin. This is not practical, since its power-handling capacity is governed by the volume of material being stressed. Under perfect transmission conditions, the theoretical maximum power-handling capacity is about 6 watts per cubic centimeter per kilocycle, or 90 watts per cubic centimeter at 15 kc. Hence, if we design with a safety factor of about 2, as the manufacturer recommends, the ceramic elements could be loaded to a maximum of 45 watts per cubic centimeter at 15 kc. Assuming a 60-percent electromechanical conversion efficiency, approximately 1.2 watts per cubic centimeter of ceramic would have to be removed as heat.

The size of the ceramic element is therefore based on the expected strain and hence driving field potential, the required acoustic power output at the operating strain level, the number of ceramic elements used, and the minimum thickness which can reasonably be used.

In selecting the thickness of the ceramic elements, a compromise must be made between heat removal requirements and the thickness required to prevent lateral restraint of the elements. If the ends of the element are clamped and if the wafer is thin, it operates in a laterally clamped longitudinal mode. For this case, the effective coupling coefficient is  $K_t$  and not  $K_{33}$ \*, which reduces the coupling factor by about 25 percent. To fully realize  $K_{33}$ , the length of the crystal should be such that the thickness resonance is below any lateral resonance. In this type of transducer, such design is generally not practical; but if the crystal elements are thick enough to permit partial relief of the transverse stress, a coupling coefficient intermediate between  $K_t$  and  $K_{33}$  can be achieved by effectively coupling the faces of the ceramic elements to the faces of the metal members if the latter are an integral part of the resonant system, so that the lateral displacement of both the ceramic and the metal are about equal.

Transducer systems developed during this program generally satisfied these conditions.

---

\*  $K_t$  is the transverse coupling coefficient (laterally clamped longitudinal mode).

$K_{33}$  is the coupling coefficient obtained when the crystal is excited in the thickness mode and predominant strain is also in the thickness mode.

## B. Transducer Design

Ceramic transducer materials possess very low tensile strength; hence they must be maintained under bias compressive stress so that the vibratory stress imposed during operation never results in a tensile strain on the ceramic. For an operating  $Q$  in the welder transducer-coupling system of up to 10, which seems reasonable, a maximum alternating stress of 3500 psi (rms) is indicated; i.e., with a peak of 4900 psi, a static bias of 5000-6000 psi should be adequate.

This bias can be applied in several ways, such as via a center tension bolt or a tension shell. The tension shell concept was devised for use here, because no other practical geometry appears capable of properly relating the strain characteristics of the tension member with the strain characteristics of the compressed members; other advantages of the shell design are that it provides an enclosed system for protection from high voltages, facilitates circulation of cooling air, and provides a protective housing for the brittle ceramic elements.

The tension shell design involved a resonant system comprised of two ceramic elements separated by a center spacer, two end sections of approximately three-quarter wavelength, and the tension shell. The required bias stress was applied during assembly, and a threaded collar, inserted between the threaded end of the shell and one end section, maintained this bias stress.

The center spacer was made of a low expansion alloy, Invar 36, and contained curved radial channels to permit flow of cooling air. The end sections were fabricated from aged beryllium-copper alloy. The various stages in the evolution of this final configuration are discussed below.

## C. Transducer Evaluation Technique

There are two traditional methods of evaluating transducer performance. The first, vector impedance loop measurements and subsequent determination of  $Q$ , can be used with free and lightly loaded systems, but does not necessarily provide a reliable indication of performance at high power under varying load conditions. The alternate method, of incorporating the transducer in a welder and evaluating welding performance, is complex, laborious, and not necessarily accurate.

During the Phase I effort, a direct method for evaluating transducer performance was devised. The vibratory energy output of the transducer was conducted into an energy absorber where it was degraded into heat and was measured calorimetrically. The device was subsequently improved to reduce indeterminate heat losses and to permit rapid measurement of the heat produced.

This acoustical calorimeter, shown in Figure 6, takes power from two sources, the transducer and a standard a-c power line. All the energy from both sources is removed from the calorimeter by tap water that flows through a copper tube coil embedded in the body of the absorber. Inlet and outlet water temperatures, as well as water volume, are monitored.

In operation, the device is stabilized at some elevated temperature based on a pre-set level of input electrical power from the regular a-c power line feeding resistance wires embedded in the body of the absorber. When acoustic energy from the transducer is introduced, power from the a-c line, which is monitored by a calibrated wattmeter, is decreased to maintain the temperature differential between the input and the output water at a constant value. Essentially, the electrical power is decreased by the amount of vibratory power delivered into the absorber. Thus, the vibratory power is equal to the observed decrease in a-c power, and the overall energy balance is checked by computing the power delivered into the flowing tap-water heat sink. The absorber, enclosed in a tall vacuum chamber at a pressure of about 2 millimeters of mercury, was insulated against heat losses.

This acoustical calorimeter, which provides a reproducible test load for transducer evaluation, has been a major contribution to transducer development.

#### D. Early 2-Kilowatt and 3.3-Kilowatt Assemblies

The initial design of a tension-shell transducer was a 2-kilowatt unit, with the metal components all being made of beryllium-copper because of its low loss characteristics in vibratory power transmission. Standard "V"-type threads were incorporated between the tension shell and the end sections.

Early power tests indicated that only about half of the design power could be developed. The unit, however, was successfully powered up to 600 watts and showed conversion efficiencies up to 84 percent. Data from calorimetric tests are shown in Table IX, together with comparable tests from a standard laminated nickel-stack transducer (which showed an efficiency of only about 35 percent).

The difficulties in achieving full power with this unit were traced to voltage breakdown in the electrical plug adapter, arcing between the spacer and the inside of the tension shell, and microscopic cracking, resulting from differential expansion between the center spacer and the ceramic washers, of the ceramic elements. The arcing problems were attributed to corona sites (such as sharp edges from high-potential surfaces); these were eliminated by radiusing and polishing the edges on these surfaces. The differential expansion between the ceramic disks and the central spacer were minimized by fabricating the spacer of Invar 36, which has thermal expansion properties more closely matching those of the ceramic, and by increasing the thickness of the spacer.

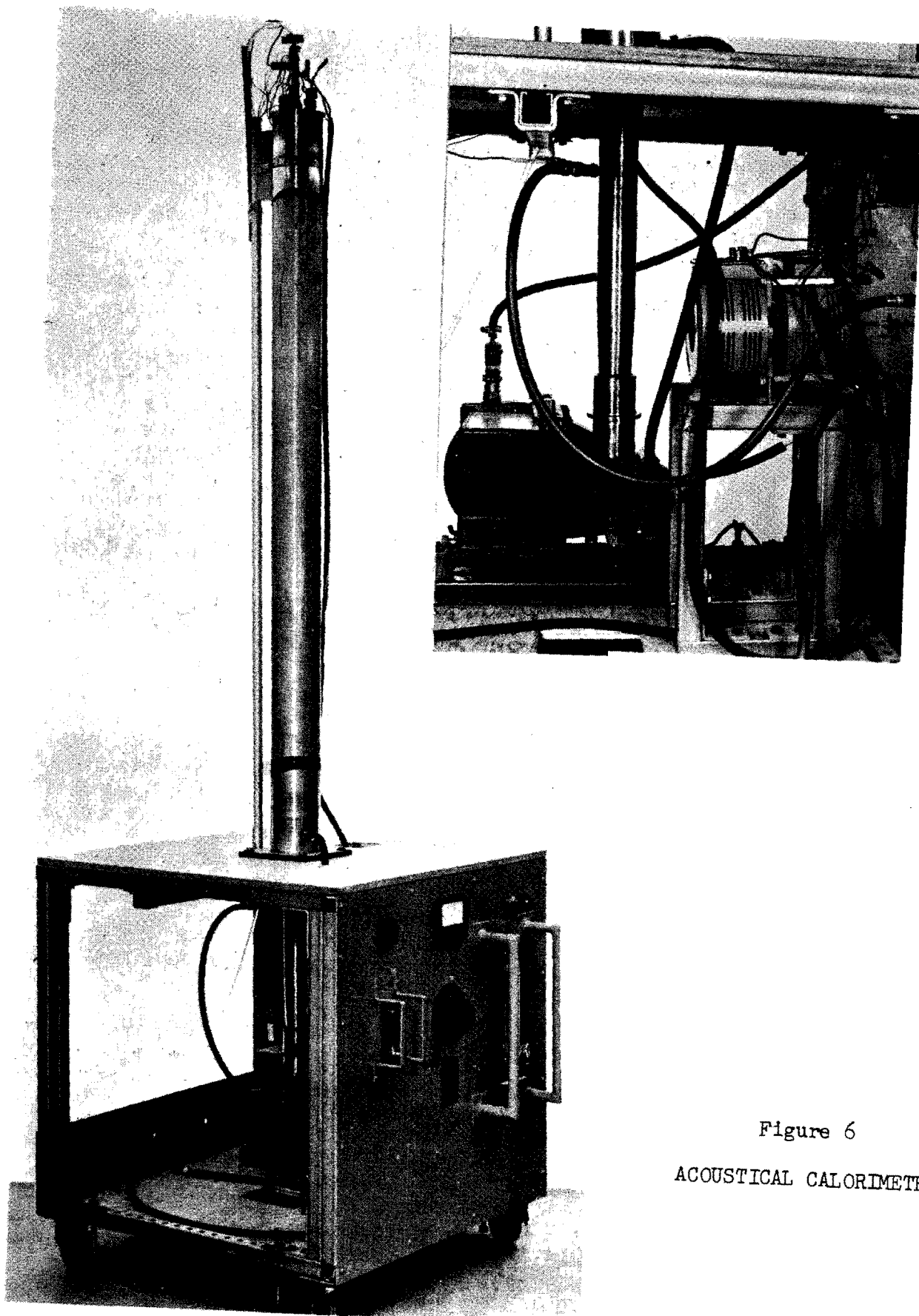


Figure 6  
ACOUSTICAL CALORIMETER

Table IX

SUMMARY OF ACOUSTICAL ENERGY ABSORBER DATA FOR A NICKEL AND A  
CERAMIC (PZT-4) TRANSDUCER UNIT OF 2-KILOWATT POWER-HANDLING CAPACITY

Transducer	Input Power		Water Temperature		Water Flow (gm/sec)	Power Absorbed by Water P <sub>3</sub> (watts)	Transducer Efficiency	
	Transducer P <sub>1</sub> (watts)	To Heater P <sub>2</sub> (watts)	Inflow (°C)	Outflow (°C)			P <sub>2</sub> /P <sub>1</sub> (percent)	P <sub>3</sub> /P <sub>1</sub> (percent)
Nickel	1000	0	23.5	37.0	6.31	356		36
	0	350	23.5	37.0	6.31		35	
	1650	0	23.5	50.0	5.26	583		35
	0	575	23.5	50.0	5.26		35	
2-kw PZT-4	500	0	23.5	37.5	6.31	370		74
	0	370	23.5	37.5	6.31		74	
	600	0	23.4	42.6	6.31	507		84
	0	480	23.4	42.6	6.31		80	
	300	0	23.0	33.7	*	-	-	-
	0	200	23.0	33.7	-	-	67	-

\* Water flow was not accurately measured.



In addition, on the manufacturer's recommendation, the ceramic elements were heat-cycled before use at temperatures above those that would be achieved during operation. Apparently it had just been learned that the PZT-4 behaved anomalously in its thermal expansion properties as a function of temperature.

A further difficulty in driving the units at full power arose from the fact that the ceramic elements are voltage-sensitive, high-impedance devices, characterized by a high static capacitance, and thus present a highly reactive load to the driving power. This difficulty was minimized by the use of a high-Q neutralizing coil.

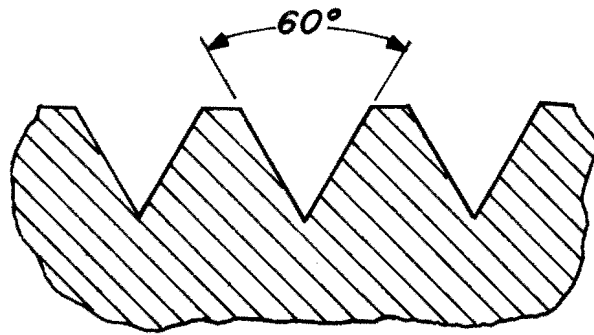
In order to reduce the driving voltage and matching coil requirements, a 3.3-kilowatt transducer was assembled with four, rather than two, ceramic disks, and the disks were thicker. The power density was thus reduced to less than 3 watts per cubic centimeter per kilocycle, and heat removal was simultaneously facilitated. The spacers were redesigned to project beyond the circumference of the disks and to incorporate air-cooling channels.

Conversion efficiencies obtained with this four-wafer unit ranged from 52 to 69 percent, compared to 75-92 percent previously achieved with the two-wafer design. The reduction in efficiency was attributed to two factors: the ceramic elements were spread over such a large proportion of a half-wavelength that they were not equally stressed; and the additional interfaces (eight instead of four) between the wafers and the spacers tended to be energy dissipative. Consequently, the two-wafer design was selected for the final units.

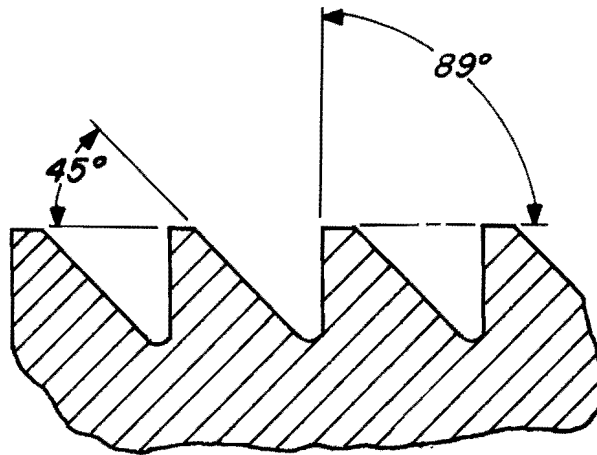
A two-element, 3.3-kilowatt unit incorporating the refinements indicated above was successfully tested up to its design power capacity. After a period of use, however, the conversion efficiency decreased, and it was found that vibratory energy was being degraded into heat by motion in the "V" threads (Figure 7-A) used between the tension shell and the end sections. The threads were replaced by buttress-type threads having a 1-degree positively inclined load-bearing face (Figure 7-B). This modification permitted continuous operation up to about 1200 watts and pulse operation up to about 2400 watts before substantial heating occurred at the threaded joints. Relative motion in the threads was further reduced by changing the thread angle to a 7-degree negative inclination (Figure 7-C). Continuous operation at 2000 watts input power was then possible with only slight heating in the thread area.

#### E. Final 4.2-Kilowatt Assemblies

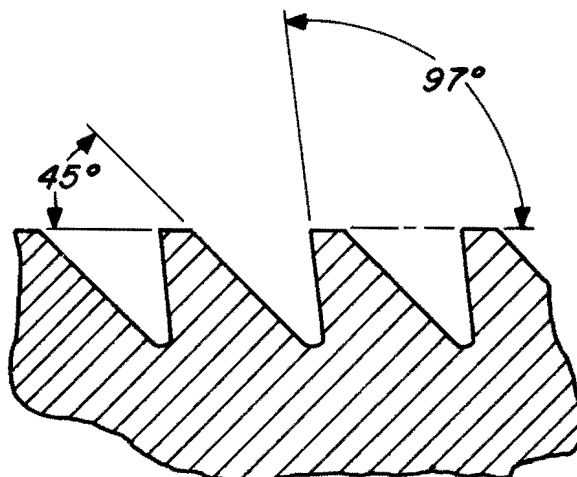
The final design of the 4.2-kilowatt transducer assembly incorporated all the refinements evolved during development of the 2.0- and 3.3-kilowatt test models, and a few additional modifications were made.



A. Standard "V" Thread



B. Modified Buttress Thread  
1° Positively Inclined  
Load-Bearing Face



C. Modified Buttress Thread  
7° Negatively Inclined  
Load-Bearing Face

Figure 7: Thread Configurations Used for the Ceramic Transducer Assembly

The beryllium-copper used for fabrication of components of the earlier assemblies had been solution-annealed. For the final assemblies, this material was age-hardened by holding under heat (600°F) for 1 hour; this resulted in a stronger material with a somewhat higher sound velocity (3940 vs. 3800 meters per second).

A further modification was made to reduce time and cost of fabrication and to simplify assembly and prestressing. Certain of the threaded connections were replaced by a shoulder, and a tensioning collar was incorporated between the shell and the coupler. The assembly of end sections, ceramic disks, and spacer was compressed to the required biasing stress level in a hydraulic testing machine. This technique eliminated former uncertainties associated with applying bias stress, and insured that the preset compressive stress was maintained on the ceramic elements.

The first of the 4.2-kilowatt units was fabricated and tested by the calorimetric technique. The results are shown in Table X. The unit operated successfully at 3000 watts of electrical power on a continuous basis, and at 5000 watts under pulse power conditions (simulating actual welding power pulses). It was thus effective at powers beyond its design power level. Calorimetric measurements indicated efficiencies generally within the range of 70 to 90 percent.

In addition, temperature measurements were made at about 10-minute intervals (with ultrasonic power momentarily turned off) using contact thermocouples at the locales of the shell thread, the shell center, the non-threaded end of the shell, and at end couplers adjacent to the shell. The maximum recorded temperature of 140-150°F was at the central section of the shell, which was the area of impingement of cooling air exhausted through the central metal spacer. The adequacy of the design was thus affirmed; with a conversion efficiency of 80 percent, 20 percent of the applied power (800 to 1000 watts), which had degraded to heat in the transducer, was adequately removed. It thus appeared that the unit would adequately accommodate heat power loss under the most severe use conditions.

The remaining five transducer assemblies were subsequently fabricated to the same specifications. These were not subjected to full-power tests on the calorimeter, but short-time tests at input powers up to 2 kilowatts indicated conversion efficiencies ranging from 82 to 88 percent. Operating frequencies for all six units were within the range of 14,935-14,955 cycles per second.

Table X

TEST DATA FOR 4.2-KILOWATT CERAMIC TRANSDUCER  
(Pulse Power: 1.5 seconds on, 1.5 seconds off)

Test Condition	Input Power, (watts)	Output Power, (watts)	Efficiency, (%)
Continuous	500	335	67
	1000	890	89
	1000	830	83
	1500	1185	79
Continuous	2000	1530	76.5
Pulse	2000	1540	77
	2500	1750	70
	3000	2160	72
	3000	2150	72
	3500	2420	69
	3500	2660	76
	4000	3040	76
Pulse	4500	3330	74
	5000*	--	--
Life Test (at 4000 watts pulse duty for 30 minutes)	4000	3400	85

\* Powered to this level to check electrical characteristics.

#### IV. COUPLER SYSTEM DEVELOPMENT

A transducer-coupling system for ultrasonic welding consists of a transducer to convert electrical to vibratory energy, a coupler or coupling system to deliver this energy to the weld locale, and a welding tip to deliver the energy into the weld zone. For the 25-kilowatt welding machine, it was preliminarily established that the transducer-coupling system must provide for:

1. Generation and transmission of 15-20 kilowatts of vibratory power.
2. Structure for normal static loads (clamping forces) up to about 5000 pounds, without seriously affecting the operating frequency of the system or losing vibratory energy through the support members.

Under Phase I, the respective merits of the reaction-anvil versus the opposition-drive system were examined, and the opposition-drive was concluded to be mandatory for delivering the requisite high power levels. This arrangement consists of two opposed transducer-coupling systems to transmit vibratory energy simultaneously into both sides of the weldment. The oscillatory strain levels in each system are thus less than one-half those of the reaction-anvil system (in which the total energy is delivered through a single transducer-coupling system), because in an anvil there must be some measure of compliance, which can be altogether eliminated in an opposition-drive system.

The opposition-drive system requires precise matching of the resonant frequency of both systems and precise mechanical and electrical phasing to achieve a 180-degree out-of-phase vibratory relationship of the two systems. A relative phase shift of either system will decrease the amount of energy delivered. Under certain circumstances, one transducer-coupling system may act as an alternator, with the opposite system serving as a motor, so that little work may be done in the weld locale.

With the ceramic transducers, precise phasing was insured by the polarization direction of the ceramic elements. The three transducers for one system were assembled with the positive polarization direction of the disks toward the center spacers, and the three for the opposite system were assembled with the positive polarization direction toward the end sections of the transducers.

The Phase I studies had also included consideration of the wedge-reed versus the lateral-drive coupling system, both of which are adaptable for the opposition-drive arrangement, as shown schematically in Figures 8 and 9. The wedge-reed system, previously used with the 2-kilowatt and 4-kilowatt welding machines, involves transmission of vibratory energy longitudinally from the transducer through a wedge-shaped coupler which drives the reed in

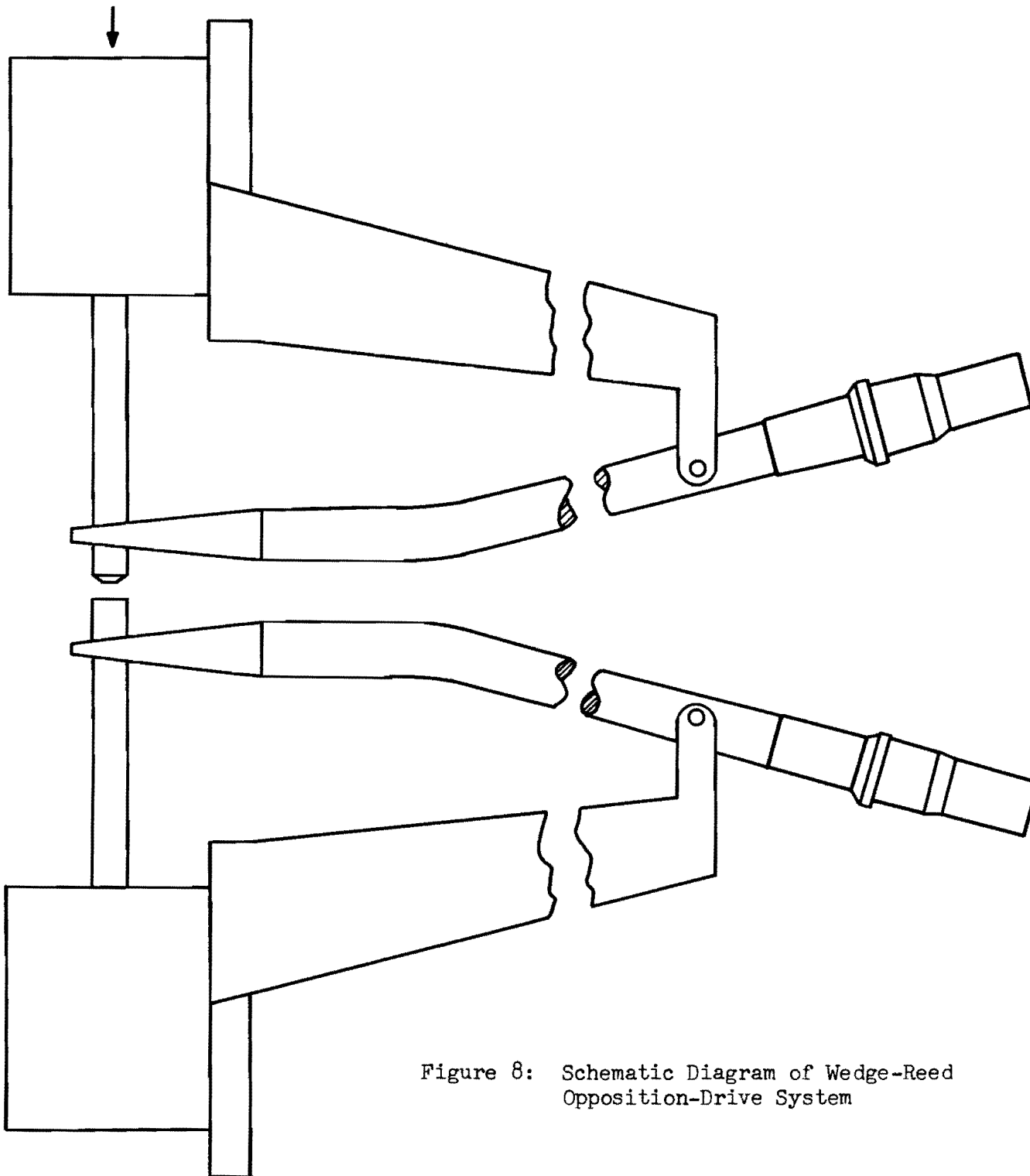


Figure 8: Schematic Diagram of Wedge-Reed Opposition-Drive System

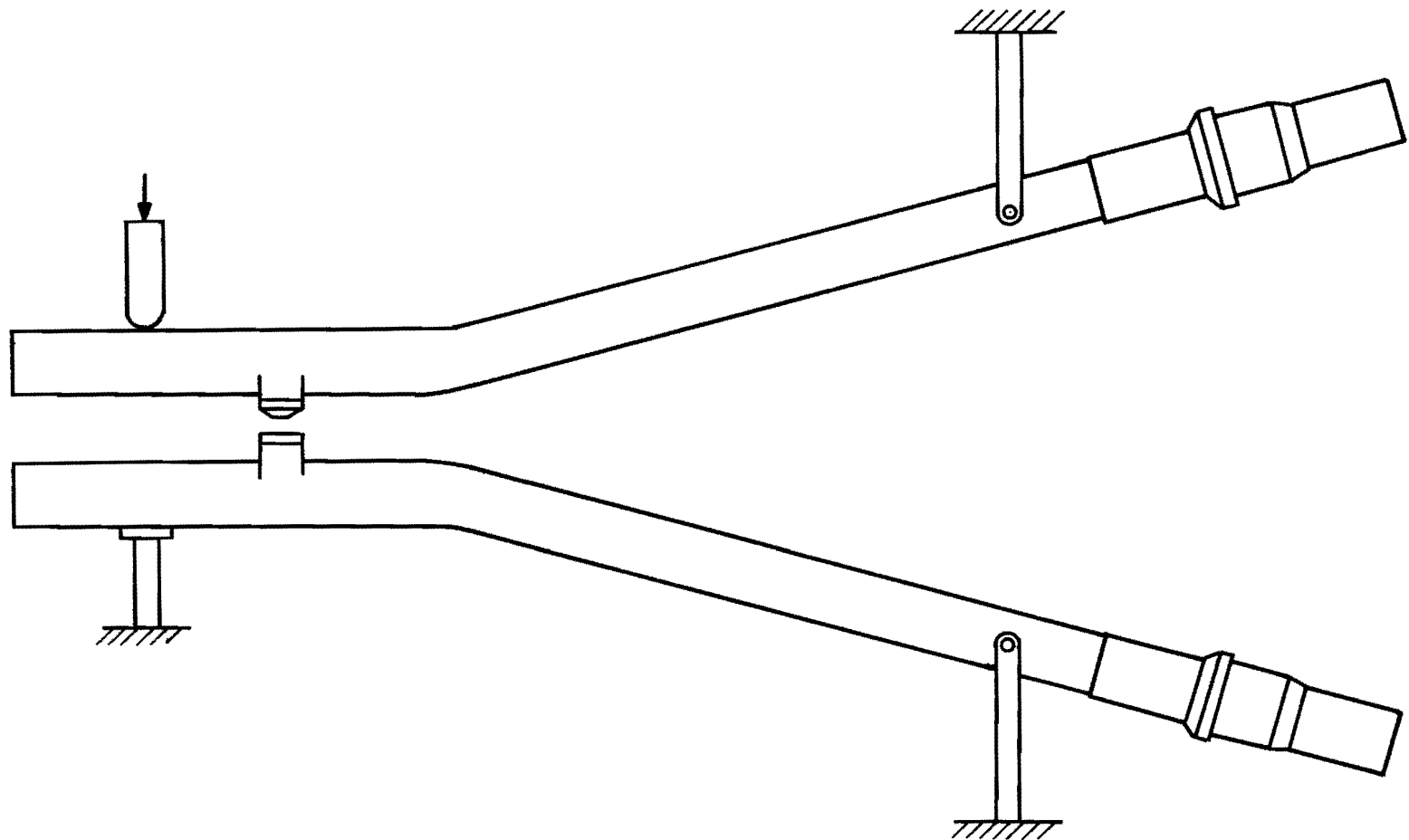


Figure 9: Schematic Diagram of Lateral-Type Opposition-Drive System

flexure. Clamping force is applied via the reed, which remains essentially stable over an extended range of the acoustical variables (force and power). With the lateral-drive system previously used only with low power systems, the clamping force is applied via bending of the coupler; this system is inherently "soft" structurally, exhibiting tip bounce and reducing the clamping force at the instant when it is most essential. The lateral-drive system was thus considered inadequate, in its then-existing stage of development, for a welding machine involving application of several thousands of pounds of clamping force.

On this basis, the wedge-reed system was initially selected for incorporation on the 25-kilowatt welding machine. As discussed later, difficulties were encountered in driving this system at high power. The stresses associated with a flexurally vibrating system are substantially greater than for a longitudinally vibrating system at the same vibratory amplitude level (see Appendix A), and associated flexural motion in the drive coupler presented serious problems. Meanwhile, concurrent effort on other welding equipment development had evolved a lateral-drive system with an overhung coupler, which essentially eliminated the problems of coupler bending and tip bounce. This overhung-coupler lateral-drive system was eventually selected for the heavy-duty welder.

#### A. Wedge-Reed System

From consideration of the wedge-reed coupler system for the 25-kilowatt welder, the necessity for design modifications was apparent in order to achieve optimum power transmission and to provide essential work clearance. These modifications involved the driving coupler attached to the reed member.

In a perfectly loaded system (i.e., one in which all the mechanical power supplied from the transducer is absorbed by the load or the weldment), the joint between the wedge and the reed should coincide with a flexural antinode on the reed. It has been empirically established in our laboratory, however, that for best transfer of power from the transducer to the reed, and ultimately to the weld, the driving point on the reed must be displaced from the flexural loop position. The result is a flexural component reflected back into the wedge coupler wherein it must be accommodated. If the driving coupler is "stiff", high stresses are introduced into the junction. Although this has not been a problem in the 4-kilowatt machines, operation at 12-13 kilowatts input power could lead to unacceptably low joint life.

Thus it was necessary to relieve the flexural stiffness of the driving coupler and develop design criteria for such a system to operate at the higher powers. This was accomplished by thinning or sculpturing the section of the wedge in the vicinity of the wedge-reed junction.

In addition, it was contemplated that the high power machine would have a throat depth of 36 inches. To provide the necessary work clearance, it was essential that the driving coupler be curved away from the plane of the weldment.



In order to evaluate these design changes, a 4-kilowatt wedge-reed system was modified accordingly, as illustrated in Figure 10, and its performance was evaluated in the welding of three intermediate gages of 2024-T3 bare aluminum alloy. The results obtained in terms of weld strength were compared with comparable weld strengths achieved with standard 4-kilowatt welding systems (Table XI). These data show that best performance was obtained with the coupling system that was sculptured only. Bending of the coupler through 4.5 degrees to simulate the final system resulted in a slight decrease in performance, but not to an unacceptably low level. The validity of the modified design was thus confirmed.

Consideration was then given to the design of the reed member, which vibrates flexurally, with a view to achieving maximum power-handling capability. A theoretical study was made (Appendix A) in an effort to (a) establish a power-capability criterion, (b) delineate limitations that might exist, and (c) indicate the effect of geometrical variations on the power-handling capability of the system. The analysis indicated that for equal impedance at a given frequency, a reed of square section would transmit 1.3 times as much power as a reed of circular cross section without increasing the associated stresses.

The 4-kilowatt system shown in Figure 10 was therefore modified to incorporate a square reed design in accordance with the usual reed criteria: resonant frequency as a free element, a standing-wave pattern existing between the drive point and the upper mass during power delivery, and variation of this pattern with time.

The system thus modified operated satisfactorily at low power levels, but at the higher power levels the brazed junction between the wedge and the reed could not be optimized to handle the vibratory stresses. Study of the microkinetics of the vibration motion indicated that no simple, practical joint could support the necessary stress level. This approach was abandoned in view of the lateral-drive system.

#### B. Lateral-Drive System

With the availability of the overhung-coupler lateral-drive system,\* there appeared to be more promise of solving the power delivery problem without overstressing. The concept of such a system in opposition drive on the 25-kilowatt welder is shown in Figure 11. This design utilizes the more efficient longitudinal vibratory mode, eliminates the necessity for mode conversion (as between the axially vibrating coupler and the flexurally vibrating reed in the wedge-reed system), and offers potentially easier control over the phase relationship between the upper and lower coupling systems. Stability of the system at high powers and high clamping forces is offered by the application of clamping force through rod E in Figure 11 at a point outboard of the welding tips.

---

\* Jones, J. Byron (Aeroprojects Incorporated), U. S. Patent 3,209,447 (issued October 5, 1965), "Transducer Coupling System."

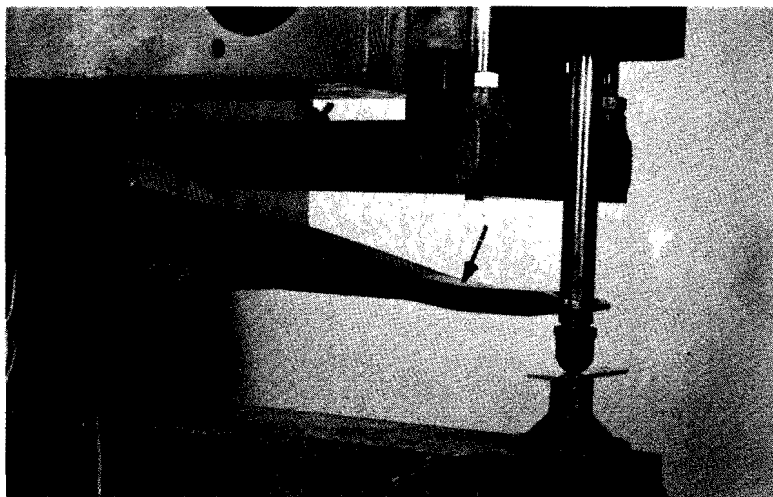


Figure 10: Curved and Sculptured Welding System  
(Curved section indicated by arrow)

Table XI

EVALUATION OF 4-KILOWATT CURVED AND SCULPTURED SYSTEM  
WELDING 2024-T3 BARE ALUMINUM ALLOY

Systems*	Material Gage, (inch)	Power, (watts)	Clamping Force, (pounds)	Weld Time, (seconds)	Number of Specimens	Weld Strength			
						Average (pounds)	Range (pounds)	Standard Deviation (pounds)	Deviation (percent)
A	0.040	2000	900	1.5	100	1030	340-1240	160	16
B		2400	800	1.5	36	950	720-1040	80	9
C		2400	700	1.5	100	950		80	
A	0.050	3700	1000	1.5	20	1050	660-1240	170	16
B		3700	1000	1.5	20	1010	440-1320	260	26
C		3800	1100	1.5	100	1070±133			
A	0.063	4000	1100	1.8	24	1520	950-1750	230	15
B		3700	1100	1.5	8	1010	760-1250	145	15
					3	800±356			
C		3800	1100	1.5	6	930	580-1500		
					3	1030±850			

\* System: A - 4-kilowatt straight sculptured system  
 B - 4-kilowatt curved sculptured system  
 C - 4-kilowatt standard system. Typical values obtained by pooling data from several ultrasonic welding systems.

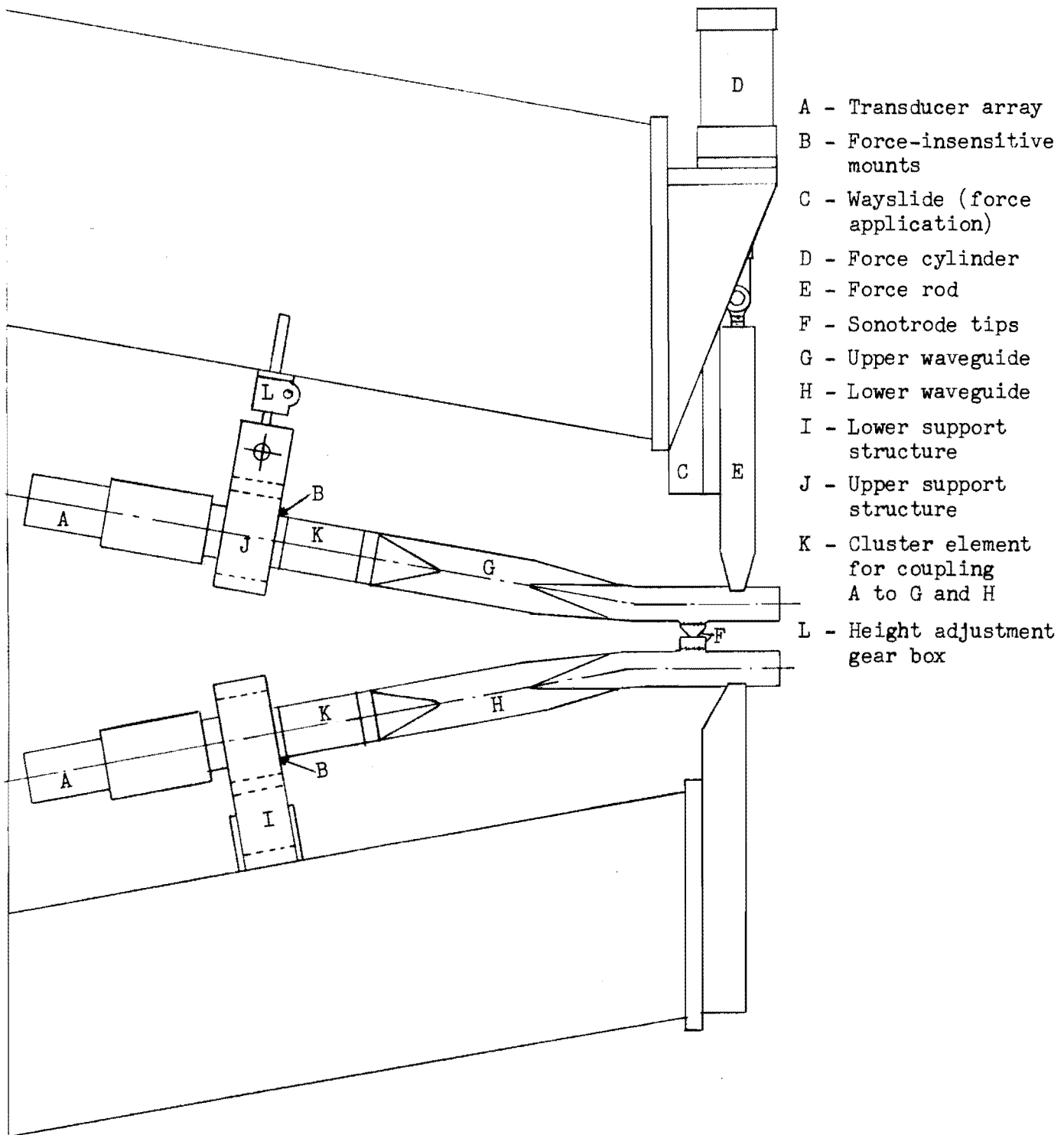


Figure 11: Ultrasonic Welding Array

A transducer-coupling system incorporating this projected design, scaled to an intermediate power level, and operating at a frequency of 17.5 kilowatts, was fabricated, assembled, and evaluated. Exploration of the system's characteristics revealed second-order factors contributing to unsatisfactory behavior. These factors were associated with the specific geometry of the coupler and an unexpected flexural response related to Poisson's ratio and the location of the clamping force arm.

Relative vibratory amplitude measurements revealed a flexural standing-wave pattern with an average separation between positions of flexural nodes and antinodes ranging from 2-3/8 to 2-1/2 inches (at clamping forces ranging from 200 to 500 pounds). Analysis of this geometry with respect to vibration beam or plate theory (24) revealed a flexural response at approximately 17.5 kc with the system force arm at a flexural node and the welding tip at a flexural antinode. It was found that this flexural response could be eliminated by adjusting the cross-sectional dimensions of the coupler to effect a slightly reduced flexural rigidity.

Further study of the design details of the secondary coupler, taking into consideration the expected clamping loads, led to minor but significant dimensional changes in the cross section geometry of the coupler in the locale of maximum stress. The revised design also permitted a somewhat more practical geometry for mechanically attached welding tips (discussed in Section V).

To evaluate performance for the overhung-coupler opposition-drive concept, the array of Figure 12 was assembled. This array incorporated two available identical low-power (1000-watt) transducer-couplings with waveguides similar to those being considered for the 25-kilowatt machine. This array was driven by two 1000-watt frequency converters, one coupled to each transducer-coupling system, and operating through a common oscillator. The system was used for welding 0.040-inch-thick coupons of 2024-T6 bare aluminum alloy at progressively increasing power and clamping force levels. The systems remained stable under all test conditions. Forty weldments made at maximum power (2000 watts into the two systems) were tested in tensile-shear, and the results, presented in Table XII, show a mean weld strength of 980 pounds, with a standard deviation of only 55 pounds. As indicated by the footnote in Table XII, these results were superior both in average strength and standard deviation to those obtained with standard wedge-reed welding machines at the same power level. System performance was thus confirmed.

### C. Coupler Materials

Under Phase I, analysis of the vibratory energy transmission properties of candidate coupler materials, including consideration of impedance matching, internal friction losses, and power-handling capacity, had indicated that either aluminum-bronze or beryllium-copper would provide superior performance, and these materials were used experimentally in various stages of coupler system development.

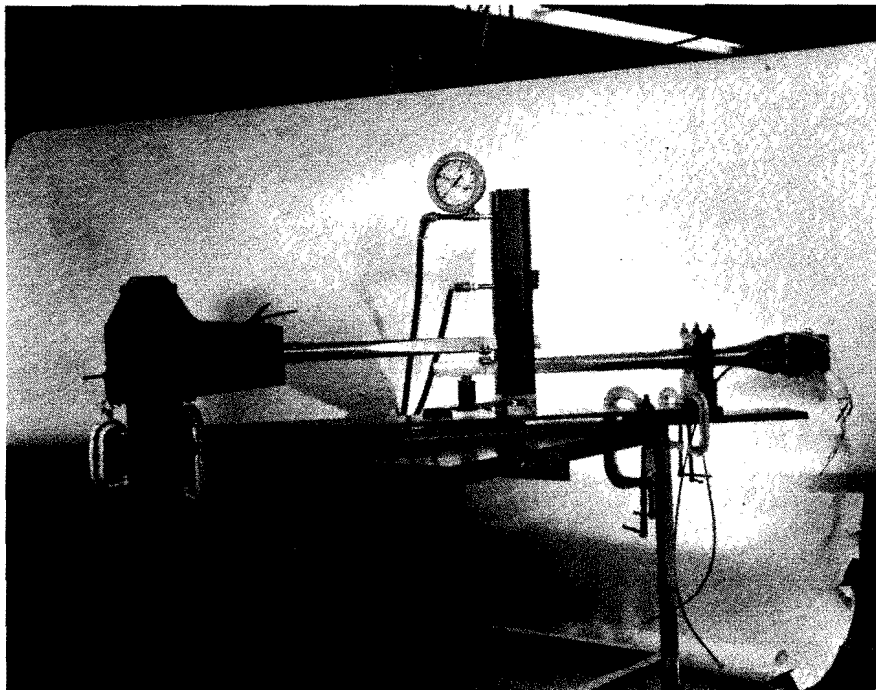


**Figure 12:** Ultrasonic Welding Setup Used for Evaluation of Double Opposed Welding System

Table XII

## EVALUATION OF DOUBLE OPPOSED TRANSDUCER-COUPLING WELDING SYSTEM

Weldment Material: 0.040-Inch 2024-T6 Bare Aluminum Alloy

Individual Weld Strengths (pounds)				Statistical Analysis
1040	1040	990	1010	
1020	840	1050	870	Mean $\bar{X}$ = 987 lb*
940	1030	1040	1000	
1010	1020	1000	1015	Standard Deviation $\sigma$ = 55 lb*
980	1070	1010	1050	
1000	990	970	1000	
890	980	855	970	
1020	980	1050	940	
980	1020	1045	1030	
860	870	1005	980	

\* The range for similar data obtained with standard 2-kw ultrasonic welding machines incorporating wedge-reed transducer-coupling systems was as follows:

Mean  $\bar{X}$  = 910 to 965 pounds

Standard Deviation  $\sigma$  = 70 to 130 pounds

However, this preliminary work revealed several problem areas with beryllium-copper and aluminum-bronze. These materials perform best in the annealed condition, but the design stress loads required that they be heat-treated in critical areas, particularly at the joints between members and the point of welding tip attachment. Brazing, which appeared to be the only acceptable joining method, degraded the strength properties of the materials. Furthermore, both alloys proved to be difficult to braze. Rapid alloying of the braze metal with the base metal produced a brittle joint, and altered the vibratory transmission characteristics by an indeterminate amount.

Consequently, potential coupler materials were reconsidered. The power loss vs. strain characteristics (Figure 13) had shown K Monel to be the next most effective material. Prior experience with K Monel had indicated it to be satisfactory as a transmission member, and fabrication problems were less severe. In addition, K Monel has a longer wavelength ( $\lambda/2 = 5.86$  inches at 15 kc, compared to 5.34 inches for aluminum-bronze and 5.12 inches for beryllium copper), so that the locales of certain junctions, such as welding tip location and the point of clamping force application, are less critical. The longer wavelength also permits a greater amplitude at the tip.

K Monel was therefore selected for the final coupler assemblies. It was used in the annealed condition, with subsequent heat treatment in certain critical areas. It presented difficulties in brazing due to intergranular penetration of braze metal, but these were not as severe as with the aluminum-bronze or beryllium copper. Brazing was accomplished with Handy and Harmon Alloy 560 at a temperature of 1350°F. Extreme care was taken to prevent overheating (which would induce excessive intergranular penetration). The metal was heated only to the extent absolutely necessary to achieve flow of the brazing alloy.

#### D. Final Coupler Design and Fabrication

The final transducer-coupling system satisfied the requirements for high-power operation. The components and assembly are shown in Figure 14. For each system, three of the 4.2-kilowatt transducer assemblies transmitted vibratory energy through three transition couplers into a single coupler adapter and thence into the terminal coupler. The couplers were exponentially tapered to provide amplification of the vibratory amplitude. The total amplification achieved with each system was about 5:1.

Figure 15 shows the two systems installed on the 25-kilowatt welding machine.



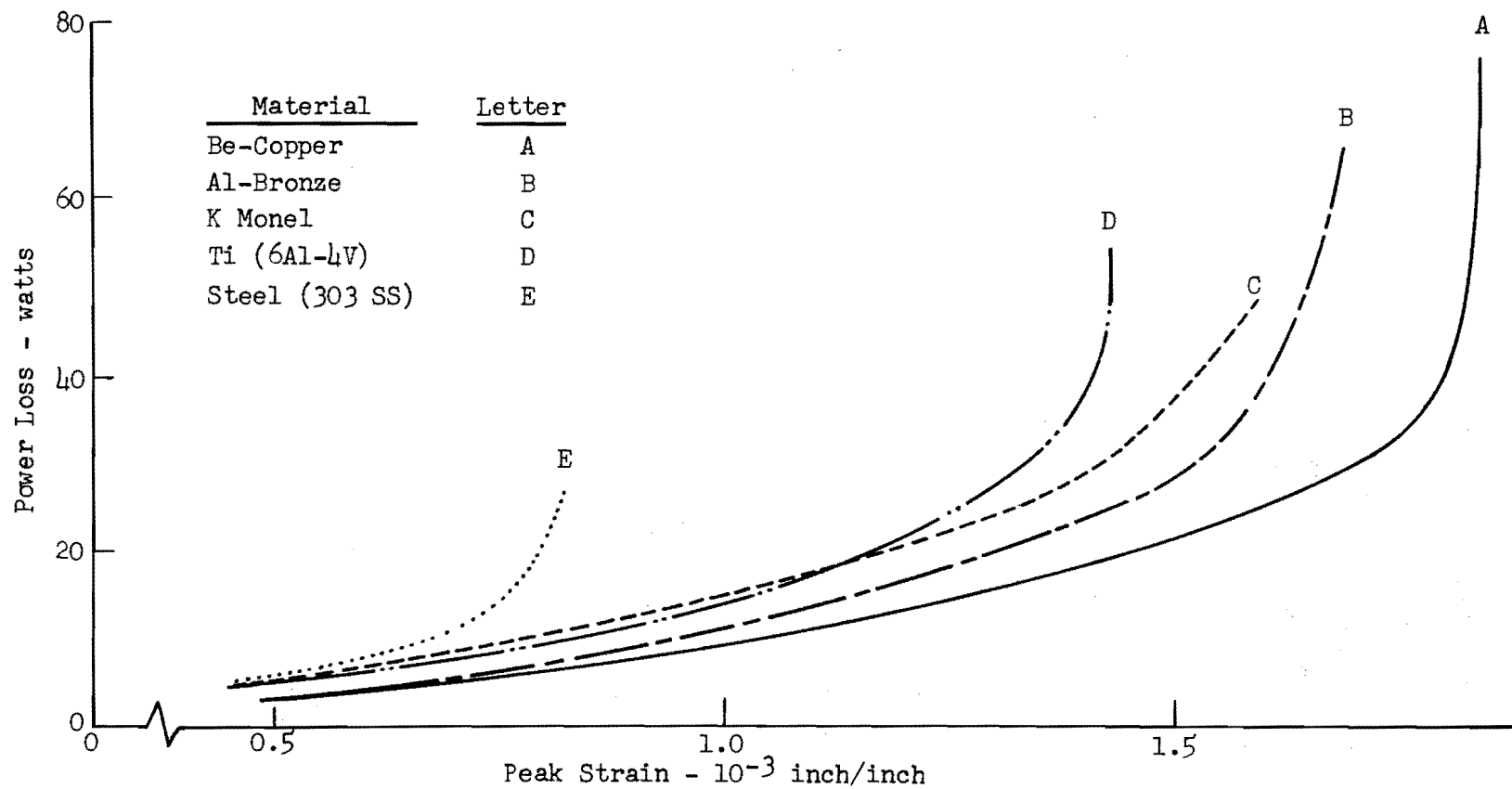
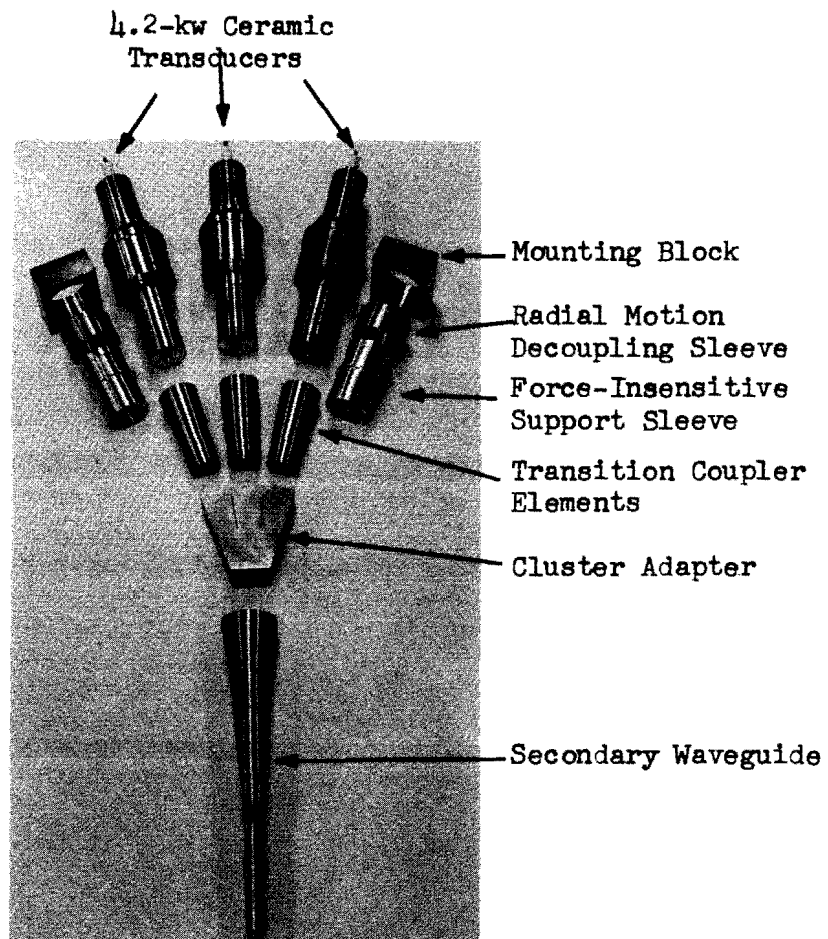
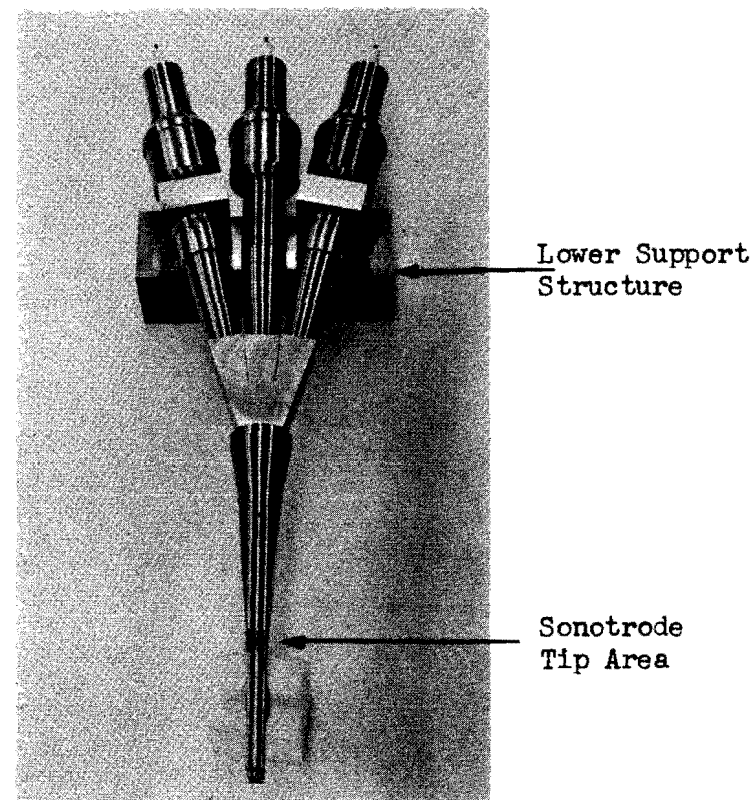


Figure 13: Power Loss vs. Strain Characteristics  
of Candidate Coupler Materials

(Frequency - 15 kilocycles per second)



A. Disassembled Components



B. Assembled But Not Brazed

Figure 14: High-Power Welding Transducer-Coupling System (Lower)

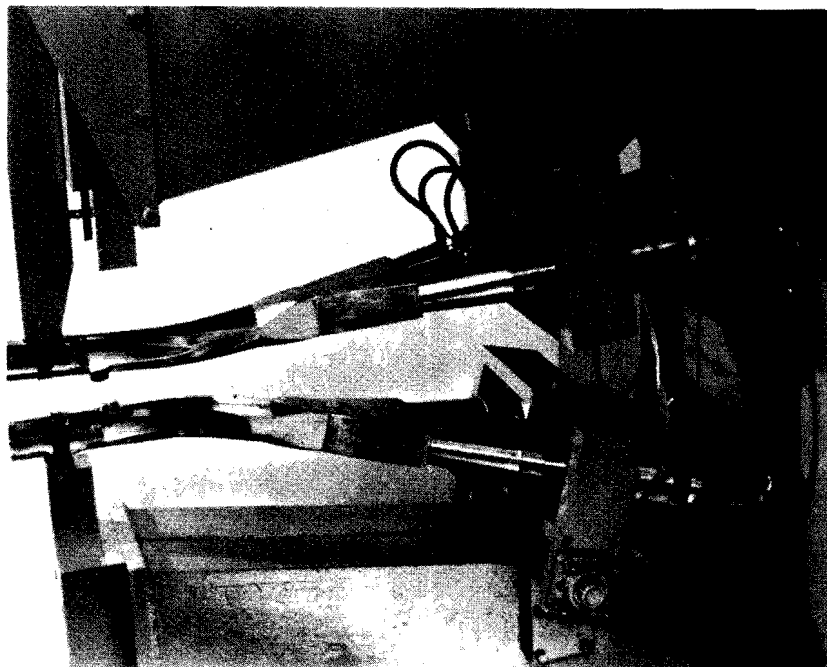


Figure 15: Lateral-Drive Transducer-Coupling Systems  
Mounted on Welding Machine

## V. WELDING TIPS

Problems associated with welding tips for the high-power welding machine were critical because of the unusual concentration of vibratory stress in these members. The stress on these tips is imposed in shear, which is an unfavorable method of loading, and it is accompanied by substantial, though transient, heating (up to about half the absolute melting temperature of the weldment material). Prior experience in welding the refractory metals and alloys, even in thin gages and at comparatively low power levels, had revealed continuing welding tip problems.

Extended consideration was given to tip materials and geometries, and to methods of attaching the tip to the primary coupler.

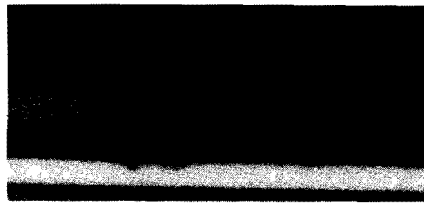
### A. Tip Materials

Welding tips for operation at high power levels and with the refractory materials must be tough and resistant to wear, without tendencies to deform, spall, erode, or crack, and the physical properties of the tip material must be retained at elevated temperature. Tips of tool steel and Inconel X-750, which are satisfactory for welding most common materials, are inadequate for the refractory metals. Phase I had included evaluation of a variety of candidate tip materials, and it appeared that the nickel-base alloy Astroloy would probably perform satisfactorily.

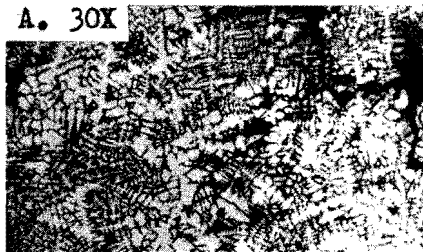
Astroloy, however, was an experimental alloy; its mechanical properties and metallurgical processing were not well established and varied from one lot to another. Investigation of welding tips fabricated from this material in cast and wrought form were continued.

In experimental welding, a number of Astroloy tips fabricated from vacuum-melted and cast material failed prematurely. Radiographic examination of a cast bar (Figure 16-A) revealed centerline shrinkage cavities, and metallographic inspection of a failed tip (Figure 16-B) indicated that the poor performance probably resulted from macrocracks in the damaged tip contact area, which followed these shrinkage cavities. Closer inspection disclosed a system of transdendritic microcracks, which could have been extensions of the macrocracks. Prematurely failed tips fabricated from the wrought material also displayed intergranular cracks.

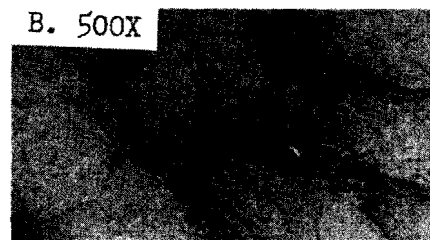
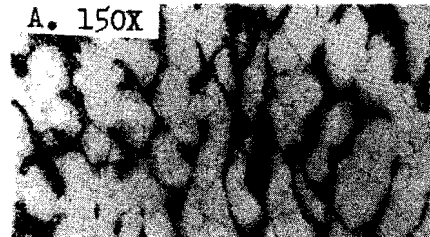
Meanwhile, other promising tip materials of similar composition were located, and these also were considered. Tables XIII and XIV summarize the chemical composition and physical properties of these materials. Udimet 700, a material being used for high-temperature jet engine applications, appeared particularly promising. This material is similar in composition and mechanical properties to Astroloy, but it was more readily available in wrought forms and its heat-treatment procedures were standardized. Udimet 500 and Nicrotung appeared to be somewhat less heat-resistant.



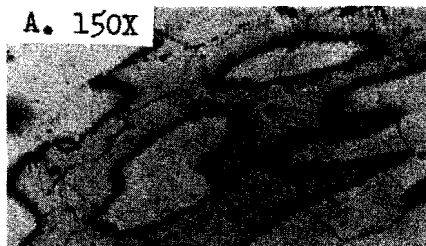
A. X-Ray of Cast-Bar Astroloy  
(note shrinkage cavities)



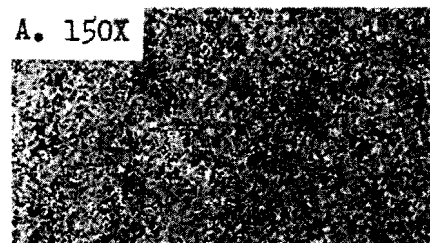
B. Photomicrograph of a Cast-Bar Astroloy Tip After Premature Failure



C. Extruded Astroloy in As-Fabricated Condition



D. Hot-Rolled Astroloy in As-Fabricated Condition



E. Rolled-Bar Udmet 700 Stress-Relieved at 1975°F for 3 Hours and Air-Cooled

Figure 16: Metallographic Structure of Candidate Tip Materials  
(Reduced to approximately one-fourth for reproduction)

Table XIII

## CANDIDATE TIP MATERIALS: SOURCE AND COMPOSITION

Material	Source	Chemical Composition											
		Ni	Co	Cr	Mo	Al	Ti	C (percent)	Fe	Mn	Si	B	Other
Astroloy	Wyman-Gordon Co.	56.8	15	15	5.25	4.40	3.5	0.06	0.02*	--	--	0.03	--
Nicrotung	Westinghouse	Bal	10	12	--	4.00	4.0	0.10*	--	--	--	0.05	8.00 W 0.02 Zr
Udimet 500	Special Metals, Inc.	Bal	13	15	3.00	2.50	2.5	0.15*	4.00*	0.75*	0.75*	0.01	--
Udimet 700	Special Metals, Inc.	Bal	17- 20	13- 17	4.50- 5.75	3.75- 4.75	3.0- 4.0	0.15*	1.00*	--	--	0.10	--

\* Maximum

Table XIV

CANDIDATE TIP MATERIALS: MECHANICAL PROPERTIES  
IN FULLY HEAT-TREATED CONDITION

Material and Heat Treatment	Elevated Temperature Characteristics			Elongation in 2 Inches (percent)	Reduction of Area (percent)	Stress Rupture
	Tempera- ture (°F)	Tensile Strength (psi)	Yield Strength (psi)			
Astroloy (A)	Room	190,000	138,000	12	13	
	1400	150,000	122,000	15	16	23 hr at 85,000 psi (1400°F)
Microtung	Room	130,000		5		
	1600	88,000		4		
	1800	66,000		6		
Udimet 500 (B)	Room	175,000	110,000	15	15	100 hr at 73,000 psi (1350°F)
	1200	175,000	110,000	17	17	100 hr at 44,000 psi (1500°F)
	1600	95,000	70,000	23	23	100 hr at 30,500 psi (1600°F)
Udimet 700 (C)	Room	204,000	140,000	17	20	
	1400	150,000	120,000	33	40	48 hr at 85,000 psi (1400°F)
	1800	52,000	44,000	28	28	48 hr at 20,000 psi (1800°F)

Heat Treatments

A. 1975°F, 4 hours, air cool (rapid)  
1550°F, 4 hours, air cool  
1400°F, 16 hours, air cool

B. Not Specified

C. 2150°F, 4 hours, air cool  
1975°F, 4 hours, air cool  
1550°F, 24 hours, air cool  
1400°F, 16 hours, air cool

Hot-rolled and extruded bars of Astroloy in the "as-fabricated" condition and hot-rolled bars of Udimet 700 in the stress-relieved condition were procured and examined metallographically. Because the extruded Astroloy exhibited a dendritic structure with evidence of coring and heavy interdendritic segregation (Figure 16-C), it was tentatively eliminated from further consideration as a tip material. The hot-rolled Astroloy (Figure 16-D) showed a somewhat more uniform grain structure, with residual dendritic segregation. Udimet 700 had a finer, more uniform grain structure (Figure 16-E).

Several tips were fabricated from the hot-rolled Astroloy and the hot-rolled, stress-relieved Udimet 700. After machining, the tips were heat-treated in accordance with the schedules in Table XV. Examination of the microstructure after completion of the heat-treat cycle showed the two alloys to be indistinguishable (Figure 17).

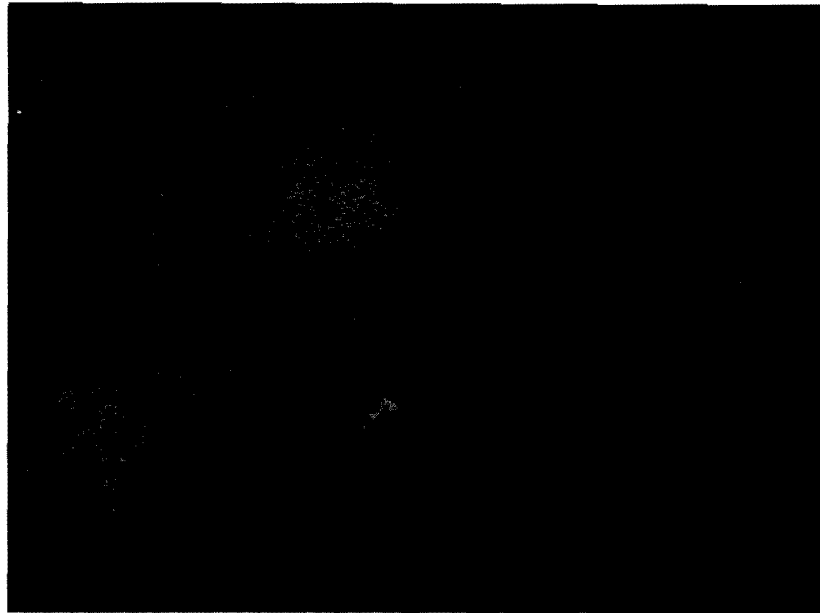
Table XV  
HEAT TREATMENT OF UDIMET 700 AND ASTROLOY TIP MATERIALS

	<u>Udimet 700 AC*</u>		<u>Astroloy AC*</u>	
Hardness Rc: As Supplied	34		32	
After Heat-Treatment	38-41		39-42	
	<u>(°F)</u>	<u>(hours)</u>	<u>(°F)</u>	<u>(hours)</u>
Solution Treatment	2150	4	2140	4
Preliminary Aging	1975	4	1975	4
Stabilization	1550	24	1550	4
Final Aging	1400	16	1400	16

\* Air-cooled

These tips, fabricated with spherical radii varying from 0.25 to 1.0 inch, were evaluated by welding thin gages of Cb(D-31), Mo-0.5Ti, and 304 stainless steel (half-hard) at different machine settings. Their performance with the two refractory alloys is summarized in Table XVI. This table also summarized work performed on a concurrent program (16) requiring the welding of 0.060-inch-diameter wires to plates.





A. Astroloy



B. Udimet 700

Figure 17: Photomicrographs of Heat-Treated Astroloy and Udimet 700

Magnification: 500X  
Etchant:  $\text{HF} + \text{HNO}_3 + \text{H}_2\text{O}$

Table XVI

## PERFORMANCE COMPARISON OF UDIMET 700 AND ASTROLOY TIPS

<u>Number</u>	<u>Material</u>	<u>Radius (inch)</u>	<u>No. of Welds</u>	<u>Results and Comments</u>
<u>A. Welding Refractory Sheets</u>				
1a	Udimet 700 wrought	1.0	80	Surface cracks noted. Tip re-ground, designated tip No. 1b.
1b	Udimet 700 wrought	1.0	180	Tip damaged. Can not be re-covered by regrinding.
2a	Astroloy wrought	0.25	181	Surface cracks noted. Tip re-ground, designated tip No. 2b.
2b	Astroloy wrought	1.0	180	Tip damaged, can not be re-covered by regrinding.
3	Astroloy wrought	0.75	83	Tip removed, no apparent damage.
<u>B. Welding 0.060-inch Diameter Wires to Plates of Refractory and Other Alloys*</u>				
4a	Udimet 700 wrought	3	250	Surface cracks noted. Tip re-ground, designated tip No. 4b.
4b	Udimet 700 wrought	3	390	Surface cracks noted. Tip re-ground, designated tip No. 4c.
4c	Udimet 700 wrought	3	372	Tip removed, no apparent damage.
5a	Astroloy wrought	3	951	Surface cracks noted. Tip re-ground, designated tip No. 5b.
5b	Astroloy wrought	Grooved	654	Tip damaged and removed.
6,7,8	Astroloy cast	3	approx. 50 ea.	Spalled beyond salvage.
9a	Udimet 700 wrought	3	338	Surface cracks noted. Tip re-ground designated Tip No. 9b.
9b	Udimet 700 wrought	3	144	Tip damaged and removed.

\* Control welds in 0.040-inch 2024-T3 aluminum alloy interspersed.

In these initial tip performance studies, the anvil surface for the acoustic terminal element was fabricated from Astroloy in the as-cast condition. Occasional surface pitting was observed, and it was necessary to reposition the anvil after every 20 to 40 welds. Surface regrinding was necessary after approximately 150 welds. Pitting was particularly noticeable when the material being welded was Mo-0.5Ti.

One anvil faced with cast Astroloy was discarded after approximately 1600 welds and another after 1200 welds. To lengthen surface life, rolled Astroloy plate was heat-treated before being used to make new anvil faces.

As a result of extended testing, it appeared that both Astroloy and Udimet 700 would perform satisfactorily as tip materials, and there was no significant difference in welding performance or service life. Udimet 700 was used for the tips installed on the 25-kilowatt machine.

#### B. Tip Geometry

Throughout the evolution of the ultrasonic welding process, a spherical-radius tip and a flat reactive anvil have almost invariably been used for spot-type welding, except when this combination has been unsuitable for workpieces of a specific geometry. In the opposition-drive system developed for the 25-kilowatt welder, the combination of one spherical tip and one flat tip was used.

Prior photoelastic investigations (21, 25) indicated that the most effective welds are obtained when the welding tip radius is between 50 and 100 times the thickness of the sheet adjacent to the tip. Table XVII shows the range of tip radii from 50t to 100t for sheet thicknesses from 0.005 to 0.100 inch. The data indicate that four tips having respective radii of 0.85, 1.75, 3.7, and 6.0 inch will probably be adequate for this sheet thickness range.

Consideration of the stresses acting on the welding tip indicate that the spherical geometry is probably not optimum for spot-type welding. With such tips there exists a complex stress field involving compressive and tensile stresses immediately ahead of and behind the tip in the direction of welding excitation; oscillating shear stresses exist in the weldment along the sides of the spot. Metallographic information obtained during the course of several years' work indicates that when cracks occur in such welds, there can be three types of defects:

1. Internal tension cracks at the weld interface in front of and behind the direction of tip excursion.
2. Cracks on the outer surface, also resulting from tension stresses in the same locale.
3. Non-bonding defects.

Table XVII

## TIP RADII ASSOCIATED WITH WELDING VARIOUS SHEET THICKNESS

Tip Radius in Multiples of Sheet Thickness (t)	Tip Radius in Inches for Sheet Thickness in Inches of											Required Tip Radius (inches)
	0.005	0.010	0.015	0.020	0.030	0.040	0.050	0.060	0.080	0.090	0.100	
50	0.25	0.50	0.75	1.0								0.85
100	0.50	1.0	--	-								
50			--	-	1.5	2.0	2.5					1.75
100			1.5	2.0	-	-	-					
50					-	-	-	3.0	4.0	4.5		3.7
100					3.0	4.0	-	-	-	-		
50							-	-	-	-	5.0	6.0
100							5.0	6.0	8.0	9.0	10.0	

Cracks resulting from shear forces to the sides of the direction of excitation have not been noted.

Furthermore, it has recently become apparent in other work that even brittle materials such as beryllium show less tendency to crack during formation of ring welds made with a torsionally vibrating annular tip. In this case, far less tensile or compressive stresses are involved than in spot welding.

It appears that the cracking tendency observed in spot welding the refractory metals and alloys might be substantially reduced by modification of the tip geometry to minimize the tensile stresses immediately ahead of and behind the tip, with correspondingly increased shear stresses along the sides. This may be accomplished by elongating the tip in the direction of vibration, i.e., by contouring the tip to compound radii rather than to a spherical radius. Appendix B provides a theoretical analysis of such geometric changes, including computations of the initial contact area for tips having a range of values for the principal radii, and comparison with initial areas of contact for the case of a spherical tip and flat anvil.

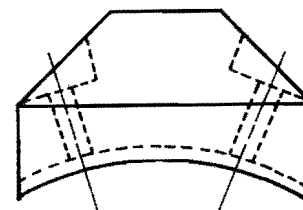
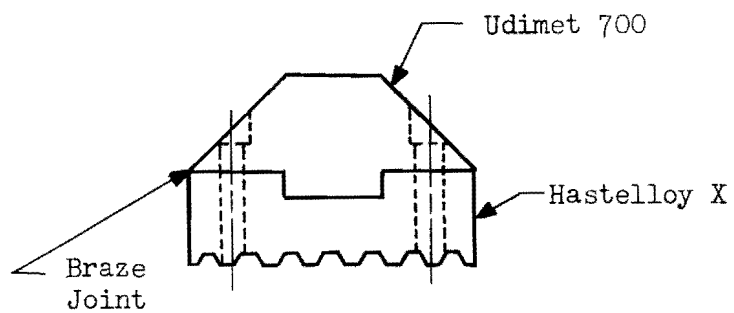
Time and funds available did not permit exploration of this approach, although it constitutes an important avenue for much-needed further improvement of the welding capability of the 25-kilowatt machine.

### C. Final Tip Design and Fabrication

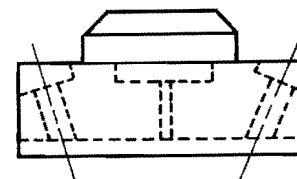
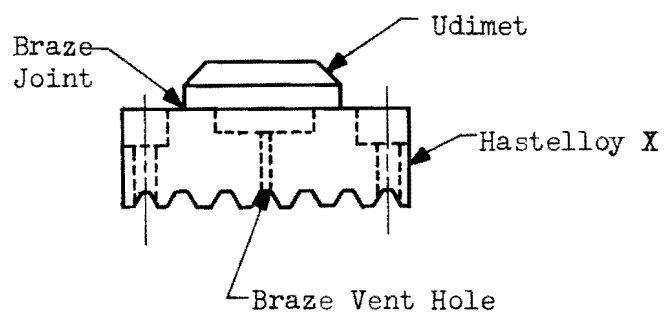
For practical reasons, the tips must be mechanically interchangeable. It was decided to provide a screw-on attachment of the tip to a base pad on the terminal coupler. In order to achieve sufficient integrity at the coupling joint to transmit the full level of vibratory stress, the mating surfaces of the tip and the base pad were serrated to maximize the area of contact. Such serrations, however, were difficult to machine in the hard Udimet 700 tip material. Consequently the tips were a composite of Udimet and Hastelloy X.

The design is shown in Figure 18. Initially the Hastelloy surface was radiused in one direction to mate with the coupler contour, as in Figure 18-A. However, in order to insure efficient power transfer via the serrated surfaces, a diamond-paste handlap fit between the tip and the coupler was necessary. This was difficult and time-consuming, and improper seating resulted in differential transverse motion leading to extensive and repeated hold-down screw failures.

The design was subsequently modified as shown in Figure 18-B, wherein the mating surfaces were flat. Lap precision fitting was still required, but this was more easily accomplished, and no hold-down screw failures occurred.



A.



B.

Figure 18: Mechanically Attached Welding Tips  
(Lower, flat tips shown.)

The designs in Figure 18 represent only the lower, flat-faced tips. The upper tips were identical, except that after fabrication their welding surfaces were ground to an appropriate radius. Figure 19 shows the tips installed on an experimental welding array.

Serious tip problems were encountered during welding evaluation of the assembled welding machine when attempts were made to weld the Mo-0.5Ti and TZM alloys and tungsten. At input power levels of about 10 kilowatts, even with the use of power-force programming, (which substantially reduced tip scuffing and pitting), tip sticking and tip damage were so severe that welds usually were broken during extraction from the machine, and tip redressing after each weld was necessary.

It is apparent that realization of the potential of the equipment necessitates further study and evaluation of tip materials, power-force-programming requirements, high-integrity mechanical attachment methods, and tip contouring.

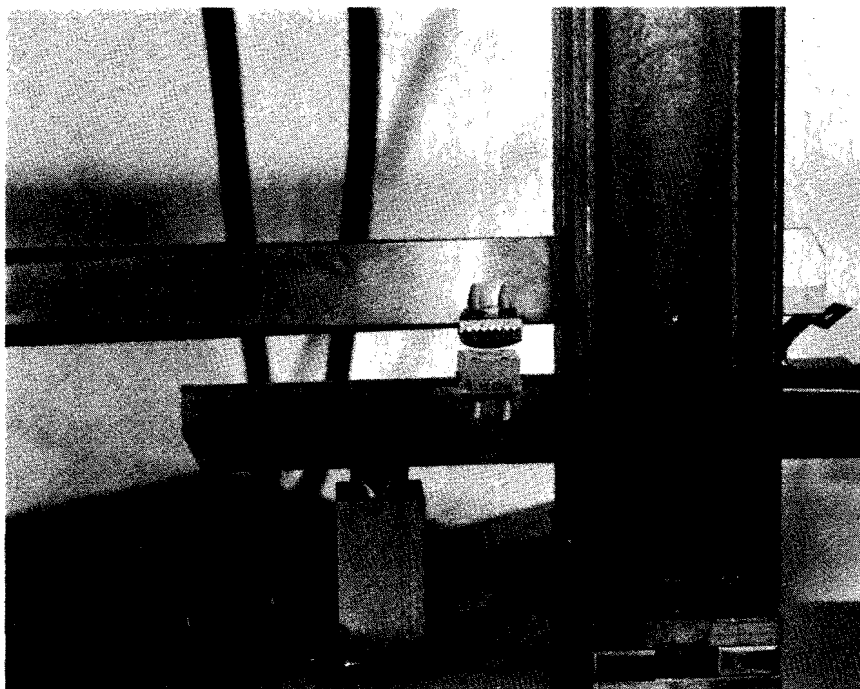


Figure 19: Close-up View of Sonotrode Tips on Double Opposed Ultrasonic Welding Test System



## VI. FORCE APPLICATION SYSTEM

The clamping force applied to the weldment materials during ultrasonic welding serves two major functions: (a) it holds the materials in intimate contact and prevents slip under the superimposed oscillating shear forces; and (b) it operates to provide an impedance match between the welding tip and the weld material. As described elsewhere (21, 26), a suitably selected clamping force, as determined from threshold curves, permits welding under minimum energy conditions.

Under Phase I, clamping force values for welding the thinner gages of the materials were approximated, as shown in Figure 20. Extrapolation of these curves produced the values shown in Table XVIII for clamping forces required to weld 0.10-inch thicknesses of the respective materials.

Table XVIII  
ESTIMATED CLAMPING FORCE VALUES FOR WELDING  
0.10-INCH MATERIALS

<u>Weldment Material</u>	<u>Clamping Force (pounds)</u>
Cb (D-31)	3760
Inconel X-750	3440
Mo-0.5Ti	3120
PH15-7Mo	3280
Rene 41	2240
Tungsten	3840

Since the maximum required clamping force appeared to be about 4000 pounds, it was reasonable to design the force system to provide a controllable force range of from 350 to 5500 pounds. For workpiece accessibility, a 4-inch travel was selected.

These travel and force range requirements indicated the need for either a high-pressure, high-volume hydraulic system, or an air-hydraulic system with air pressure operating on a relatively large piston which would act as a booster for the hydraulic pressure derived via a hydraulic piston. The latter has the advantage over the all-hydraulic system in that very high pressures can be generated with relatively few components, and rapid response

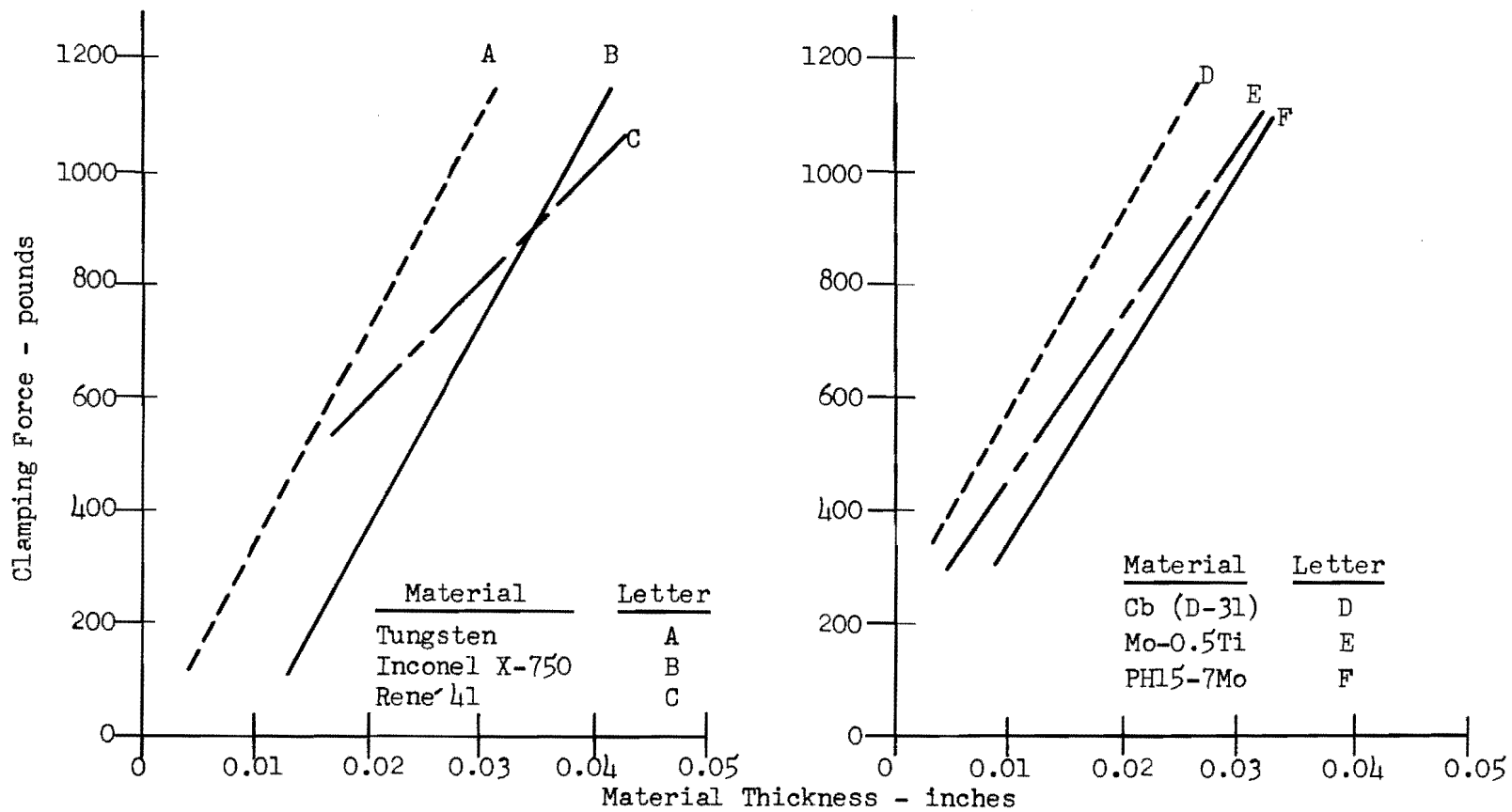


Figure 20: Clamping Force as a Function of Material Thickness

is easily achieved. Design and assembly of such a system were straightforward, and no unforeseen difficulties were encountered.

Figure 21 shows the basic air-hydraulic booster system.\* In principle, air is directed to the booster of piston area  $A_1$  at a controlled pressure  $P_1$ . The force so generated ( $F = P_1 A_1$ ) is applied to the piston in the oil chamber of area  $A_2$  to yield an oil pressure  $P_2 = F/A_2 = P_1 A_1/A_2$ . The pressure amplification ( $P_2/P_1 = A_1/A_2$ ) varies as the ratio of the piston areas. The higher pressure (oil at  $P_2$ ) is subsequently applied to the force piston to provide a clamping force ( $F_c = P_2 A_3$ ).

By proper selection of the components (Figure 22), the entire clamping force range of 350 to 5500 pounds can be achieved by control of the air pressure.

A further advantage of this system is that the total volume of oil required to displace the force piston 3 over the necessary 4 inches of travel is not supplied by the displacement of booster piston 2. The initial travel of the piston is derived from the air-oil reservoir by direct air pressure through a passageway near the bottom of the oil chamber. This passageway is sealed by force piston 2 during pressurization to effect high pressure only near the end of the travel (shown as shaded area of the oil chamber).

Force programming (described in Section VII) was obtained by controlling the oil pressure on two sides of force piston 3 with a preprogrammed servo-controlled bypass. Force controlling elements were developed under a subcontract with Minneapolis-Honeywell Company, whose engineers cooperated in testing the units.

In the welding machine, clamping force from the air-hydraulic system (Figure 23) was applied through a force rod to the overhung portion of the upper terminal coupler. The resultant bending moment on the coupler provided reaction on the welding tips.

The system as designed required only minor modifications in assembly. It was calibrated by placing a 6000-pound-capacity Dillon Universal Force Gauge between the welding tips. The clamping force as a function of applied pressure was determined, and the pressure-gage dial (Figure 22) was renumbered to indicate applied clamping force.

---

\* Purchased from Miller Flow Power, Melrose Park, Illinois.

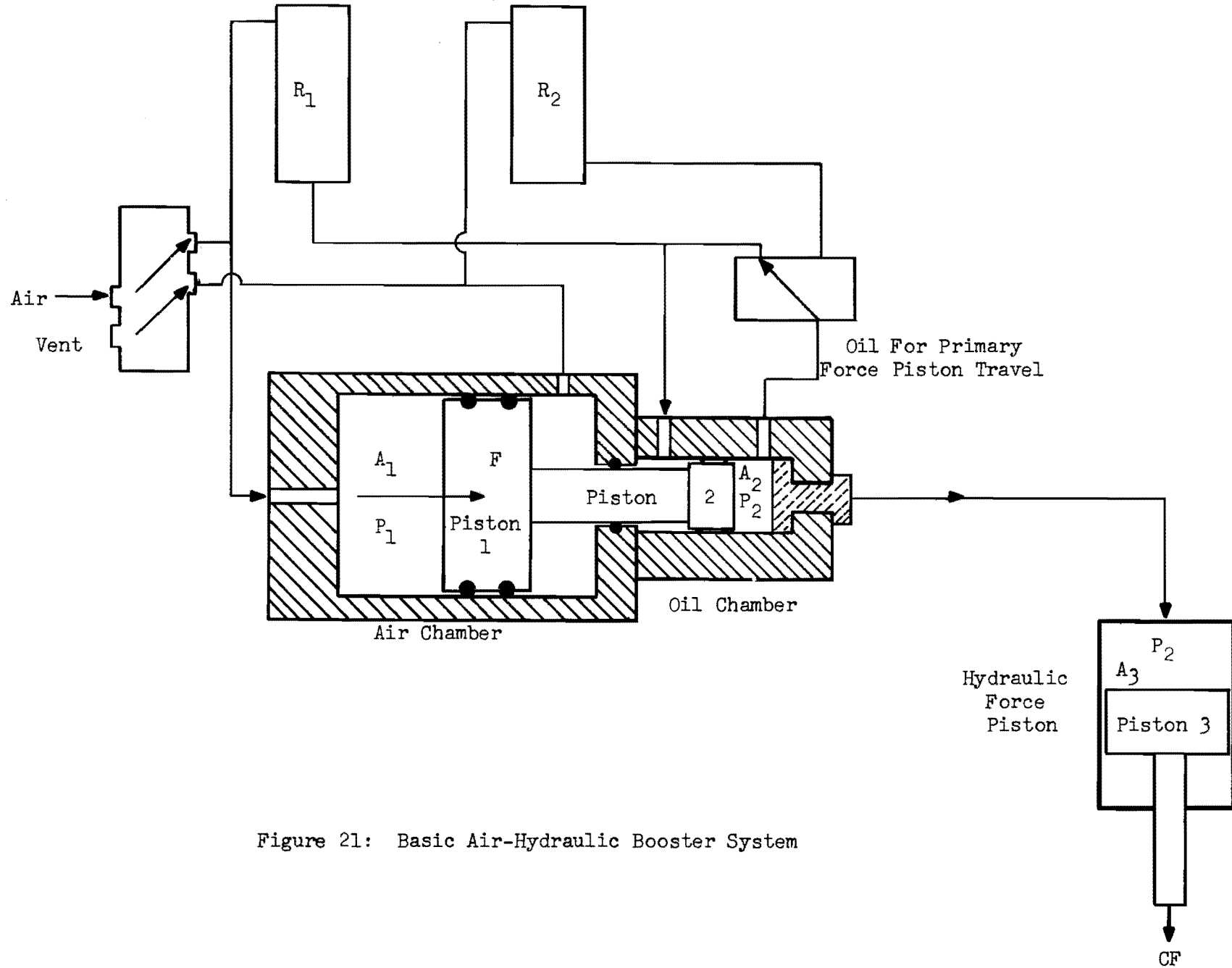


Figure 21: Basic Air-Hydraulic Booster System

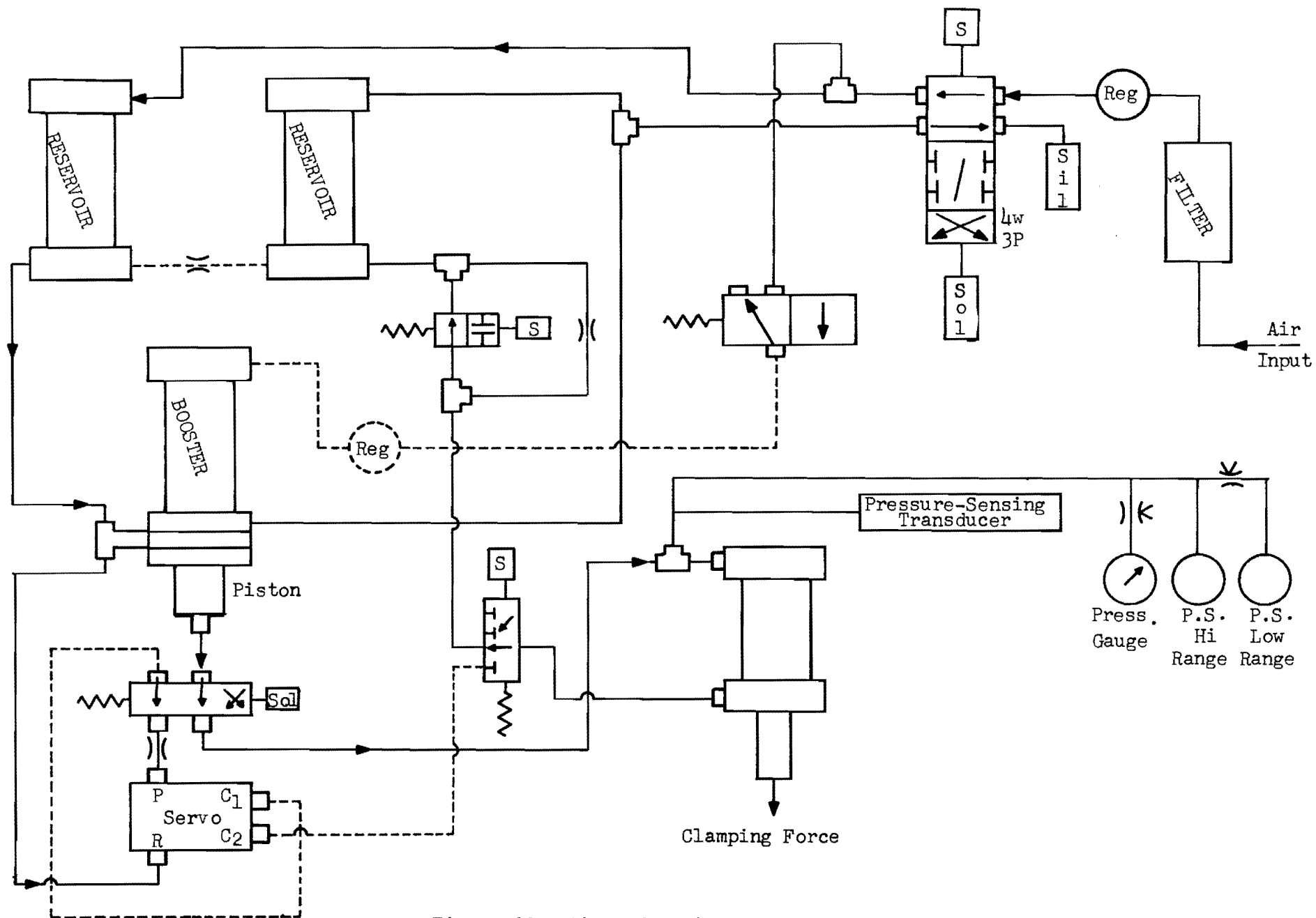


Figure 22: Air-Hydraulic Force System

(Arrows indicate direction of flow  
for pressurization)

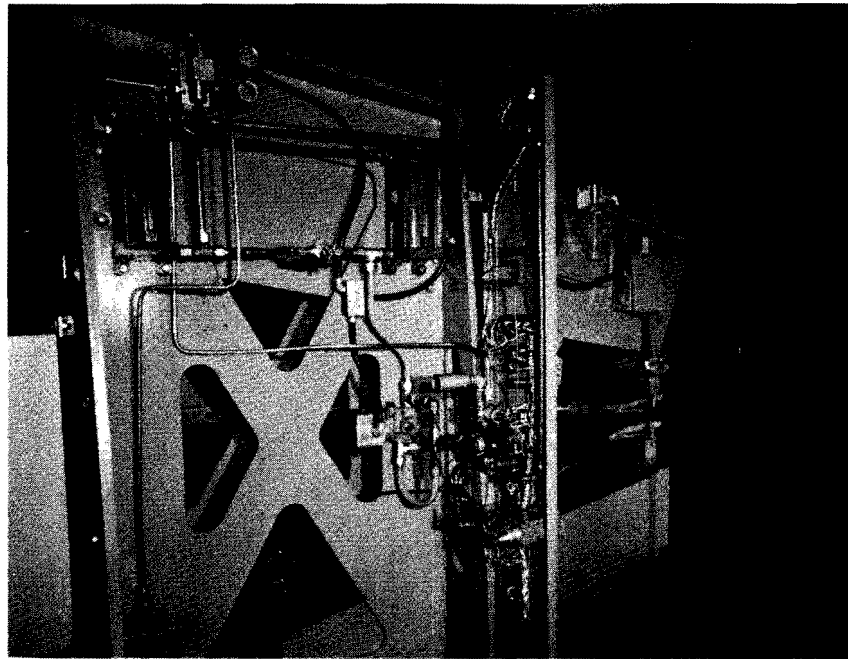
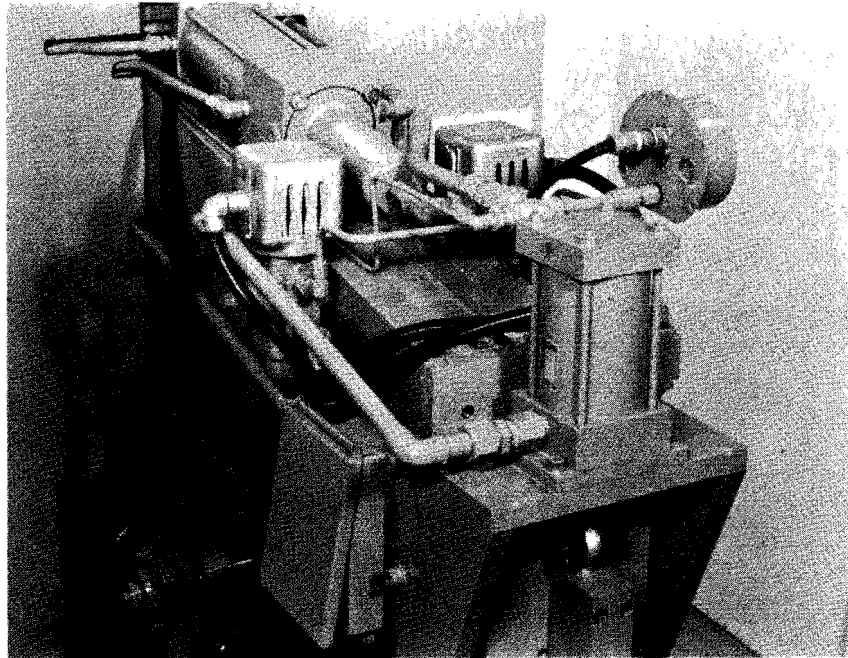


Figure 23: Air-Hydraulic Force System Installed on Welding Machine

## VII. POWER-FORCE PROGRAMMING

Other experience in welding the refractory metals and alloys (1, 2) has provided preliminary evidence that improved ultrasonic welds can be obtained in these materials with the use of power-force programming, i.e., with incremental variations in the ultrasonic power and the static clamping force during the weld cycle. Programming of clamping force partially compensates for changes in impedance during weld formation. Power programming offered a means for controlling weld quality and reducing the total input power requirements.

The major components of the power-force programming system developed hereunder were:

1. A peg-board type master control panel,
2. A time-base control circuit,
3. Function control relays for directing the signals,
4. A resistance divided network for the command signal level,
5. A magnetic contactor for primary power control,
6. A servo-valve with 400-cycle power supply, for force control,
7. A servo-amplifier,
8. A feedback pressure transducer.

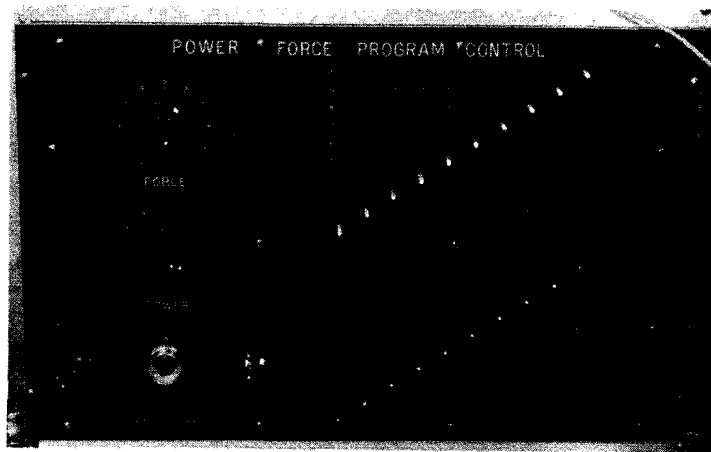
The control panel, shown in Figure 24-A, incorporated a matrix system of ten increments each, for adjusting the power and force by increments of 10 percent of the full power or force value. The addition of a percent time-base increment for any given weld interval provided a 10-square matrix control system for each of the two parameters.

The time-base control circuit (Figure 25) consisted of ten transistorized variable delay relays, with two variable series resistors for precision adjustment. This circuit had a response time of 0.0005 second. Within the range of 0 to 1.0 second, the initially measured time setting reproducibility was 0.2 percent. The reset time was 0.050 second.

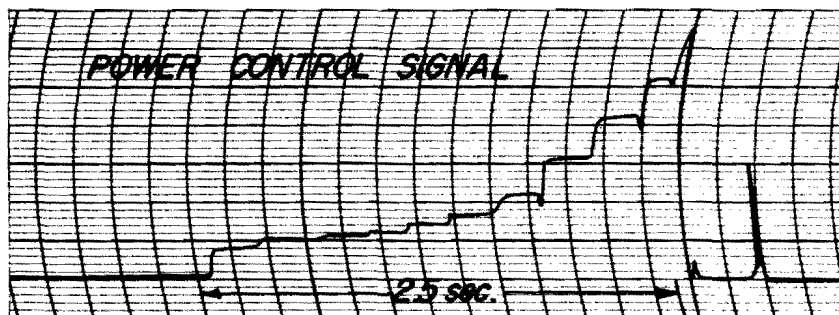
The function control relays, of the air-reed type, had a response time of 0.007 to 0.017 second. These auxiliary controls permitted control of both force and power at each time increment.

It was originally planned that variation in power would be provided by switching series resistive loads into or out of the power transmission line. However, at the high power levels involved, arcing across shorting switches presented a problem. The use of silicon-controlled rectifier (SCR) switching networks would provide rapid response, but this would also involve a major development effort for the frequency and power level involved.

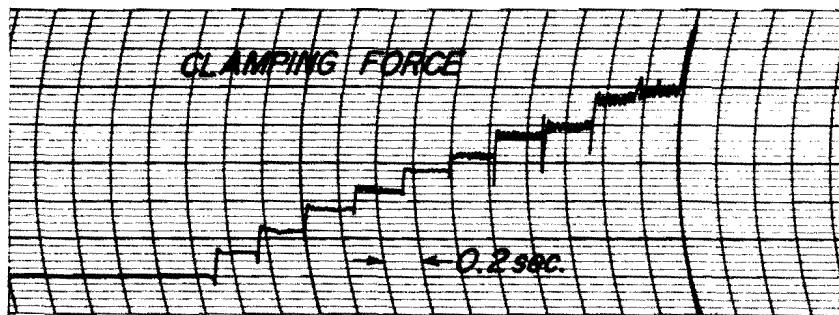
As an interim measure, power switching was accomplished by varying the alternator field current via phase control in the direct-current rectifier circuit, and using a magnetic contactor for switching power on and off.



A. Power-Force Program Control Panel Set for Progressive Increases of Each Parameter



1



2

B. Recorded Power Control Signal and Recorded Clamping Force for Settings Shown in "A" Above

Figure 24: Power-Force Programming System



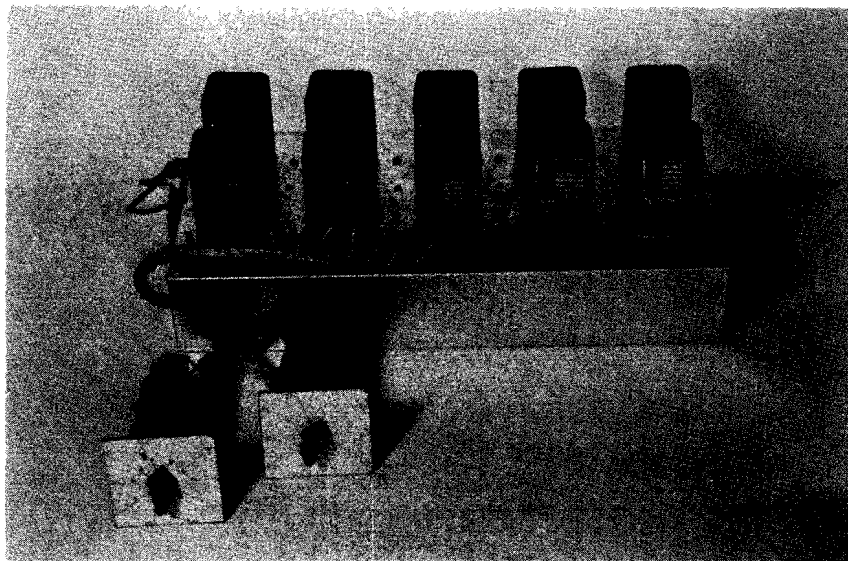


Figure 25: Timing Circuit for Power-Force Programming Unit

The level of phase shift was adjusted by the resistance divider on the power section of the peg board. The response of this arrangement to the command signals was slower than could be achieved with the SCR networks.

The components for force control are shown on the schematic diagram of the air-hydraulic force system (Figure 22). The underlapped servo-valve functioned as a variable orifice for control of oil pressure, and the pressure sensing transducer provided a feedback signal for comparison with the command signal. When the two signals balanced, via the feedback loop, the appropriate level of clamping force was established.

Figure 26 provides the general circuit arrangement for the power-force programming, showing the first three time interval sections of both power and force program boards with the associated time-delay relays (TDR) and function control air-reed relays (AR). To facilitate description, X's are shown at the intersections of the peg-board wiring grids to represent an arbitrarily set program. During operation, the total weld time interval desired is set via the two time-control step switches. Each TDR during activation is closed for just one-tenth of this preset value. A signal derived from this TDR is used to close two contacts on the associated AR. The AR contacts, upon closing, connect the peg-board programmed signal to the power and force control circuits. At the conclusion of the first tenth weld interval, TDR-1 provides a trigger signal simultaneously with its opening to initiate TDR-2 for control of the power and force over the second tenth of the weld interval. This sequence of events prevails over the full time cycle. At the end of the cycle, a signal from the last TDR resets the cycle to the beginning.

After assembly, this power-force programming system was evaluated in conjunction with a 4-kilowatt wedge-reed welding system and a 7.5-kilowatt motor alternator frequency converter. Response time (i.e., rise time and decay time for each time increment) was found to be in the vicinity of 0.010 second for both force and power. Figure 24-B shows typical oscillograph recordings obtained with the programmed pattern on the peg board shown in Figure 24-A.

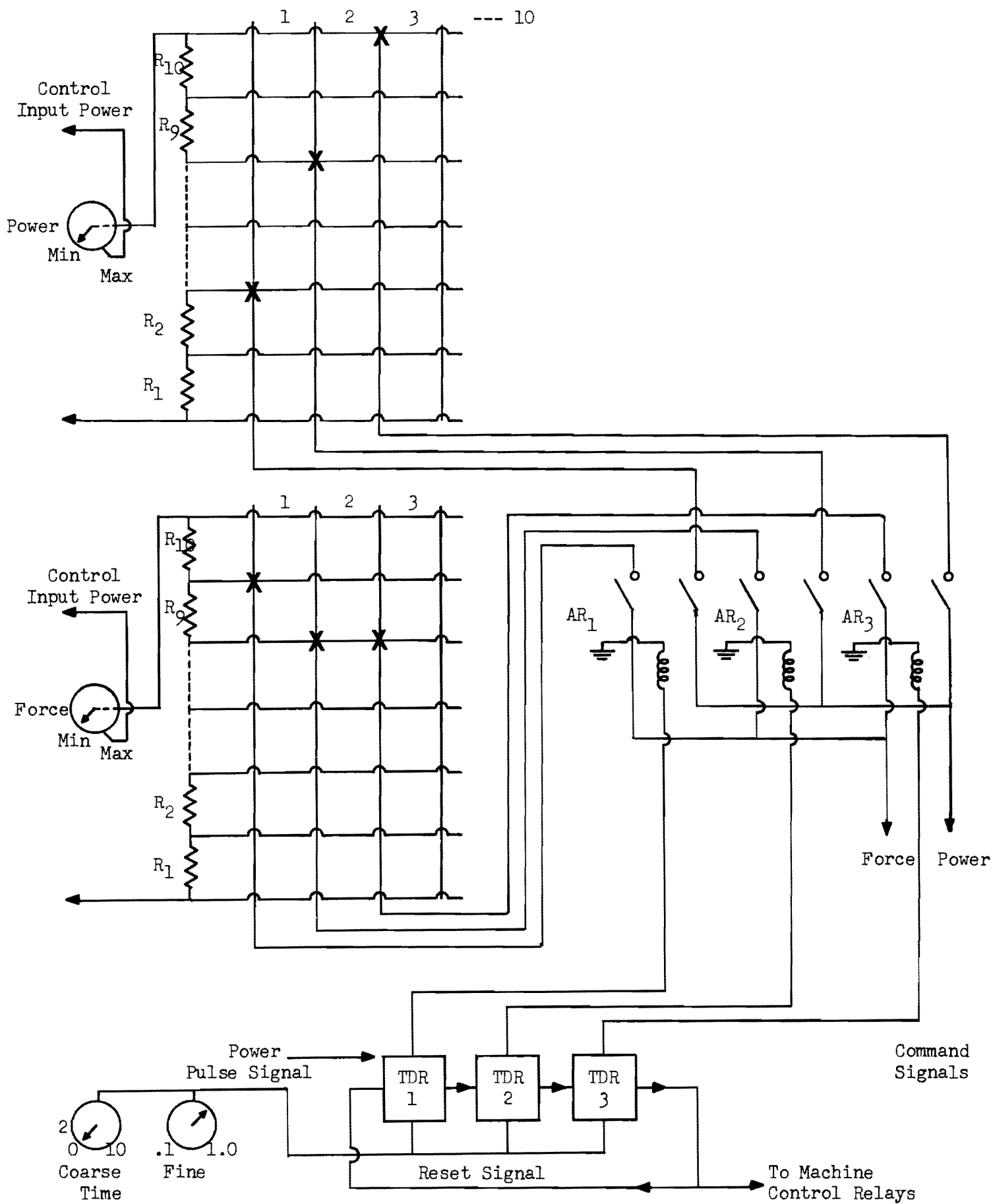


Figure 26: Power-Force Program Circuit Detail  
(Three Sections shown)

## VIII. FREQUENCY CONVERTER

Operation of the ultrasonic welding equipment required a frequency converter to supply 25 kilowatts of high-frequency electrical power to the transducers at the design frequency of the systems (nominally 15,000 cycles per second). The frequency converter should be characterized by: (a) frequency stability; (b) capability for rapid voltage and current buildup to full power; (c) efficiency in the conversion of low-frequency line power into high-frequency power; and (d) practicality of cost, assembly, and maintenance.

### A. Types of Frequency Converters

Three types of frequency converters were considered in terms of their applicability to a high-power spot-type welding machine.

#### 1. Electronic

Appropriately designed oscillators and electronic amplifiers provide satisfactory frequency stability during operation; voltage and current buildup to full power is virtually instantaneous. However, the efficiency of such devices is not high, since nearly half the input power is utilized as standby power, i.e., for filament heating, etc. Moreover, as the capacity of such units is increased, problems of complexity, physical size, and maintenance of such large "radio broadcasting station" type power sources achieve serious magnitude, raising doubt concerning their industrial practicability.

#### 2. Solid-State

Developments in our laboratory have evolved solid-state frequency converters which are promising for high-power operation. Frequency stability and power control present few problems, maintenance is low, physical size is substantially smaller than the other types at equivalent high power, and efficiency should be higher, since little power is utilized for standby operation. In spite of these advantages, the choice of this type of converter was prohibited because such equipment for the necessary high power was not available and its development required extensive effort to meet any reasonable schedule associated with this equipment.

#### 3. Motor Alternator

Standard commercial motor alternators, although available in high powers at reasonable cost, do not have the required frequency stability and control for operation with ultrasonic welding equipment; in addition, power buildup to full load can be slow. However, earlier effort in our laboratories had been devoted to solving these problems; available alternators had been modified to incorporate a "hard-drive" system to eliminate belt slip, a differential epicyclic-type transmission to eliminate frequency sag and instability, and switch gear to achieve full power with adequate promptness. The motor alternator was thus an effective potential frequency converter for the 25-kilowatt welder.

To evaluate the performance of such a system, a 7.5-kilowatt motor alternator with precision adjustable drive was placed in continuous pilot-plant use on commercial ultrasonic welding equipment for a period of several months; during this time its performance consistently equalled or exceeded the tentative specifications set. The output frequency, nominally 15,000 cycles per second, was maintained at  $\pm 8$  cycles per second over a full 24-hour period. Frequency adjustment precisely to  $\pm 3$ -5 cycles per second was straightforward. Frequency output values recorded over a period of approximately 1 hour on each of two separate days are shown in Table XIX. Adequate frequency stability was indicated.

Table XIX

FREQUENCY OUTPUT DATA FOR 7.5-KILOWATT MOTOR ALTERNATOR

(Frequency Output Setting: 14,924 cycles per second)

Test Day: 6 hours

Test Day	Measured Frequency (cycles/second)			Number of Measurements	Frequency Value	
					Average (X) (cycles/second)	Standard Deviation(s) (cycles/second)
1	14,921	14,924	14,922	13	14,922	3
	14,923	14,926	14,925			
	14,924	14,923	14,922			
	14,918	14,919	14,916			
	14,923					
2	14,924	14,924	14,927	20	14,926	2
	14,928	14,928	14,926			
	14,924	14,924	14,925			
	14,927	14,925	14,926			
	14,927	14,926	14,925			
	14,928	14,926	14,927			
	14,928	14,924				

The satisfactory performance of this 7.5-kilowatt motor alternator demonstrated the practicability of this type of frequency converter for heavy-duty spot-type welding equipment, and the data contributed to the specifications for the 25-kilowatt alternator.

## B. Design and Specifications for Motor Alternator

The 25-kilowatt frequency converter was designed to include the following components: a primary drive motor, a variable-speed differential transmission, a speed-matching transmission with oil pump and heat exchanger for the oil, the high-frequency alternator, and a supporting base for mounting the assembly. The block diagram of Figure 27 shows the electromechanical train associated with the conversion of 60-cycle per second, 440-volt power to a nominal 15,000-cycle per second, frequency-controllable 25 kilowatts of high-frequency power.

The specifications for the various components were established partly on the estimated power requirements for the machine, partly on our experience with the 7.5-kilowatt unit, and partly on calculations supplied by the Bogue Electric Manufacturing Company, Paterson, New Jersey, who designed and manufactured the alternator. Other suppliers furnished the various other components in accordance with our specifications.

The specifications were as follows:

### 1. High-Frequency Alternator

(Obtained from Bogue Electric Manufacturing Company)

Power output, continuous duty: 25 kilowatts nominal  
30 kilowatts maximum

Shaft speed: 5560 rpm

Center output frequency: 15,000 cps

Single-phase output at two levels: 100/125 volts rms or  
200/250 volts rms

Enclosure to provide for self-cooling

### 2. Primary Drive Motor

(Obtained from Allis-Chalmers, Milwaukee, Wisconsin)

Synduction type: 100 horsepower

Shaft speed: 1800 rpm

Full load current: 200 amperes wired for 440 volts

Locked rotor current: 1750 amperes

Overall weight: 1280 pounds

### 3. Variable-Speed Differential Transmission

(Obtained from Stratos Division, Fairchild Stratos Corporation,  
West Babylon, L. I., New York)

H-5 modified P.I.V. (positive, infinitely variable) unit, with control levers properly connected to appropriate differential shafting

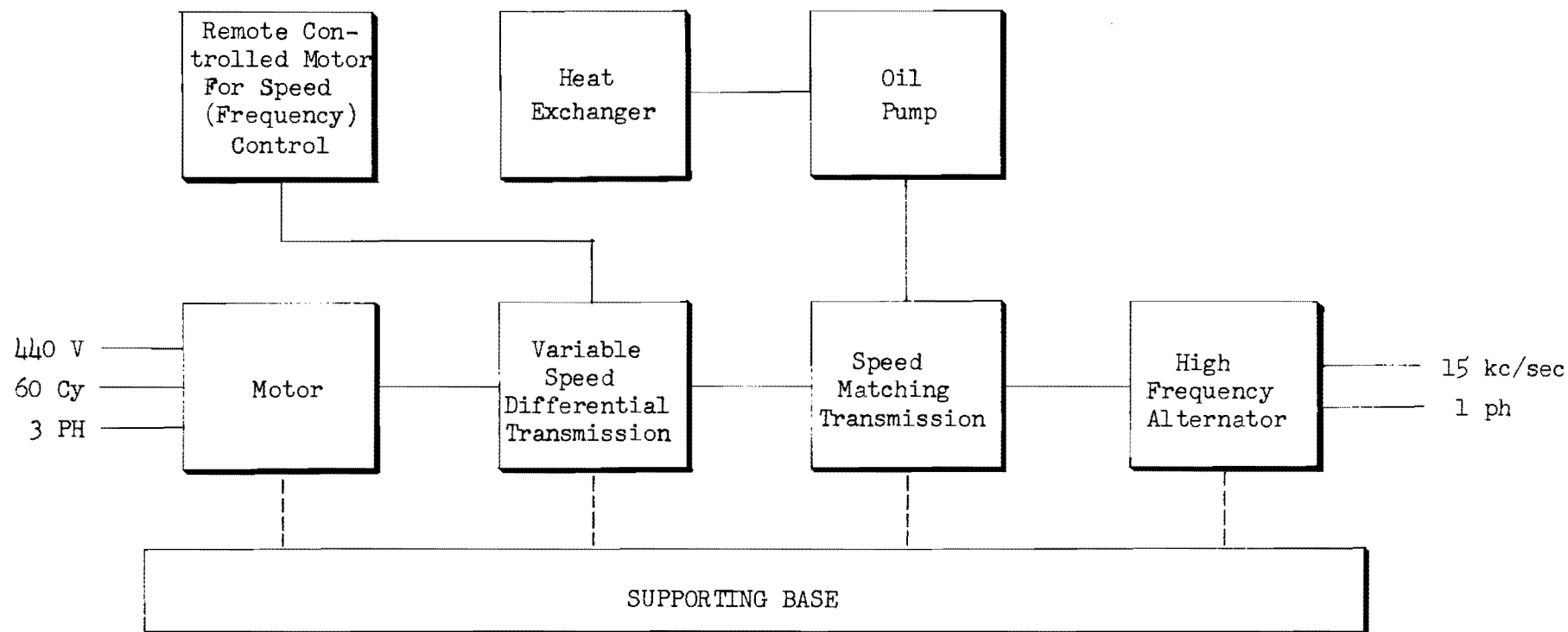


Figure 27: Components of 25-Kilowatt, 15-Kilocycle Frequency Converter

Set of coupling media to connect H-5 P.I.V. to differential transmission

Output speed: 2780 rpm  $\pm$  3.5%  
Output load: Running 65 horsepower  
Output inertia ( $wR^2$ ): 161 lb-ft<sup>2</sup>  
Weight: 1900 pounds

#### 4. Speed-Matching Transmission

(Obtained from Foote Brothers Gear and Machine Corporation, Chicago, Illinois)

Transmission ratio (input to output): 1:2.0  
Total inertia: 161 lb-ft<sup>2</sup>

The supporting structure was fabricated by the Wiedemann Division, Warner and Swasey Company, King of Prussia, Pennsylvania, and the complete unit was assembled by Fairchild Stratos Corporation.

The equipment as originally obtained utilized a hand crank and clamp lock on the crankshaft for altering and setting the alternator drive speed (and hence frequency). To obtain increased precision, the hand crank was replaced by a low-speed, geared, reversible motor\* (spring-loaded and self-locking when not electrically powered). The control for this motor was located on the front panel of the welding machine for easy access.

#### C. Switching

The exceedingly short time intervals (usually less than 1 second) characteristic of ultrasonic spot-type welding, require that full power be available promptly when the weld is to be made. To achieve this abrupt full power, it is necessary to drive the alternator output into a dummy load and provide for switching it into the welding circuit when required, and also to switch dummy resistors into and out of the power transmission line to provide the step power variations for power programming.

In the electrical industry, power at high levels is routinely switched by means of magnetic contactors which are remote-controlled, and this system was investigated initially. Preliminary measurements of the switching performance of parallel banks of magnetic contactors equipped with arc-suppression coils indicated a response satisfactory for our requirements. However, the service life of such units was doubtful.

The performance of high-current solid-state switches was therefore investigated. At full power, the triggering of the solid-state switches was

---

\* Master Gear Motor type 383L21-CP with Master Unibrake, manufactured by Reliance Electric and Engineering Co., Columbus, Indiana.



found to be unreliable, due to their sensitivity to the voltage-current phase relationship existing in the transmission line at the instant switching was initiated; however, rapid and reliable switching of partial loads into or out of a loaded transmission line was achieved. It appeared that the problem might be resolved by incorporating magnetic contactors into the machine as primary switching elements to achieve the necessary "on-off" response and by utilizing solid-state switches to achieve the power-step response required in power programming. In further tests, however, the solid-state switch proved insufficiently perfected to assure satisfactory step control.

Differential power control, as well as the "on-off" function, was ultimately furnished by a large contactor-type switch on the main transmission line, via a field-current control system whereby step-type command signals altered the phase in the phase-controlled SCR's supplying of d-c current to the alternator field.

#### D. Evaluation

After assembly of the complete frequency converter (see Figure 2), including the switch gear, comprehensive acceptance tests were carried out at the Dayton T. Brown Testing Laboratories, Bohemia, Long Island, New York. Figure 28 shows schematically the instrumentation assembly used in these tests.

The frequency converter output was driven into a dummy load consisting of six 230-volt, 5000-watt Calrod heaters attached to the output terminals of the alternator in a parallel combination. Output power was computed on the basis of the resistance of the load (which was calculated and measured at 1.7 ohms) and measurements of the voltage across the heaters.

Line current and voltage were monitored with the instrumentation indicated in Figure 28. The output of a current transformer, consisting of four turns of instrument lead wire coiled around one leg of the power lines into the frequency converter, was viewed on an oscilloscope, and the relative values between peak (or starting) current and running current were determined.

The frequency range of the assembly was determined by establishing a Lissajous pattern between a precalibrated reference oscillator and the output of the alternator.

Data from these tests (Tables XX, XXI, and XXII) indicate that the assembly met or exceeded the specifications established, with the following major variations:

1. The total inertia of the alternator speed-matching transmission exceeded by approximately 4 lb-ft<sup>2</sup> the 161 lb-ft<sup>2</sup> value originally requested.

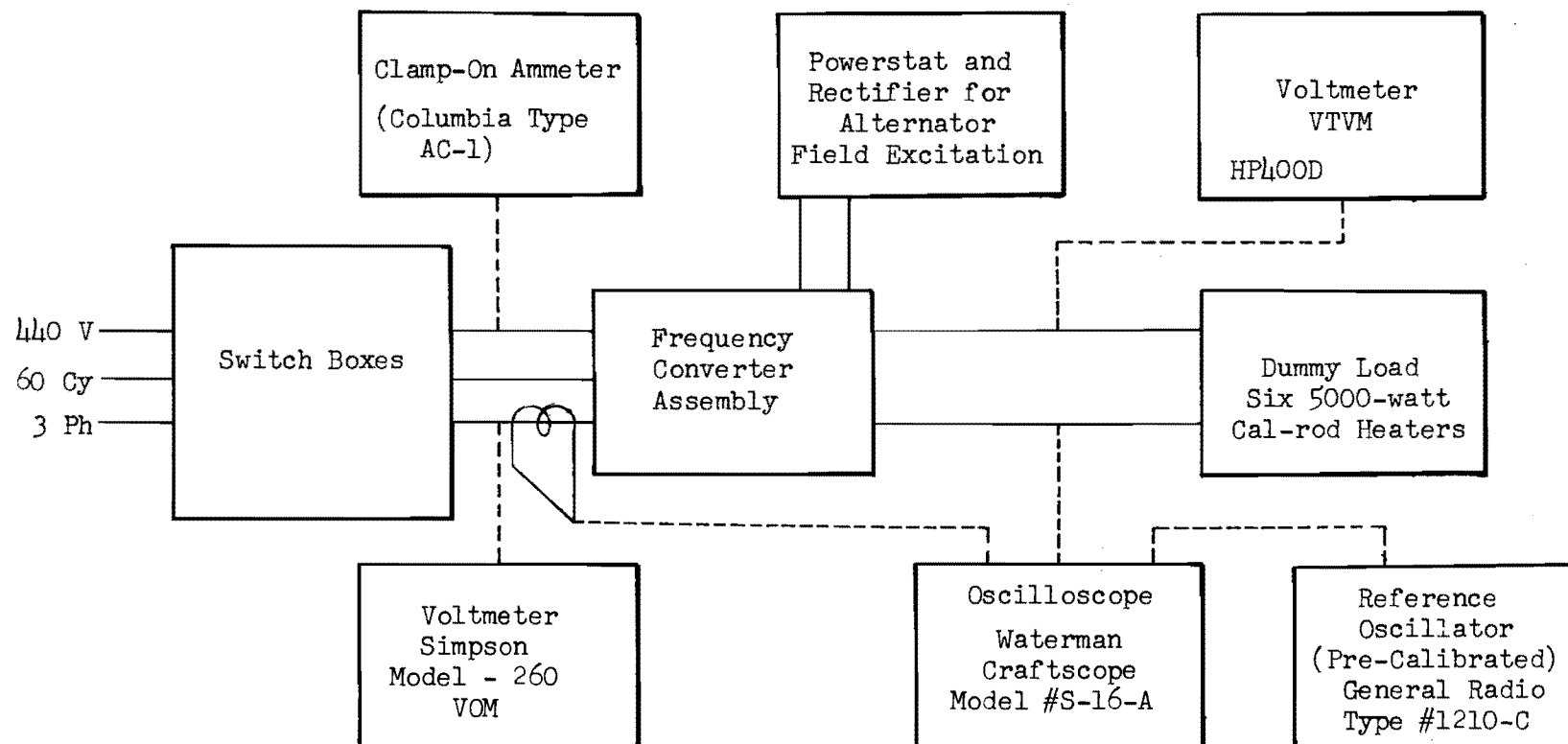


Figure 28: Equipment Array for Frequency Converter Acceptance Tests

2. The speed-matching transmission ratio was originally requested to be 1:2.0 and was delivered at 1:2.0217.
3. The no-load voltage of the alternator was 265 volts instead of the requested 250 volts.

These deviations could be accommodated, and the unit was considered acceptable for the intended purpose.

Table XX

25-kw ALTERNATOR HIGH-FREQUENCY TESTS

	Requirements	Test	Differences
Power (kilowatts)	30 (max.)	35.3	+ 5.3
Alternator Shaft Speed as governed by variable-speed and speed-matching transmissions.			
Variable-Speed Transmission Shaft Speed (rpm)	2780 $\pm$ 3-1/2%		
Speed-Matching Transmission Ratio	1:2	1:2.0217	+ 1.085%
Shaft Speed (rpm)	5750 to 5370	5820 to 5420	+ 70 to 50
Alternator Frequency (cycles per second)	15520 to 14480	15700 to 14625	+ 180 to 145
Alternator Inertia (lb-ft <sup>2</sup> )	161	165 <sup>x</sup>	+ 4

<sup>x</sup> Calculated

Table XXI

## 25-KW ALTERNATOR FREQUENCY CONVERTER TESTS

Field Set Position	Current-amperes* Input Power Line			Voltage Across Dummy Load	Approximate Power Into Load
	Line 1	Line 2	Line 3	Volts	Watts
0-(no field)	110	117	117	0	0
1	104	130	130	100	5650
2	120	140	130	142	13000
3	120	130	130	173	17000
4	140	155	150	210	25000
5	140	155	155	225	28700
6	-	-	-	250	35300

\* Measurements were made with a clamp-on ammeter which is sensitive to orientation of the plane of the clamp jaws to the axis of the conductor.

Input line voltage - 465 V across phases.

Table XXII

## 30-KW ALTERNATOR TEST DATA

Motor 100 hp

3 Ø - 440 v - 60 cycle

## Alternator and Speed-Matching Transmission (only)

Friction and Windage losses . . . . .	4.4 kw
Iron losses . . . . .	7.1 kw
Power input at full power . . . . .	46.0 kw
Output power . . . . .	30.0 kw
Efficiency . . . . .	65 %
No load torque at input to transmission . . . . .	11 ft-lb

## Differential Variable-Speed Transmission

Efficiency . . . . .	80 %
No load - no field input power . . . . .	5.5 kw
Full load input . . . . .	58.0 kw
No load - max. field input . . . . .	14.5 kw

## Complete Assembly

Overall efficiency . . . . .	51.8 %
A. No field - torque . . . . .	21.6 ft-lb
B. With field - torque . . . . .	57.0 ft-lb
C. 30-kw load - torque . . . . .	227.0 ft-lb

A = 120 amps      B = 125 amps      C = 160 amps at . . . . 465 volts

## Motor

No load - no field . . . . .	7.5 hp
No load - with field . . . . .	19.5 hp
Full load . . . . .	77.6 hp

## IX. ASSEMBLY AND CHECKOUT OF EQUIPMENT

The previously described components for the 25-kilowatt welder were assembled and operationally checked prior to assembly into the complete equipment array. Meanwhile the machine framework was fabricated, and the air-hydraulic force system was installed thereon. Instrumentation and controls were added and checked for proper functioning, using an experimental low-power welding assembly temporarily mounted on the frame. Finally the transducer-coupling systems were installed, and operation of the complete assembly was carried out.

### A. Machine Structure

The framework for the welding machine was designed to provide structural rigidity with applied clamping force as high as 5500 pounds, a throat depth of 36 inches, and a total welding head movement of 4 inches. Figure 29 shows the conceptual layout of the machine, with significant dimensions indicated.

The basic structure was the welded, rigid steel framework shown in Figure 30. The frame was mounted on lockable casters, with the base dimensioned to prevent upset under reasonable casting forces. Stress analysis indicated that the structure had adequate torsional rigidity, and the expected elastic deflection at the ends of the support arms under a clamping force of 5500 pounds was a maximum of 0.035 inch. This value was considered satisfactory, since the upper transducer-coupling system was supported by movable extension arms extended from a double eccentric cam to provide parallel and vertical alignment of the welding tips.

### B. Instrumentation and Controls

The minimum controls required for ultrasonic welding equipment consist of those for clamping force adjustment, high-frequency electrical power delivered to the transducer, weld pulse time, and output frequency of the frequency converter. Because the 25-kilowatt machine represents a significant advance over previous models in power capacity\* and is intended for welding a broad range of metallic materials and gages, additional instrumentation was incorporated to facilitate establishing welding machine settings and to provide for certain fundamental measurements.

The basic function controls for the machine are located on the left front panel of the machine, as shown in Figure 31-A. This panel also includes the clamping force adjustment and clamping force indicating gage, so located because of proximity to the air-hydraulic force system components. Other controls and read-out instruments are located on the right front panel (see Figure 1) and to the right of the machine (Figure 31-B.)

---

\* Power is up by a factor of five to six over largest previous production model.

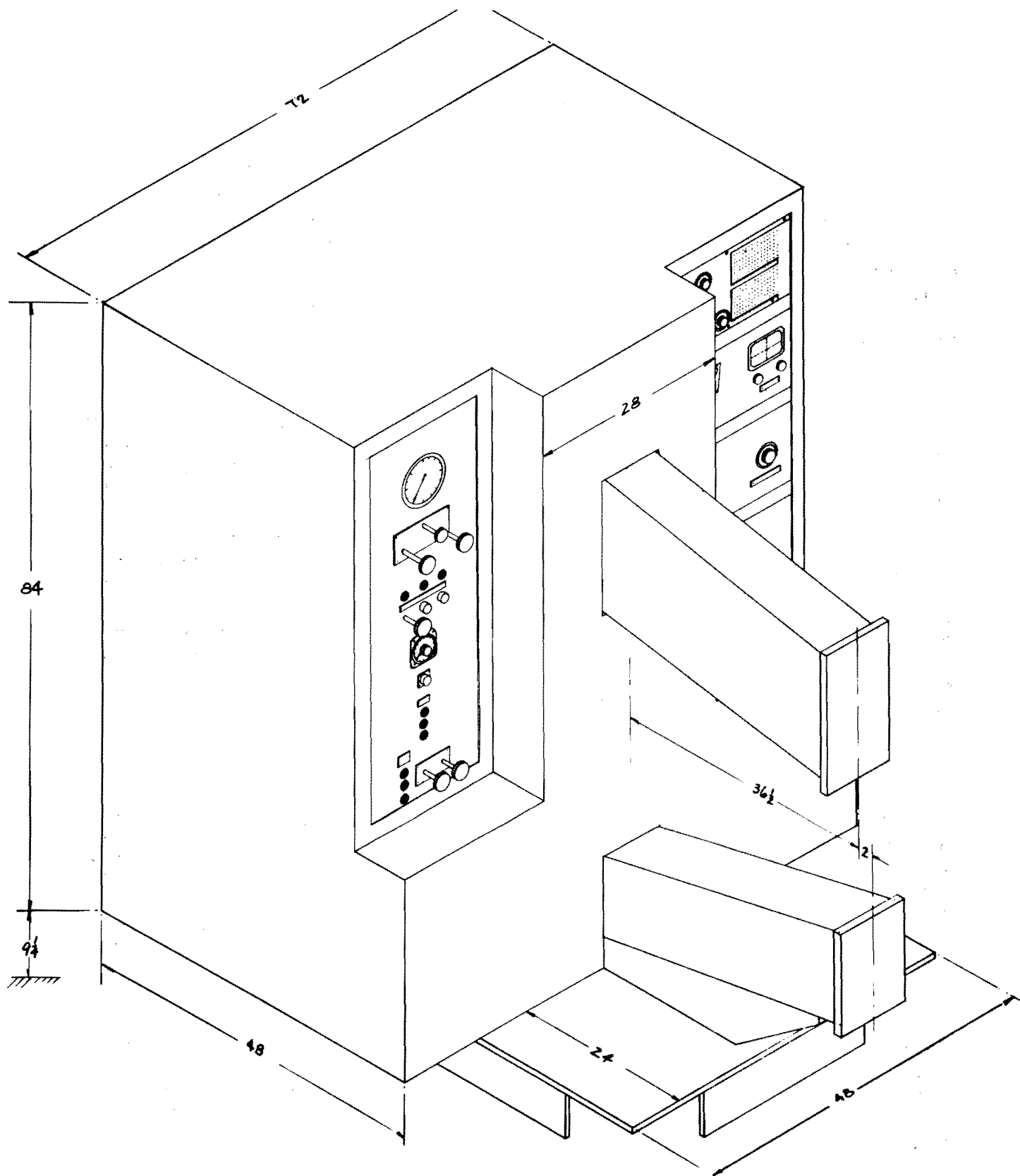


Figure 29: Instrument and Cabinet Arrangement for 25-Kilowatt Welding Unit

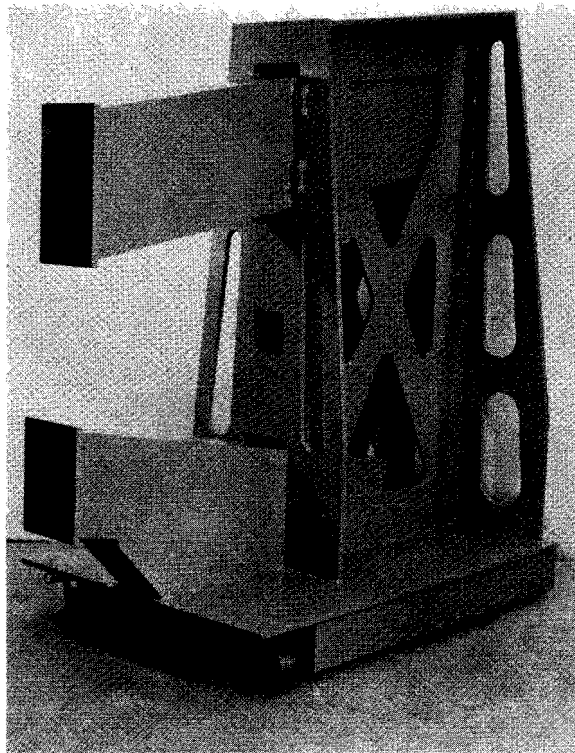
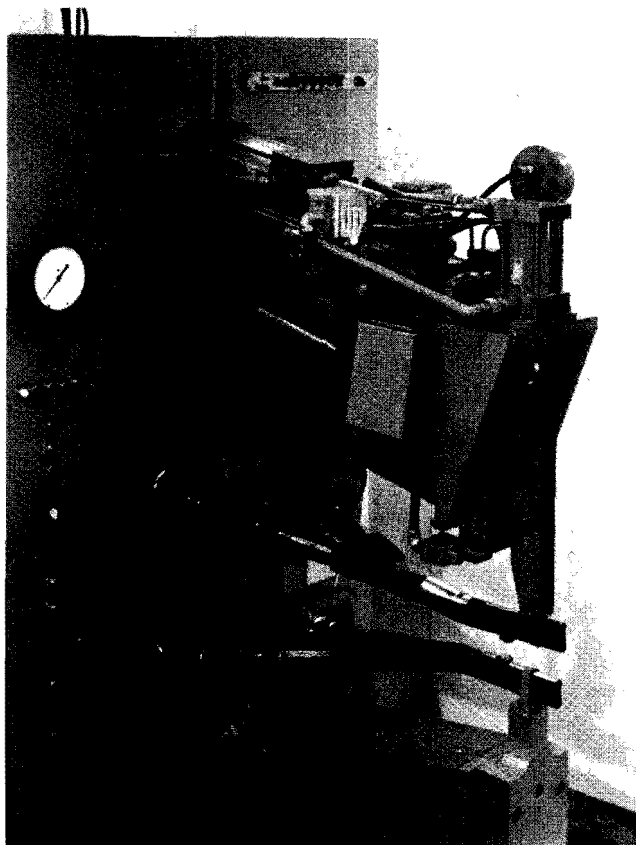
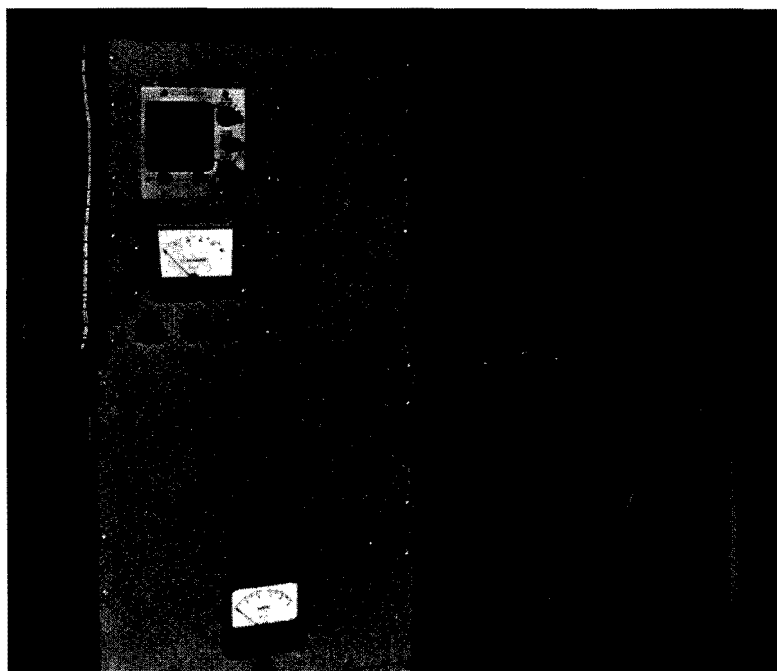


Figure 30: Framework for 25-Kilowatt  
Spot-Type Welding Machine





A. Left Front Panel



B. Right Side Controls

Figure 31: Instrument and Control Panels

The only instrumentation or controls not located on the welding unit itself are the disconnect and reduced-voltage electrical hardware for starting the primary motor of the frequency converter. This equipment is located on the converter itself, which is remote (about 75 feet away) from the welding unit.

The location and specific function of the various controls are described below.

LEFT FRONT PANEL (See Figure 31-A)

Pressure Gage - Indicates level of clamping force, used only during setup. It is subsequently closed off from hydraulic pressure by a gage cut-off valve located immediately below.

Machine Sequence Indicating Lights (Described in left to right order)

Standby: When on, this light indicates that electrical power has been applied to all control and instrument circuits, that force control air pressure is on, and that the welding head is in the fully retracted position.

Lower Head: Indicates that the sequence-initiating foot switch has been depressed and that latch relays controlling solenoid valves for clamping force have been activated.

Clamping Force: Indicates that the preset level of clamping force has been achieved.

Ultrasonics On: Indicates that the weld time interval has been initiated and that high-frequency power is being delivered to the transducers.

Reset: Indicates that timing circuit is being reset for subsequent welding. This light will remain on until the welding head has been completely retracted.

Master ON-OFF (Immediately below Sequence Indicating Lights)

Two push-button switches, with an ON indicating light, activate and deactivate all electrical circuits of the machine.

Automatic-Manual-Adjust - This three-position switch permits selection of the mode of operation (automatic or manual - described later), and in the Adjust position provides for manual cycling of the machine without ultrasonic power being applied.

Clamping Force Air Pressure - Used to adjust to desired maximum clamping force by controlling air pressure acting on air-hydraulic booster.

Cut-Off Valve (Located to left of Air Pressure Regulator) - Cuts off hydraulic pressure from the low-range pressure switch.

Field ON-OFF - Because of the high initial inrush current to the synchronous motor of the frequency converter during start-up, the motor is started without current through the alternating field windings, thus assuring minimum start-up load. This field current control circuit is activated by depressing the FIELD-ON push-button switch.

Pressure Switches, LO-HI Switch - The low pressure switch is used to set contact closure for clamping forces within the range of about 350 to 2000 pounds. For operation above this range, the Selector Switch is set for HI, and the low pressure switch cut-off is closed.

Power Indicating Light - This light at the bottom of the panel merely indicates that electrical power is available in the machine.

#### RIGHT FRONT PANEL (See Figure 1)

Frequency Counter (at extreme top of panel) - Provides rapid indication of operating frequency of frequency converter. Electrical signals for this counter are obtained by sampling the no-load voltage on the high-frequency transmission line feeding into the large magnetic contactor used for primary ultrasonic power ON-OFF control.

Frequency Control (below top indicating meter on panel) - This two-position switch directs 60-cps power to the speed control motor on the frequency converter, thus effecting adjustment of frequency.

Acoustic Watt Meter - In conjunction with standing-wave-ratio measurements, this meter indicates acoustic power delivery to the weldment. The controls below provide for ON-OFF power, RANGE, and ADJUSTMENT.

#### RIGHT SIDE OF MACHINE (See Figure 31-B)

Oscilloscope (top left) - Used to determine standing-wave ratio in ultrasonic coupling system. Standard oscilloscope controls are included.

Electrical Watt Meter (below oscilloscope) - This instrument samples a fraction of the voltage and current of the high-frequency transmission line to indicate the electrical power delivered to the high-voltage matching transformer used to drive the transducers.

Servo-Valve Amplifier and Null Control (to right of oscilloscope and watt meter) - This vertical row of controls governs the force control servo-valve used for force programming.

D-C Power Supplies (below electrical watt meter) - The lower three panels house d-c power supplies for all instruments and for the alternator field. The meter in the center indicates the value of field current utilized and provides an independent method for high-frequency power adjustment.

Power-Force-Program Panel - Operation of this system has been described previously. On the lower left of this panel is the weld timer which permits setting of the weld power pulse at any value from 0.01 to 10 seconds. A COARSE ten-position switch provides step time increments of 1, 2, . . . 9 seconds; a FINE ten-position switch provides step time increments of 0.10, 0.20, . . . 1.0 second. Intermediate weld time can be achieved by programming the power and force to terminate at less than the full time interval set on the position switch.

Function control for the welding machine is effected by electrical relays and solenoid control valves, all of which are housed in industrial type NEMA cabinets. Switches and solenoids are heavy-duty industrial quality. Appropriate electrical interlocks are provided by switches or mechanically activated microswitches to preclude accidental powering of the ultrasonic system without clamping force application.

### C. Equipment Operation

The welding equipment may be operated either manually or automatically. If the operation is automatic, the following is the sequence of events:

1. Turn on power to frequency converter.
2. Turn on Master Switch on welding machine.
3. Turn Manual-Automatic-Adjust switch (on left front panel) to Automatic.
4. Set clamping force (left front panel) to the maximum desired value.
5. Set ultrasonic power (peg board control panel) to the maximum desired value.
6. Set timer (on peg board control panel) to desired weld time.
7. Establish desired program patterns for power and force.
8. Insert materials to be welded on lower welding tip.
9. Depress foot switch. This automatically triggers the following sequence of events:
  - a. The system is activated by closing of a latching relay.
  - b. The upper sonotrode lowers to contact weldment material supported on lower sonotrode and to apply clamping force.

- c. Clamping force builds up to the preset level, and the welding power pulse is initiated.
  - d. The programmed power-force-time cycle is completed.
  - e. Signal voltage is directed to the unlatch coil of the latching relay, thus deactivating the sequence-controlling circuits.
  - f. The system deactivates, ultrasonic power cuts off, and the upper sonotrode retracts.
10. With retraction of the sonotrode, remove welded material from the machine or relocate for a subsequent weld.

Once the required welding machine settings are established, repetitive welding is accomplished by repeating only steps 8, 9, and 10.

If manual operation is desired, as in the case of experimental welding, the Manual-Automatic switch is set on Manual. Then the foot switch becomes a two-position switch. With the first depression, the upper sonotrode lowers to contact weldment materials; clamping force builds up to the preset level, but no other events are triggered. This permits time for adjustment of clamping force or the other variables, if so desired, before weld power is introduced. A second depression of the foot switch then actuates the weld cycle, which is completed automatically if the foot-switch is held in the depressed condition.

The scram button, shown to the right of the foot switch in Figure 1, may be used to interrupt a weld cycle at any instant, since it abruptly cuts off power to all control functions.

#### D. Checkout of Equipment

After the complete assembly of equipment, the welding array was tested under power conditions for electrical and mechanical phase adjustment and for resonant frequency.

##### 1. Electrical Phase Adjustment

It was previously noted (page 26) that a high-Q neutralizing coil is essential for use with ceramic transducer elements. Maximum power delivery will occur when the capacitive reactance of the transducer array, as viewed by the frequency converter, is balanced out by resonance tuning with the correct value of inductive reactance. In order to handle up to 10 amperes of high-frequency electrical current and the circulating reactive currents of resonance without dissipating a significant portion of this power by internal coil heating, ten high-Q, high-current coils were fabricated and assembled in two parallel arrays. These were mounted on wooden shafts, with provision, by proximity coupling, for incremental adjustment of inductance.

The correct value of inductance was based on the relative phase between the voltage and current into the high-voltage transformer. The inductance was adjusted under power for a power factor of about 0.9, which experience with ultrasonic welding systems has shown to be approximately optimum. The factor alters with variations during delivery of ultrasonic power to the weldment.

## 2. Mechanical Phase Adjustment

The opposition-drive transducer-coupling system was designed so that upper and lower ultrasonic systems would be as nearly identical as possible, in order to preclude the possibility of different phase relationships occurring under power conditions. Assembly of the two sets of ceramic elements with reversal of polarization direction within the transducer assembly yielded an out-of-phase relationship for the vibratory motion of the two systems. To check this relationship under power-pulse conditions, small ceramic transducers were epoxy-bonded onto the free end surface of each waveguide. The relative phase between these systems on repeat power pulses remained essentially at 180 degrees. The unit, at least at low power, functioned according to the design.

## 3. Frequency Check

After assembly, both transducer-coupling systems were bench-checked as free units and were adjusted to drive at precisely the same frequency (14,970 cycles per second). Due to impedance changes, the correct operating frequency for a system under loaded conditions does not necessarily coincide with the resonant frequency of the unloaded systems. For these assemblies, the frequency of maximum response of each system under loaded conditions was observed by vibration probe measurements at the weld-tip locale at frequencies approximating the free resonant frequency. Maximum response for both systems occurred with the systems loaded at frequencies ranging from 14,870 to 14,890 cycles per second, or about 100 cycles per second below the unloaded situation. To anyone skilled in the technology, the effectiveness of force-insensitive mounting is then obvious.

## E. Preliminary Welding

Preliminary evaluation of the welding capability of the equipment was made with coupons of 0.040-inch-thick 2024-T3 bare aluminum alloy, using about half the vibratory energy required with standard nickel-transducer welding systems (1000 watts power, 900 pounds clamping force, and 1.5 seconds weld time, compared to 2000 watts, 900 pounds, and 1.5 seconds with the nickel system). Good welds were not obtained, and monitoring of the system during attempted welding indicated two trouble areas:

1. The mechanically attached welding tips, which depended upon the mating of serrated surfaces for transfer of vibratory energy, were not well-matched to the coupler along the serrated surfaces. The tips were removed and hand-lapped to achieve a more precise fit.
2. The force bar used to transmit clamping from the piston to the overhung upper terminal coupler showed resonant response at the operating frequency. This resonant response was eliminated by altering the geometry of the force bar.

After these modifications, good welds were made in 0.050-inch 2024-T3 bare aluminum alloy at settings of 2000 and 4000 watts power, 900 pounds clamping force, and 0.5 second weld time. As power input to the welder was increased, other difficulties became evident. A summary of the preliminary welding data, with annotations of the difficulties encountered, is presented in Tables XXV and XXVI of Appendix C.

In spite of these difficulties and the delays required for rework, it was clear that the overall performance of the machine met the design projections. An early indication of this was obtained when, in a first attempt to weld at 7.5 kilowatts input power, two reasonably good welds were made in 1/4-inch-thick 6061-T6 aluminum alloy plate.

Throughout the welding evaluation (described in Section X), various debugging type problems were encountered and solved.

One of the major difficulties arose from the loss of ultrasonic energy at the various mechanical joints of the transducer-coupling systems. In our ultrasonic apparatus technology, the general practice for mechanically joining various components of an ultrasonic system involves the use of a butt-type screw couple, with a soft aluminum or copper shim inserted to maximize area contact at the interface. Such joints, located at vibratory antinodal positions, are satisfactory in a partially loaded system operating at relatively low power. With this arrangement in the high-power system, upon coupling of the welding tips to the work, the stress waves associated with ultrasonic power delivery introduced transverse loads on the joint between the terminal coupler and the adapter coupler; these stress waves effected transverse motion in the system, loosened joints, and caused detrimental heating.

Various efforts to rework this assembly were fruitless. Eventually the complete system was disassembled and the critical joint was remade by brazing. No further heating was encountered.

Other problems, especially those associated with the welding tips, have been discussed in Section V. It was not possible, within the limitations of the program, to solve all problems that have become evident in this new equipment that potentially increases the power-handling capacity of ultrasonic welding equipment by 500 to 600 percent.

## X. EVALUATION OF WELDING PERFORMANCE

For initial evaluation of the equipment performance, welds were made in a range of gages of aluminum alloys, stainless steel, and selected refractory metals and alloys. No effort to establish the complete capability of the machine or to drive it at maximum power was contemplated. The problems encountered during debugging, particularly welding tip problems, which were not completely solved, caused delays and limited the scope of the evaluation efforts. Nevertheless, sufficient data were obtained to indicate that this equipment has the potential to achieve its design objectives once certain problem areas are resolved.

Performance capability was determined for bare aluminum alloys 2024-T3 and 2014-T6, in gages up to 0.071 inch and 0.080 inch respectively, and for those gages of the high-strength and refractory metals up to which tip performance could be maintained.

Welding machine settings were approximated on the basis of data previously derived. Input energy requirements for the various materials and gages, shown in Figures 32 and 33, were obtained from the curves of Figures 4 and 5, with the assumption that ceramic transducer-coupling systems are about twice as efficient as those incorporating nickel transducers. The points shown on the curves of Figures 32 and 33 represent actual values used. Clamping forces were estimated from the curves of Figure 20.

Although time did not permit exploration of power-force programming for these materials, some of the later welds were necessarily made with an arbitrarily selected power program to alleviate the tip problem, which it did. The oscillograph of the power program is shown in Figure 34. This program provided a step-wise buildup to full power, and a drop to half power just before the completion of the weld cycle. It was reasoned that preliminary heating of the weld metal may impart some ductility to it prior to the application of full power and that tip loading is thus alleviated. Sufficient data were not obtained for evaluation of these effects.

The tables in Appendix C present, in chronological order, the weld data obtained with the machine, together with interspersed comments indicating difficulties encountered. Table XXIII provides a summary of data from welded coupons that were tensile-shear tested. The indicated number of weldments do not include specimens reserved for metallographic study nor those kept for record purposes, nor those in which the weld spot was not centrally located (and thus would not yield representative shear strength data).

Altogether, welds were made in more than 200 specimens of aluminum alloys in five gages, about 140 specimens of stainless steel in two gages, and about 60 specimens of the various superalloys and refractory metals in thicknesses up to 0.060 inch. A few bimetallic welds were made between Rene'41 and Mo-0.5Ti alloy.



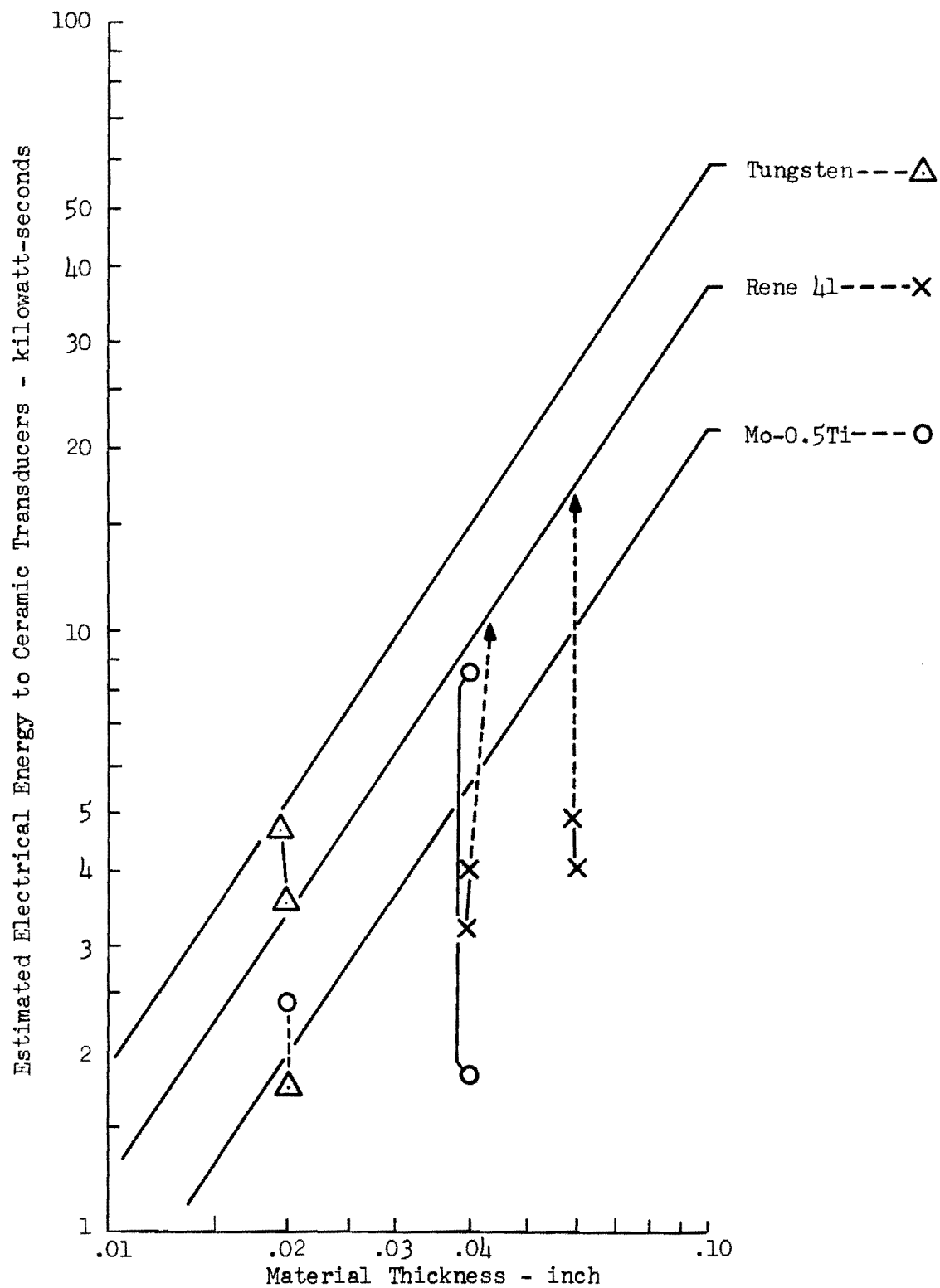


Figure 32: Estimated and Actual Input Energy Required for Welding with Ceramic Transducers

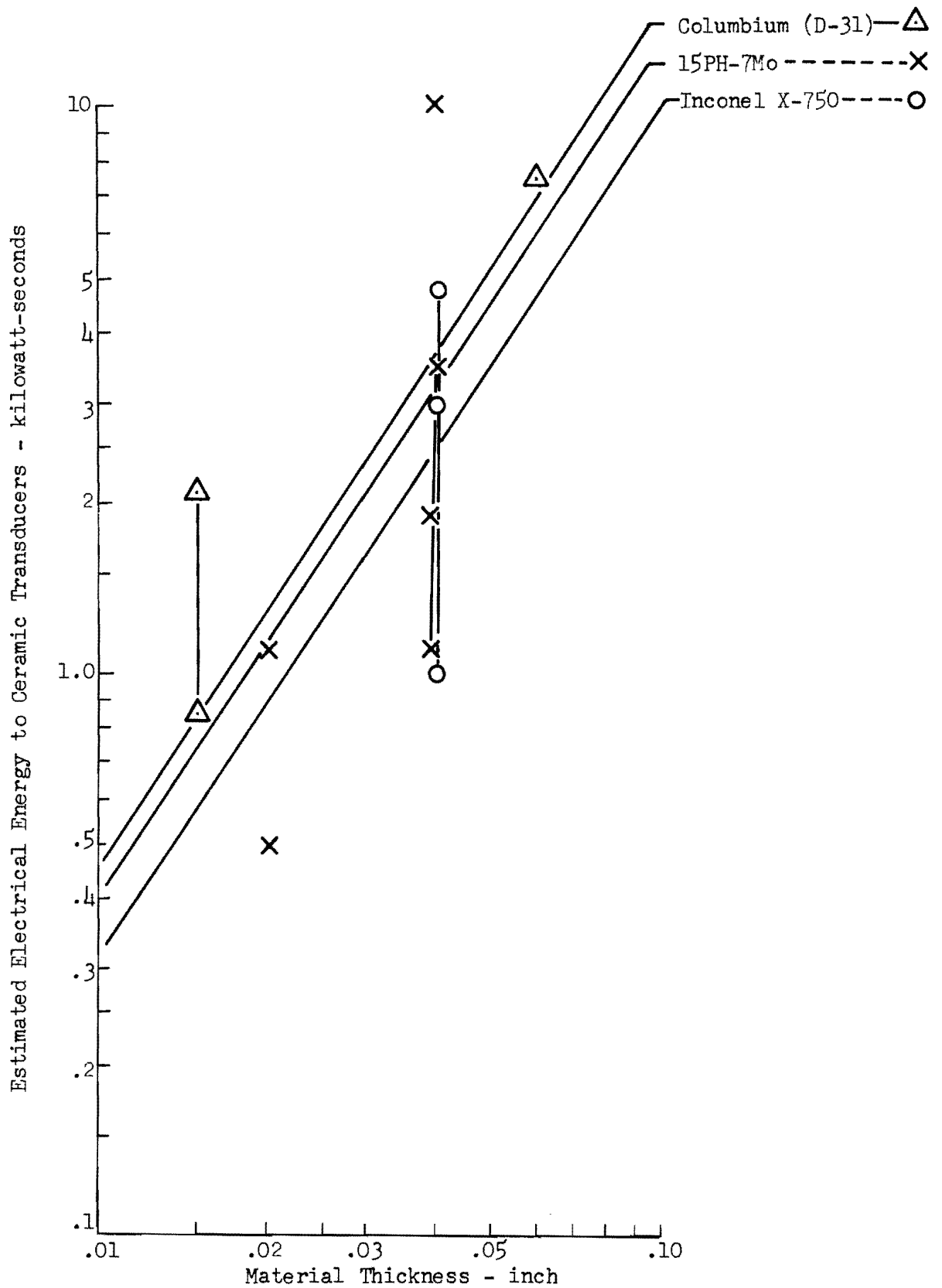


Figure 33: Estimated and Actual Input Energy Required for Welding with Ceramic Transducers

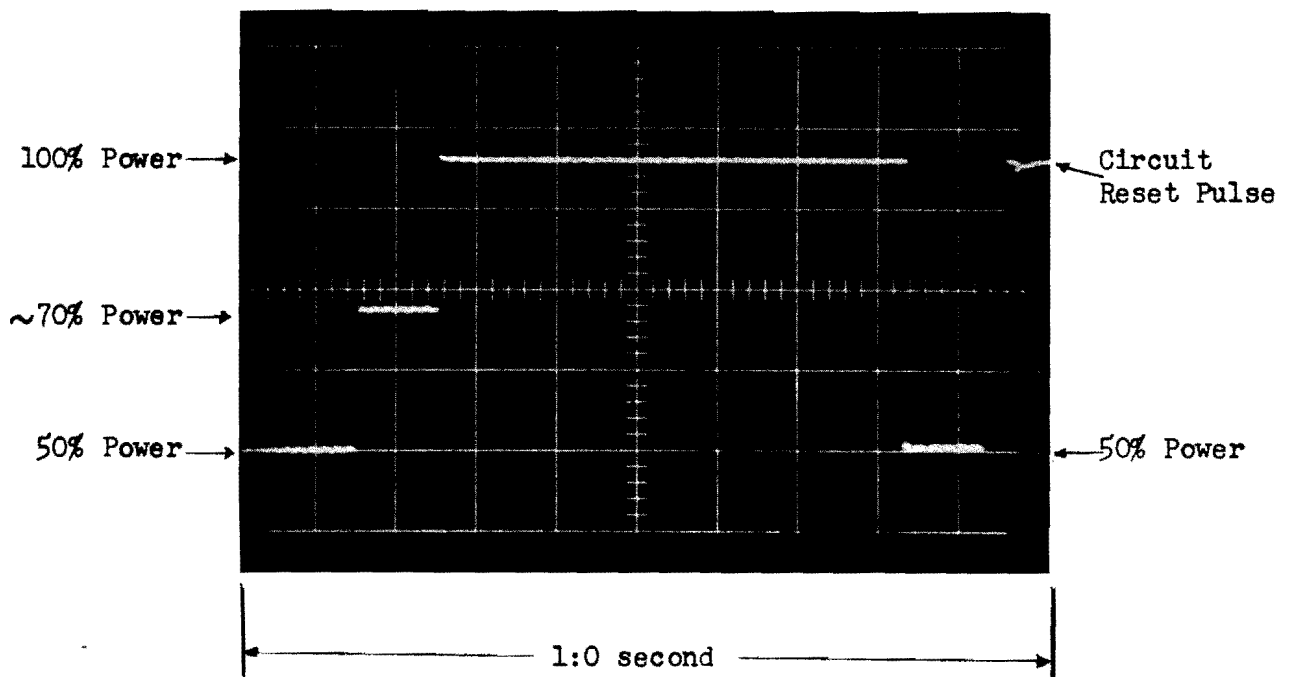


Figure 34: Oscillograph of Power Programming Command Signal for Peg-Board Schedule for Welding Refractory Metals

# ULTRASONIC WELDING

Table XXIII

SUMMARY DATA OF WELDS MADE WITH 25-KILOWATT ULTRASONIC WELDER

Weldment Material		Input Energy (kw-sec)	No. of Welds Tested	Average Tensile- Shear Strength (lb/spot)	Reference Strength Data* (lb/spot)	Comments
Type	Gage (inch)					
Aluminum Alloy	0.040	2.5	10	1277	950	Excessive energy for this material and gage.
2024-T3 <i>al</i>	0.050	1.0-2.1	91	1363	1250	
	0.060	1.5-2.3	52	1903	1450	
	0.070	4.0	33	2353	1850	
2014-T6 <i>al</i>	0.080	4.0	3	2680	--	Improper tip coupling.
	0.080	4.0	4	1170	--	
Stainless Steel	0.040	1.9-4.6	23	1060	--	
AISI 304						
PH15-7Mo <i>SS</i>	0.020	0.5	6	589	1265	Clamping force too high.
	0.040	1.9-3.5	9	689	--	Clamping force too high.
	0.040	10.0	3	2367	--	
	0.040	1.1-1.7	81	1940	--	
Rene'41 <i>NiB</i>	0.040	3.2-4.0	9	2510	(490 lb for 0.030")	
	0.060	4.0	2	1065	--	
	0.060	4.9(PFP)	8	1978	--	Clamping force low.
	0.060	4.9(PFP)	1	3200	--	Increased clamping force.
Inconel X-750 <i>NiB</i>	0.040	1.0-3.1	8	325	1100	
	0.040	4.8	2	1495	1100	Large spot (~1/2" dia).
Columbium						
Alloy C103 <i>Co</i>	0.015	0.8-2.1	6	327	205	
	0.060	7.4	2	370	--	
Mo-0.5Ti <i>Mo</i>	0.020	2.4	1	130	235	
	0.040	1.8-8.7(PFP)	5	197	--	
Bimetallic Welds						
0.060" Rene'41 to						
0.040" Mo-0.5Ti		7.4-10.4(PFP)	3	696	--	

\* Data obtained previously, either in Phase I or in other work. Blank spaces represent combinations that had not previously been attempted or successfully welded.

*NiB, Mo*  
DISSIMILAR JOINING

Table XXIII includes, in addition to strength data for these welds, representative data previously obtained for welds in the same material and gage, where such data were available. It is noted that in most instances the new welding machine produced stronger welds. Welds of lower strengths than previously obtained were generally damaged because of tip degradation or tip sticking; this was especially true for the columbium and molybdenum alloys.

#### A. Weldment Characteristics

##### 1. Aluminum Alloys

Except in those cases where the welding power and/or time (weld energy) was either inadequate or excessive, the welds were characterized by high strength and minimum deformation. The weld spots were larger in diameter than those produced with older, lower-power machines. Failure in tensile-shear usually occurred from parent metal fracture, either by nugget tear-out or by fracture of the metal adjacent to the weld nugget. Figure 35 shows the significantly increased strength of the welds in these materials, compared to previously reported data obtained with a 4-kilowatt welder (26).

Microscopic inspection of the surfaces revealed light scuffing on the surface contacted by the lower, flat welding tip, and a relatively smooth (although slightly indented) surface contacted by the upper, spherical welding tip.

##### 2. Stainless Steel and Rene'41

The stainless steels (PH15-7Mo and AISI 304) and Rene'41 welded relatively easily and at less than the estimated energy level; they responded to clamping forces other than those estimated; and they possessed similar weld appearances with little deformation. Microscopic inspection of the surfaces showed scuffing and occasional pitting on the back surfaces (contacted by the flat welding tip) of both the stainless steel and the Rene' weldments. One Rene'41 specimen was cracked diametrically across the weld.

As shown in Table XXIII, the use of power programming with Rene'41 effected a significant improvement in weld strength in the 0.060-inch material and alleviated the tip problem.

##### 3. Inconel X-750 and Columbium Alloys

Only a few welds were made with these materials and general conclusions are not possible. Weld energy and clamping force requirements appeared higher than predicted, but the contribution of the tip problem is difficult to estimate. Two welds in 0.040-inch Inconel X-750 made with increased energy showed high strength; no high-strength welds were obtained in the columbium alloys. Weld surfaces were generally rough due to tip sticking; deformation was not excessive.

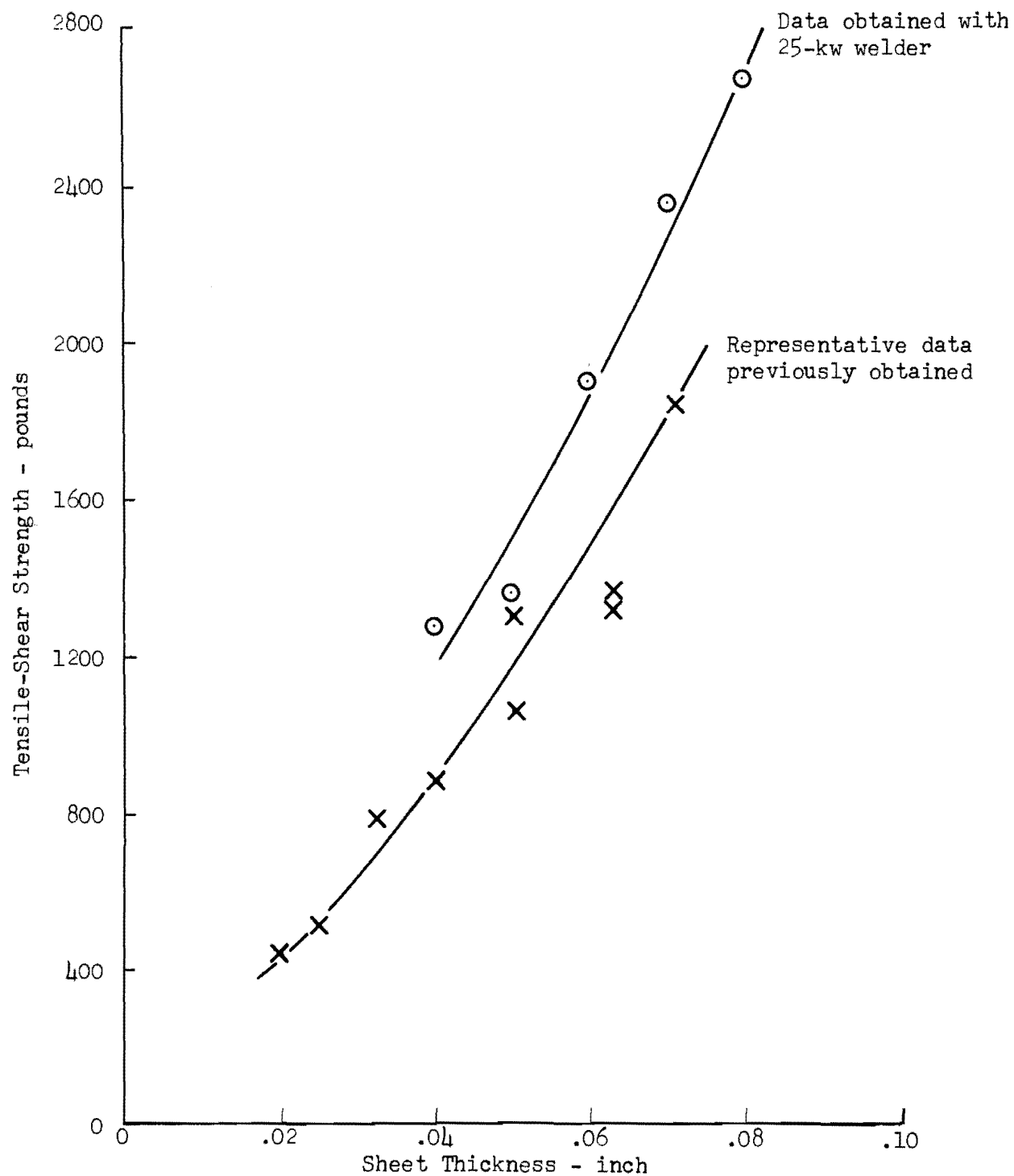


Figure 35: Strength of Ultrasonic Welds in 2024-T3 and 2014-T6 Aluminum alloys

Effective welding of these materials requires effort to determine the minimum energy condition (MEC) and suitable power-force programming for achieving quality welds. Solutions to the tip difficulties will facilitate welding.

#### 4. Molybdenum Alloys and Tungsten

The problems encountered in welding these alloys related to the ability of the tips to transmit the vibratory stresses without "self-mutilation." These alloys tended to crack during weld formation, and delamination occurred with the tungsten. Such problems were encountered in prior efforts to weld the thinner gages of molybdenum alloy and tungsten (1, 2). Improved welding tips and effective utilization of power-force programming should provide means for achieving quality welds in heavier gages than the maximum (0.060 inch) here investigated.

#### 5. Bimetallic Welds

To obtain some indication of the capability of the machine in welding bimetallic combinations, several welds were made between 0.060-inch Rene 41 and 0.040-inch Mo-0.5 Ti alloy, with no effort to optimize welding machine settings. Tensile-shear tests on three of these welds revealed strength values of 590, 600, and 745 pounds per spot.

#### B. Metallographic Examination of Welds

Representative samples of welds in various materials and gages were sectioned and polished for metallographic examination. All specimens were sectioned parallel to the vibratory direction. Microscopic observations are presented in Table XXIV, and photomicrographs are shown in Figures 36 through 47.

The weld microstructures illustrate the high ultrasonic energy density and attendant weld zone heating obtained. Since a systematic determination of the minimum energy condition (MEC) for each material could not be undertaken, and actual welding machine settings were chosen by comparison or extrapolation of existing data, the weld microstructure obtained can not be construed as "typical," but rather as indicative of the particular welding conditions employed.

Structural modifications in the weld zone resulting from the combined effects of ultrasonics and local heating were observed in all specimens examined. The welds in the aluminum alloys 2024-T3 (Figure 36) and 2014-T6 (Figure 37) show the quasi-viscous behavior of the metal at the interface and the resulting extremely fine unresolvable grain structure. Local surface melting and surface liquation were also observed in both types of welds (Figure 38), and this is clearly indicative of welding tip slip, i.e., improper coupling, a situation that can probably be resolved with proper power and clamping force programming.

Table XXIV  
MICROSCOPIC EXAMINATION OF WELDS

Material	Gage (inch)	Specimen No.	Remarks
Rene'41	0.040	48	Satisfactory weld; edge extrusion; no cracks or voids
Rene'41	0.060	6	Satisfactory weld; no edge extrusion; no cracks or voids
Inconel X-750	0.040	13	Incipient weld; modified grain struc- ture; no cracks or voids; very slight recrystallization
Inconel X-750	0.060	20	Satisfactory weld; no edge extrusion; modified grain structure; extensive recrystallization
2024-T3 Al Alloy	0.060	92	Satisfactory weld; predominantly peripheral; modified grain structure; surface (not interfacial) melting (tip slip)
2014-T6 Al Alloy	0.080	3	Satisfactory weld; edge extrusion; modified grain structure; surface (not weld locale) melting (tip slip)
PH15-7Mo	0.040	31	Satisfactory weld; edge extrusion; modified grain structure
C-103 (Columbium)			Edge-crack thru sheet; weld interface satisfactory
Tungsten			Cracking throughout weld zone
TZM		38	Edge cracks; localized welding
Mo-0.5Ti		27	As above
Mo-0.5Ti		29	As above
Mo-0.5Ti		15	Edge cracks; localized interface cracks
Rene'41/Mo-0.5Ti		42	Satisfactory weld quality; edge micro- cracks in Rene'41





Figure 36: Edge of Ultrasonic  
Weld Between 0.060-  
inch Sheets of  
2024-T3 Aluminum  
Alloy  
(Keller's etch; 100X)

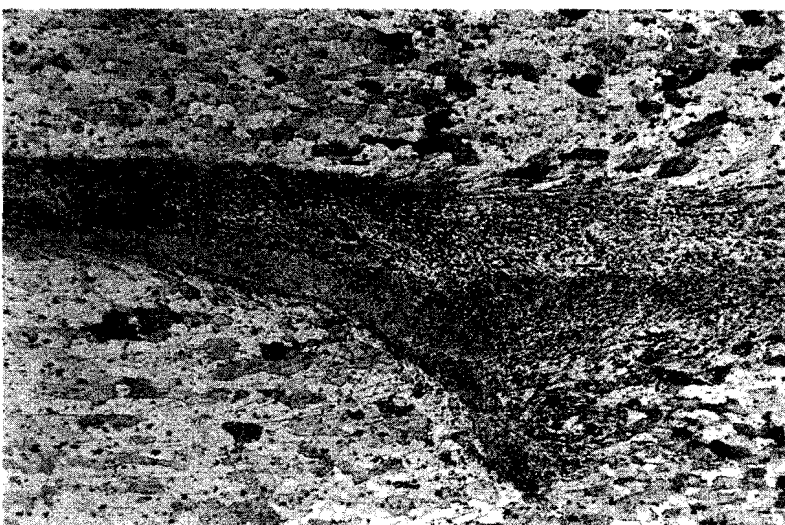


Figure 37: Edge of Ultrasonic  
Weld Between 0.080-  
inch Sheets of  
2014-T6 Aluminum  
Alloy  
(Keller's etch; 100X)

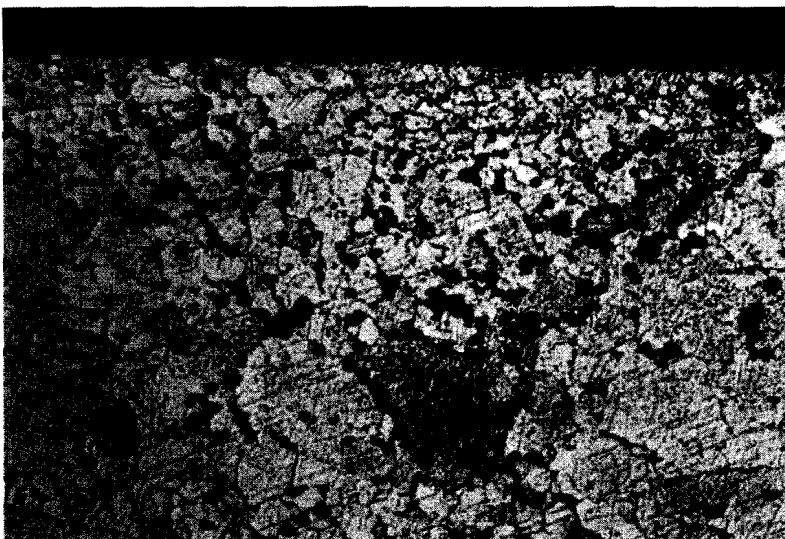
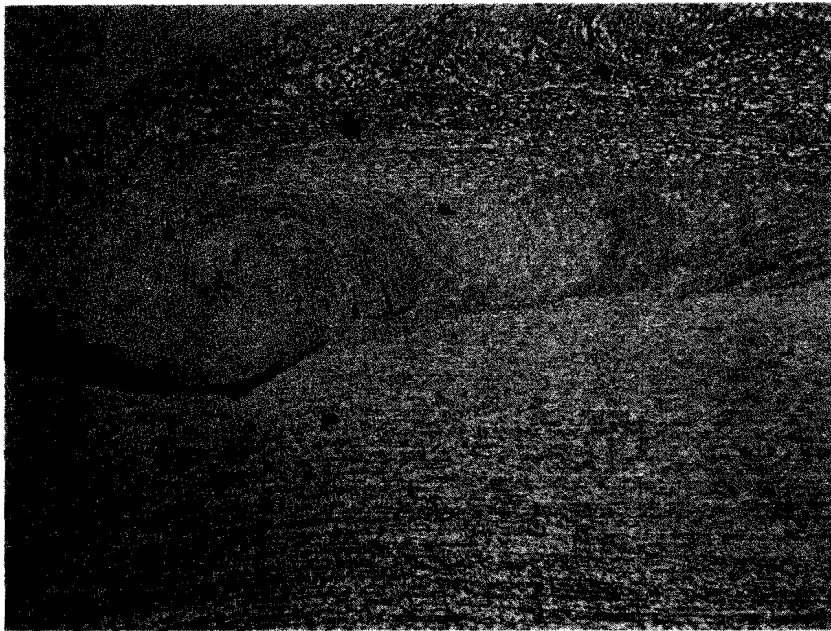
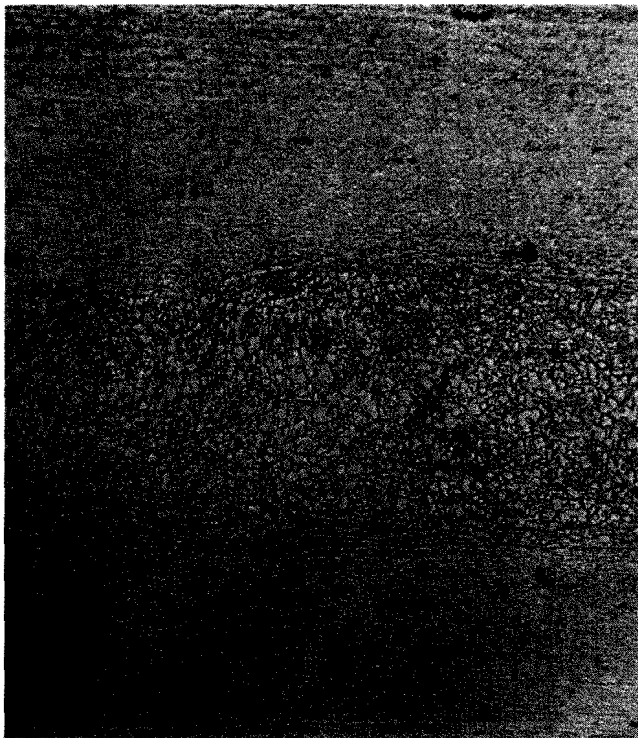


Figure 38: Surface Liquation  
in 0.040-inch  
2024-T3 Aluminum  
Alloy  
(Keller's etch; 750X)



A. Edge of Weld



B. Center Section of Weld

(Arrow indicates approximate position of original interface)



Figure 39: Ultrasonic Weld Between Sheets of  
0.040-Inch PH15-7Mo Stainless Steel  
(Etched electrolytically in oxalic acid; 100X)

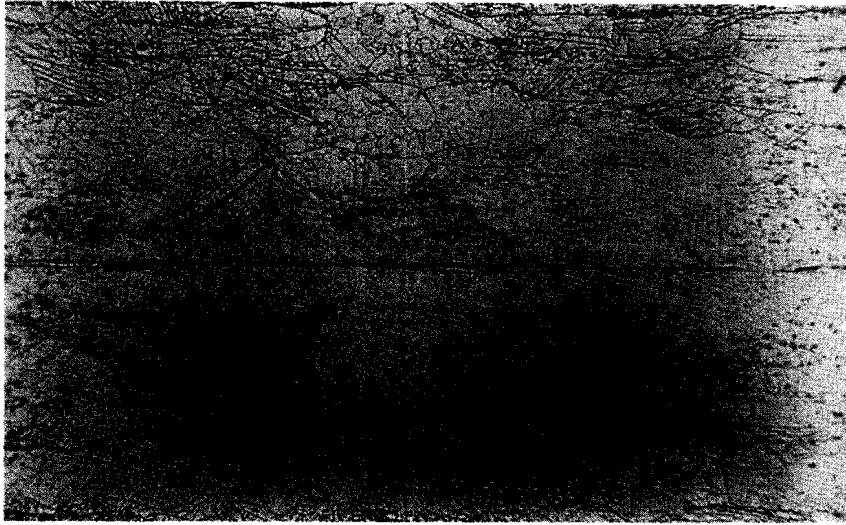


Figure 40: Ultrasonic Weld Between Sheets of  
0.040-Inch Rene-41

(Electrolytic etch in oxalic acid; 100X)



Figure 41: Ultrasonic Weld Between Sheets of  
0.060-Inch Rene-41

(Electrolytic etch in oxalic acid; 100X)

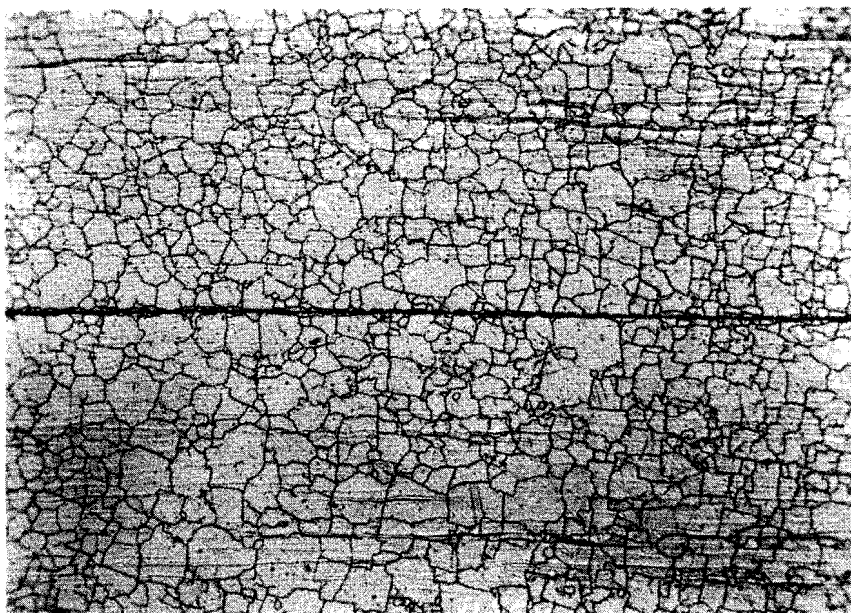


Figure 42: Ultrasonic Weld Between Sheets of  
0.040-Inch Inconel X-750

(Electrolytic oxalic acid etch; 100X)

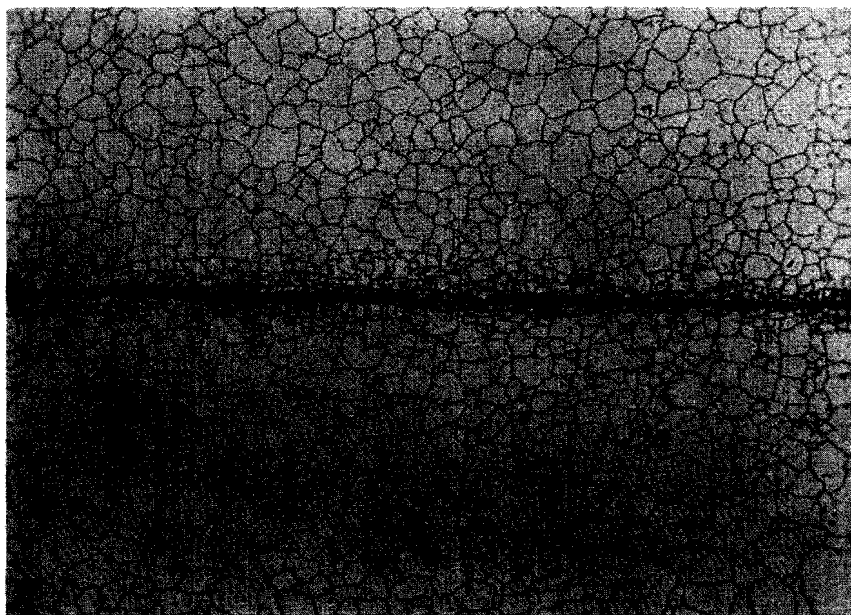


Figure 43: Ultrasonic Weld Between Sheets of  
0.060-Inch Inconel X-750

(Electrolytic oxalic acid etch; 100X)

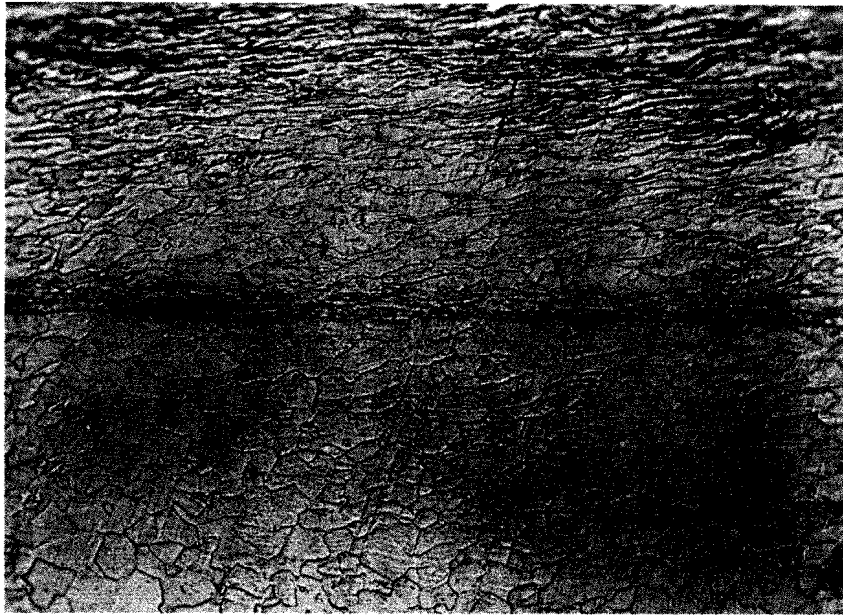


Figure 44: Ultrasonic Weld Between Sheets of  
C-103 Columbian Alloy

( $\text{HF} + \text{HNO}_3 + \text{H}_2\text{SO}_4 + \text{H}_2\text{O}$  etch; 100X)



Figure 45: Ultrasonic Weld Between Sheets of  
TZM Alloy

(Alkaline ferricyanide etch; 300X)

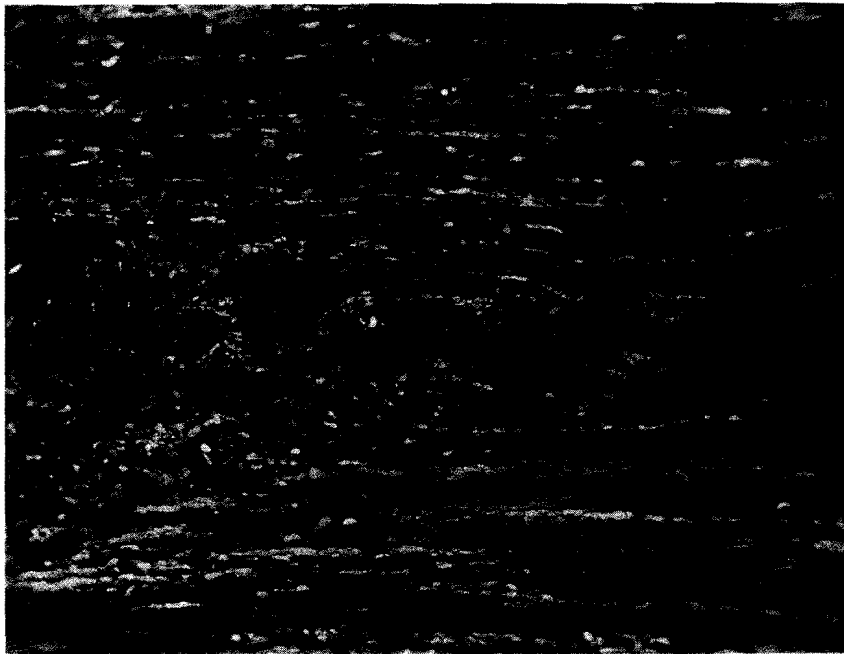


Figure 46: Ultrasonic Weld Between Sheets of  
0.020-Inch Mo-0.5Ti Alloy

(Alkaline ferricyanide etch; 300X)

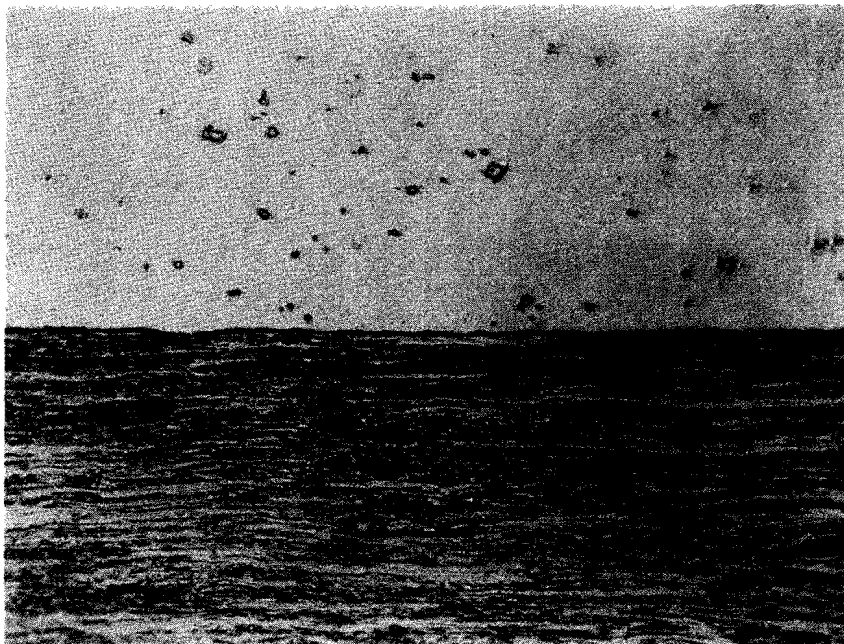


Figure 47: Ultrasonic Weld Between Sheets of  
Rene 41 (top) and Mo-0.5Ti (bottom)

(Electrolytic oxalic acid etch; 300X)



The weld microstructures illustrate the high ultrasonic energy density and attendant weld zone heating obtained. Since a systematic determination of the minimum energy condition (MEC) for each material could not be undertaken, and actual welding machine settings were chosen by comparison or extrapolation of existing data, the weld microstructure obtained can not be construed as "typical," but rather as indicative of the particular welding conditions employed.

Structural modifications in the weld zone resulting from the combined effects of ultrasonics and local heating were observed in all specimens examined. The welds in the aluminum alloys 2024-T3 (Figure 36) and 2014-T6 (Figure 37) show the quasi-viscous behavior of the metal at the interface and the resulting extremely fine unresolvable grain structure. Local surface melting and surface liquation were also observed in both types of welds (Figure 38), and this is clearly indicative of welding tip slip, i.e., improper coupling, a situation that can probably be resolved with proper power and clamping force programming.

The welds in the PH15-7 Mo stainless steel also show the viscous turbulent flow behavior at the interface, with extrusion of metal between the sheets (Figure 39). The central portion of the weld (Figure 39-B) shows the distribution of austenite and ferrite phases which presumably formed during cooling of the specimen after welding. Plastic flow at the weld interface is also shown in the 0.040-inch Rene 41 specimen (Figure 40). Partial recrystallization in the flow region can be observed. The heavier gage Rene 41 weld (Figure 41) shows less extensive flow at the welding machine settings employed.

Modification of the grain boundary configuration in the weld zone of the 0.040-inch Inconel X-750 specimen (Figure 42) is accompanied by localized recrystallization at the weld interface. A more extensive region of recrystallization is observed in the 0.060-inch weld section (Figure 43), presumably from a greater ultrasonic energy density at the interface. The alteration of the shape of the grains in the weld region has been observed in this material (as well as in some aluminum alloys, nickel, 70:30 brass, etc.) in previous investigations. The grain boundaries tend to align themselves in essentially block-like segments, oriented predominantly parallel and perpendicular to the direction of ultrasonic vibration in weld sections taken parallel to the vibratory direction.

Weld cracking was observed in the C-103 columbium, tungsten, TZM, Mo-0.5Ti, and Rene 41/Mo-0.5 Ti specimens, and this is certainly not surprising in the light of the exceedingly limited scouting work done to date. Much effort has been expended to the end of joining these materials by other processes.

The C-103 specimen contained a crack extending from the edge (periphery) of the weld through the sheet adjacent to the upper welding tip. The

portion of the weld interface shown in Figure 44 shows the satisfactory bond quality obtained. Catastrophic cracking was encountered with the tungsten. The TZM welds (Figure 45) contained some edge cracks and interface separation, and similar results were observed in the Mo-0.5Ti weld sections examined (Figure 43). Welds in both materials, however, indicate a remarkable degree of plasticity under the influence of ultrasonic energy.

The dissimilar metal weld--Rene' 41 and Mo-0.5Ti alloy (Figure 47)--exhibited good bonding at the welding conditions employed. Shallow microcracks in the Rene' 41 at the edge of the weld section were observed (not shown in photomicrograph).



## XI. CONCLUSIONS

1. The 25-kilowatt ultrasonic welding machine was assembled and operated successfully. All standard systems of the equipment, e.g., the force system, timing system, etc., functioned as intended.
2. The 25-kilowatt motor alternator (frequency converter package) functions in accordance with the projected design and supplies the required high-frequency power for this first large, high-power ultrasonic welding machine.
3. The six 4.2-kilowatt (input), 15-kc transducers function as projected with an efficiency that is about twice the efficiency obtainable with nickel-stack transducer systems. These units were evaluated at design power coupled into an acoustic calorimeter and exhibited overall electroacoustic conversion efficiencies in the range of 75-85 percent.
4. The welding tip problem is severe and crucial. In order that the effectiveness of this equipment be extended to fulfill the objectives of the project (satisfactory spot welding of 0.10-inch thicknesses of the candidate refractory and/or superalloy materials), tip development is essential; investigations and selection of significantly better tip alloys than have been available to date are necessary. The contours of these tips, because they control internal stresses in the tips and internal stresses in the weldments, also must be investigated and further developed.
5. Power-force programming improves welding performance and alleviates the tip problem (because lower powers and probably lower temperatures are thus possible). Comprehensive investigation of power-force programming is as essential to further development of this equipment as is tip development, and effort in both directions should be carried out concurrently. The room-temperature and elevated-temperature properties for the candidate refractory and superalloy materials require consideration in depth to the end of devising power and force programs for producing crack-free, superior junctions; thus, as observed, excessive tip slip, lack of acoustical coupling, and concomitant excessive surface heating can be alleviated and possibly eliminated. Appropriate power and force programs can probably be devised to control the interface temperature of the materials, thus effecting weldment material ductility.
6. The switching of power to the transducers by switching the alternator field current did not yield as rapid a buildup in power as desirable, although this aspect of the equipment is not critical. Recently developed SCR switching apparatus offers the necessary capability to precisely switch all the power of this equipment without difficulty at the projected rate.

7. Satisfactory crack-free welds were achieved in Rene'41, Inconel X-750, two high-strength aluminum alloys, and PH15-7Mo stainless steel. Further investigation is necessary to permit satisfactory joining of tungsten, Mo-0.5Ti, TZM, and columbium C-103 alloy and in gages up to 0.10 inch. The metallography of welds indicates internal metal displacement of remarkable proportions without necessarily accompanying cracks. The metallurgical changes observed in aluminum, Rene'41, Inconel X-750 follow the patterns previously observed in ultrasonic welds; in the case of the aluminum alloy, unresolvable grain structure was noted; study and evaluation of such metal would be interesting.
8. Subject to improved welding tips and a reasonable fund of practical power-force programming knowhow as it relates to the metals and alloys of interest, this equipment is ready for use to carry out comprehensive ultrasonic welding process development with the candidate superalloys and refractory metals. Further adjustment and minor improvement in the instrumentation and controls will be required as such work proceeds.

APPENDIX A

THE TRANSMISSION OF ULTRASONIC POWER BY  
FLEXURAL WAVES ON A SLENDER BAR

## APPENDIX A

### THE TRANSMISSION OF ULTRASONIC POWER BY FLEXURAL WAVES ON A SLENDER BAR

It is shown in a previous study\*, Eq. (22), that the characteristic impedance of a uniform slender bar for flexural waves is given by

$$Z_f = A\rho c_\ell \sqrt{\frac{\omega k}{c_\ell}} \quad (1)$$

where  $A$  is the area of the cross section

$\rho$  is the density

$c_\ell$  is the bar velocity  $(E/\rho)^{1/2}$

$\omega (=2\pi f)$  is the angular frequency

$k$  is the radius of gyration of the cross section about the neutral axis.

The flexural impedance equals the impedance for longitudinal waves  $A\rho c_\ell$  times the dimensionless factor  $(\omega k/c_\ell)^{1/2}$  which depends on frequency, the shape of the section and the bar velocity of sound. The power transmitted by flexural waves going in one direction along the bar is then

$$P = 1/2 Z_f \omega^2 \eta_o^2 \quad (2)$$

where  $\eta_o$  is the peak amplitude of the flexural waves. The factor  $1/2$  in Eq. (2) averages the sinusoidal time dependence of the flexural wave, which takes the form

$$\eta = \eta_o \sin(\omega t - Kx) \quad (3)$$

The angular wave number  $K$  is given by

$$K = \sqrt{\frac{\omega}{c_\ell k}} \quad (4)$$

as derived in the original work\*, Eq. (19).

---

\* Elmore, W. C., "Characteristic Impedance of Rods Used for Transferring Ultrasonic Power".

In the present report we shall examine how an upper limit to the power that can be transmitted is set by the stress fatigue limit and other material properties of the bar, as well as by certain geometrical factors related to the size and shape of the cross section of the bar. In a previous report by W. C. Elmore, "The Limitation on Amplitude Set by Maximum Strain Energy in Vibrating Systems", the effect of the stress limit on the amplitude of free-free flexural vibrations on an unloaded bar has already been considered. Here we are concerned with power transmission, and how the maximum power level can be reached by proper design of the flexural transmission line.

Let us consider first the relation between maximum surface stress  $\sigma$  and the amplitude  $\eta_0$  of the flexural wave. The following equations, proved in accounts of beam theory, pertain to this case:

$$\sigma = \frac{M}{Z} = \frac{Mh}{I} = Eh \frac{d^2 \eta}{dx^2} \quad (5)$$

where  $M$  is the bending moment at any point  $x$ ;

$Z = I/h$  is the so-called section modulus;

$h$  is the distance from the neutral axis to the most distant point on the section;

$I = Ak^2$  is the moment of inertia of the section about the neutral axis;

$d^2 \eta / dx^2$  is the curvature of the neutral section, here caused by the flexural wave.

From Eqs. (3) and (4),

$$\frac{d^2 \eta}{dx^2} = -K^2 \eta = -\frac{\omega}{c_L k} \eta \quad (6)$$

On substituting this value for the curvature into Eq. (5), and disregarding the minus sign having to do with phase,

$$\sigma_{\max} = \frac{Eh\omega}{c_l k} \eta_{\max} \quad (7)$$

This equation may be rewritten to show that the maximum (particle) velocity permitted is

$$\dot{\eta}_{\max} = \omega \eta_{\max} = \frac{k}{h} \cdot \frac{\sigma_{\max}}{\sqrt{E\rho}} \quad (8)$$

which therefore depends on the geometrical factor  $k/h$  and the material factor  $\sigma_{\max}/\sqrt{E\rho}$ . On introducing this maximum particle velocity into Eq. (2) and using Eq. (1) for the impedance,

$$P_{\max} = 1/2 \left[ \frac{A k^{5/2}}{h^2} \right] \cdot \left[ \omega^{1/2} \right] \cdot \left[ \frac{\sigma_{\max}^2}{\rho^{1/4} E^{3/4}} \right] \quad (9)$$

Equation (9) shows how the maximum power that can be transmitted depends on a geometrical factor, the frequency and a material factor. The equation can be somewhat misleading, however, in that the three factors are inter-related by the requirement that the dimension of the bar in the plane of the flexural wave (its "depth") must be kept small compared with the wavelength  $\lambda$ . Let us therefore introduce this limitation into Eq. (9) by writing

$$h = \alpha \lambda \quad (10)$$

where  $\alpha$  is a pure numeric whose maximum value would appear to be approximately 1/8, that is, the bar should have a depth no greater than one-quarter of the wavelength of the flexural wave. Since, by Eq. (4),

$$\lambda = \frac{2\pi}{k} = 2\pi \sqrt{\frac{c_l k}{\omega}}, \quad (11)$$

the maximum frequency that can be used with a given bar is given by

$$\omega_{\max} = 4\pi^2 \alpha^2 \frac{c\ell}{h} \left(\frac{k}{h}\right) \quad (12)$$

If now we introduce this maximum frequency into Eq. (9),

$$P_{\max} = \pi \alpha A \left(\frac{k}{h}\right)^3 \frac{\sigma_{\max}^2}{\sqrt{\rho} E} \quad (13)$$

which shows that the maximum power that can be transmitted is proportional to the area of the bar, a shape factor  $(k/h)^3$  and a material factor  $\sigma_{\max}^2 / \sqrt{\rho} E$ , which is identical with that limiting power transmission by longitudinal waves. [See, for example, "Fundamentals of Ultrasonic Welding". Appendix E, Eq. (9)7. To reach the maximum set by the material factor, and the geometrical factor (area times shape factor) it is of course necessary to operate at the frequency specified by Eq. (12) with  $\alpha$  as large as possible. One may look upon Eq. (12), in fact, as defining the value of  $\alpha$ . If a frequency is used less than  $\omega_{\max}$ , (corresponding, for example to  $\alpha < 1/8$ ) then Eq. (12) must be solved for the smaller value of  $\alpha$  to be used in Eq. (13) in computing the upper limit to power transmission for the given flexural transmission line. If we denote by  $\alpha_{\max}$ , its highest permissible value, corresponding to the frequency  $\omega_{\max}$ , then at lower frequencies

$$\alpha = \sqrt{\frac{\omega}{\omega_{\max}}} \alpha_{\max} \quad (14)$$

(It would appear that an experiment should be done to test the assumption that  $\alpha_{\max} = 1/8$  is a practical upper limit to the half-depth to wavelength ratio.)

Some practical implications will now be considered. In making use of them one must bear in mind that if a load is not matched to the impedance of this, or any other transmission line, the resultant standing wave pattern will reduce the maximum power that can be delivered to the load. Thus, if a standing wave ratio of 10 exists on the line, the power that can be safely delivered is reduced by a factor of 10. Any attempt to increase power delivery by increasing input power will over-stress the surface regions of the bar, and ultimately lead to fatigue failure.

Bar of Circular Section. Let us first compute  $P_{\max}$  for a circular steel rod, one-inch in diameter, for which  $\rho = 7.84 \text{ gm/cm}^3$ ,  $c_l = 5.17 \times 10^5 \text{ cm/sec}$ .  $E = 2.1 \times 10^{12} \text{ dynes/cm}^2$  and  $\sigma_{\max} = 10^9 \text{ dynes/cm}^2$  ( $\sim 15,000 \text{ psi}$ ). Then  $h = 1.27 \text{ cm}$ ,  $k/h = 1/2$ , and assuming that  $\alpha = 1/8$ ,

$$f_{\max} = 2\pi (1/8)^2 \times \frac{5.17 \times 10^5}{1.27} \quad 1/2 = 20,000 \text{ cps}$$

The maximum power (with unity standing wave ratio) is

$$P_{\max} = \pi^2/8 (1.27)^2 (1/8) \frac{10^{18}}{\sqrt{7.84 \times 2.1 \times 10^{12}}}$$

$$= 6.13 \times 10^{10} \frac{\text{ergs}}{\text{sec}} = 6,130 \text{ watts}$$

If the line is used at 15,000 cps, the maximum power, by Eq. (14), will be about 86.6 percent of this value, or 5,310 watts.

In comparison, the maximum power that can be transmitted by longitudinal waves, on the same bar by Eq. (9) of Appendix E, "Fundamentals of Ultrasonic Welding", is

$$P_{\max} = 1/2 A \frac{\sigma_m^2}{\sqrt{E \rho}} \quad (15)$$

$$= \pi/2 (1.27)^2 \frac{10^{18}}{\sqrt{7.84 \times 2.1 \times 10^{12}}}$$

$$= 6.24 \times 10^{11} \text{ ergs/sec} = 62,400 \text{ watts}$$



which is approximately ten times greater ( $32/\pi$ ). For longitudinal waves the frequency can have any value up to a maximum that makes the radius of the transmission rod an eighth of a wavelength. The maximum frequency is therefore

$$f_{\max} = \frac{c}{\lambda_{\min}} = \frac{c}{8a} \quad (16)$$

which, for the present example, gives

$$f_{\max} = \frac{5.17 \times 10^5}{8 \times 1.27} = 51,000 \text{ cps.}$$

Bar of Square Section. Next consider a steel bar of square section one inch on a side of the same material. Again  $h = 1.27$  cm, but  $k = h/\sqrt{3}$  and  $A = 4h^2$ . Hence

$$\begin{aligned} P_{\max} &= \pi/8 \cdot 4(1.27)^2 \cdot \frac{1}{3\sqrt{3}} \cdot \frac{10^{18}}{\sqrt{7.84 \times 2.1 \times 10^{12}}} \frac{\text{ergs}}{\text{sec}} \\ &= 12,000 \text{ watts,} \end{aligned}$$

which is nearly twice the power the bar of circular section can accommodate.

The maximum frequency, at which this power can be delivered, is

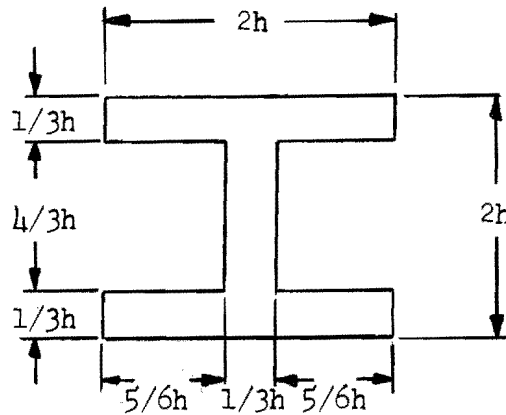
$$f_{\max} = 2\pi (1/8)^2 \frac{5.17 \times 10^5}{1.27} \frac{1}{\sqrt{3}} = 23,100 \text{ cps}$$

due to the more favorable shape factor. At 15 kc/sec, the maximum power is 80.6 percent of that at  $f_{\max}$ , or about 9,700 watts, as compared with 5,300 watts for the bar of circular section. Hence at 15 kc/sec, the increased area and shape factor result in an 83 percent increase in the capacity to transmit power. The impedance of the square bar is 37% greater than that of the circular bar because of the increased area and shape factor.

A square bar whose impedance equals that of a circular bar can transmit 1.3 times as much power without stress overload, when both bars are

operated at the same frequency. For equal impedances at a given frequency, it is found from Eq. (1) that the diameter of the circular bar must be 13.3 percent greater than the thickness of the square bar.

Bar of I Section. As a final example, let us consider the bar having the section shown as follows:



For this shape it is found that

$$A = \frac{16}{9} h^2, \quad I = \frac{244}{243} h^4, \quad k/h = 0.752$$

Using the same material properties as before and making  $h = 1.27$  cm,

Eq. (13) gives

$$P_{\max} = \pi (1/8) \frac{16}{9} (1.27)^2 (.752)^3 \frac{10^{18}}{\sqrt{7.84 \times 2.1 \times 10^{12}}} \frac{\text{ergs}}{\text{sec}}$$

$$= 11,800 \text{ watts,}$$

at the frequency

$$f_{\max} = 2\pi (1/8)^2 \frac{5.17 \times 10^5}{1.27} (.752)$$

$$= 30,000 \text{ cps.}$$

At 15 kc/sec, the maximum power would be 8,350 watts, as compared with 5,300 watts for a circular bar of one-inch diameter and 9,700 watts for a one-inch square bar.

The one-inch I section has an impedance at 15 kc/sec of 1930 kg/sec; the one-inch square bar an impedance of 3800 kg/sec; and the one-inch circular bar an impedance of 2780 kg/sec. The low impedance of the bar of I section means that such a bar can deliver considerably more power, relative to the bars of other sections, when the load has a very low impedance, such as may occur in welding. If the bar of I section has the same impedance as a bar of circular section (which requires that  $2h$  be 17.5 percent greater than the diameter of the circular bar) the maximum power that can be delivered at the same frequency is 2.3 times the power that can be delivered by the circular bar. It is evident that bars having a high section modulus make the best transmitters of ultrasonic power by flexural waves.

APPENDIX B

CONTACT AREA BETWEEN TWO BODIES  
HAVING TWO PRINCIPAL RADII

## APPENDIX B

### CONTACT AREA BETWEEN TWO BODIES HAVING TWO PRINCIPAL RADII

Two elastic bodies forced into contact, and originally having principal radii  $R_1, R_1'$  and  $R_2, R_2'$  respectively at the contact region, have a contact area that is elliptical with semi-axes given by

$$a = m \left\{ \frac{3\pi}{4} \frac{P (k_1 + k_2)}{A + B} \right\}^{1/3}$$
$$b = n \left\{ \frac{3\pi}{4} \frac{P (k_1 + k_2)}{A + B} \right\}^{1/3}$$

where

$P$  = contact force

$$k = \frac{1 - \sigma^2}{\pi E}$$

$\sigma$  = Poisson's ratio

$E$  = Young's modulus

$A, B$  are quantities depending on  $R_1, R_1', R_2, R_2'$  as defined below,

$m, n$  are constants depending on  $A$  and  $B$ , which are found by the use of the table.

As shown by Love (27),

$$2 (A + B) = \frac{1}{R} + \frac{1}{R_1'} + \frac{1}{R_2} + \frac{1}{R_2'}$$

$$4 (A - B)^2 = \left( \frac{1}{R_1} - \frac{1}{R_1'} \right)^2 + \left( \frac{1}{R_2} - \frac{1}{R_2'} \right)^2 + 2 \left( \frac{1}{R_1} - \frac{1}{R_1'} \right) \left( \frac{1}{R_2} - \frac{1}{R_2'} \right) \cos 2\omega$$

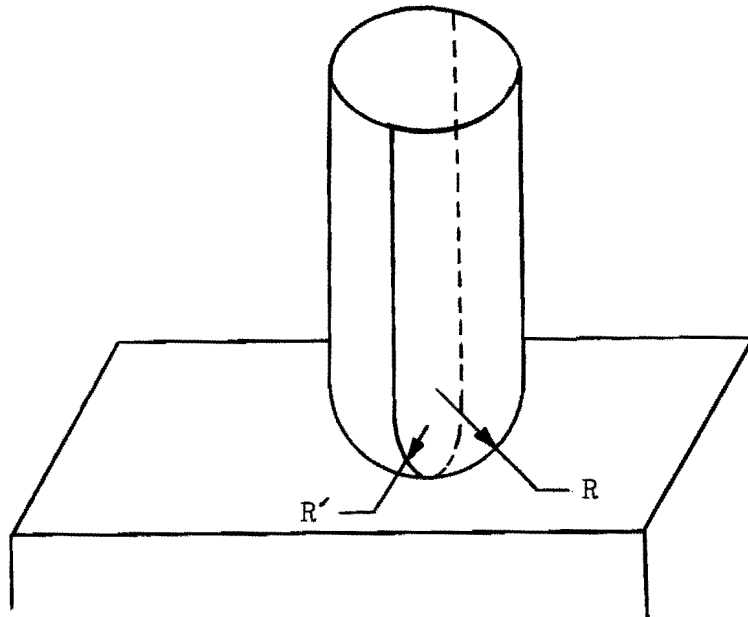
where  $\omega$  = angle between planes containing  $R_1$  and  $R_2$ . We are concerned with the case in which  $R_2 = R_2' = \infty$ , which is representative of a flat anvil.

Then

$$\left. \begin{aligned} 2(A + B) &= \frac{1}{R_1} + \frac{1}{R_1'} \\ 2(A - B) &= \frac{1}{R_1} - \frac{1}{R_1'} \end{aligned} \right\} \text{Hence}$$

$$A = \frac{1}{2R_1} = \frac{1}{2R}$$

$$B = \frac{1}{2R_1'} = \frac{1}{2R'}$$



If one defines a parameter  $\theta$  such that

$$\cos \theta = \frac{B - A}{A + B} = \frac{R - R'}{R + R'}$$

Then  $m$  and  $n$  are determined from the following table from Timoshenko and Goodier, (28):

$\theta =$	$30^\circ$	$35$	$40$	$45$	$50$	$55$	$60$	$65$	$70$	$75$	$80$	$85$	$90$
$m =$	2.731	2.397	2.136	1.926	1.754	1.611	1.486	1.378	1.284	1.202	1.128	1.061	1.000
$n =$	0.493	0.530	0.567	0.604	0.641	0.678	0.717	0.759	0.802	0.846	0.893	0.944	1.000

From the foregoing one may calculate the max. pressure at the center  $= \frac{3}{2} \frac{P}{\pi ab}$ ,  
as well as the area of contact  $= \pi ab$ .

The attached figure presents a set of curves relating contact area to the major principal radius for a series of values of the minor radius. The curves show the actual area, for typical elastic constants, and a pressure of 1000 lbs, as well as a scale applying to other elastic constants and pressures.

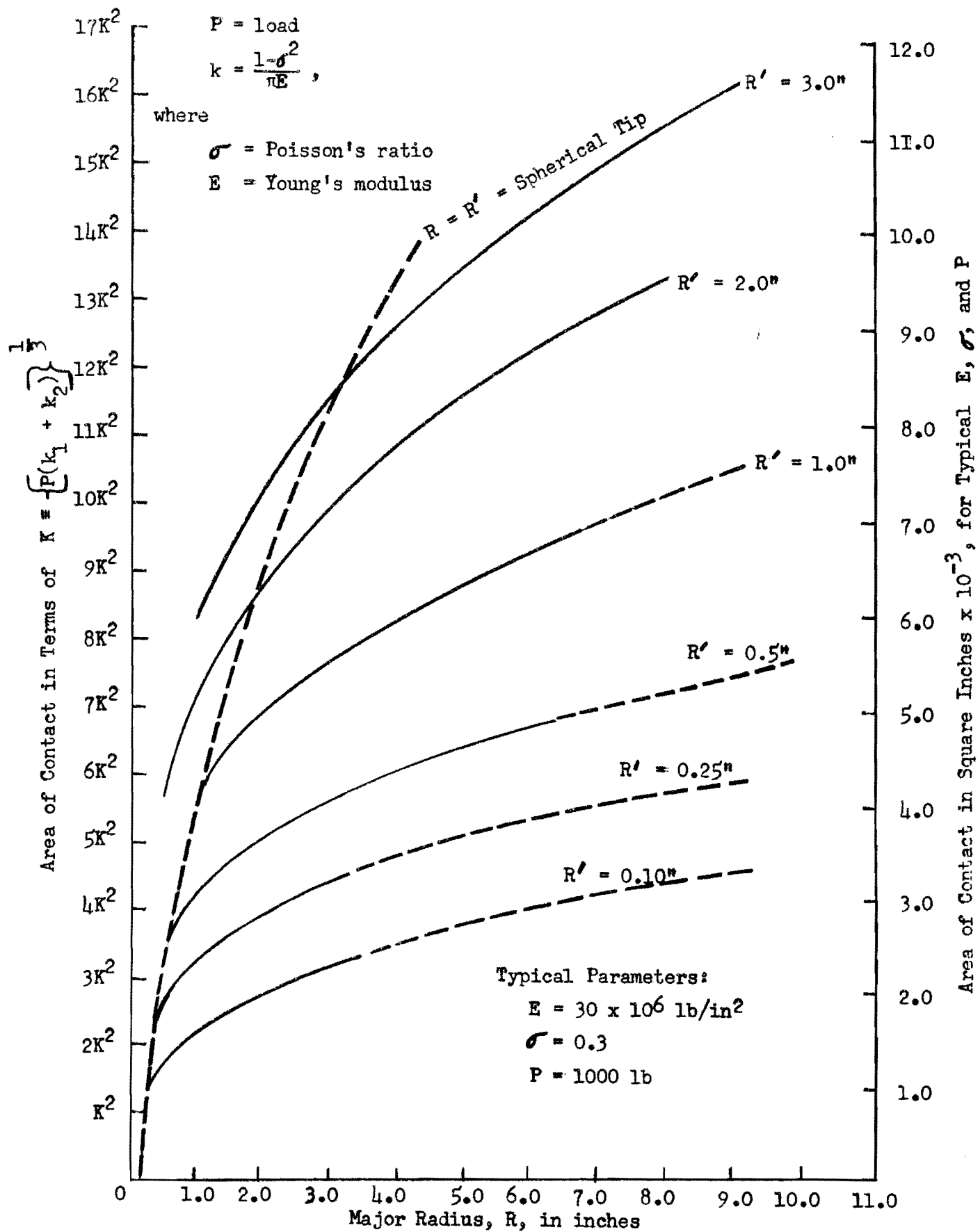


Figure 48: Area of Contact as a Function of the Larger Radius



APPENDIX C

WELDING DATA OBTAINED DURING EQUIPMENT CHECKOUT

Table XXV

## PRELIMINARY WELDING CHECKOUT DATA FOR 25-KW ULTRASONIC WELDER

Weldment Material		Input Power (kw)	Weld Time (sec)	Weld Energy (kw-sec)	Clamping Force (lb)	No. of Measure- ments	Tensile Strength (lb/spot)			Comments
Designation	Gage (inch)						Min	Max	Av	
2024-T3 Bare Al	0.050	4.0	0.5	2.0	900	6	1100	1700	1400	
6061-T6 Al	0.250	7.0	1.5	10.5	2000	2	--	--	--	Apparently good welds
Waveguide-transducer joints heating -- reworked for larger coupling screws										
2024-T3 Bare Al	0.050	4.0	0.5	2.0	900	10	1270	1700	1570	
Waveguide heating at adaptor-coupler joints -- reworked and new shims added										
2024-T3 Bare Al	0.050	2.0	0.5	1.0	900	12	880	1480	1295	
Performance level satisfactory										

Table XXVI

ULTRASONIC WELDING OF SUPERALLOYS INTERSPERSED WITH  
QUALIFICATION DATA FOR 25-KW WELDER

Weldment Material		Input Power (kw)	Weld Time (sec)	Weld Energy (kw-sec)	Clamping Force (lb)	No. of Measure- ments	Tensile Strength (lb/spot)			Comments
Designation	Gage (inch)						Min	Max	Av	
Inconel X	0.040	2.0	0.5	1.0	1000	2	218	480	349	
		2.0	1.1	2.2	1000	2	160	225	192	
		2.85	1.1	3.14	1000	4	350	415	379	
2024-T3 Bare Al	0.050	2.5	0.5	1.25	1000	6	1230	1650	1444	Qualification check
PH15-7Mo Stain- less Steel	0.020	2.5	0.2	0.50	800	6	400	780	589	
	0.040	3.75	0.5	1.88	800	1	--	--	1420	
					1000	2	320	560	440	
					1200	4	470	770	638	
		4.95	0.7	3.5	1200	2	380	970	675	
		10.0	1.0	10.0	1500	3	1800	2800	2367	
Braze-joint failure -- cleaned and rebrazed two coupler joints										
2024-T3 Bare Al	0.050	2.5	0.5	1.25	1100	9	1590	1860	1784	Qualification check
		2.5	0.3	0.75	1100	5	800	1720	1416	
Excessive breakage of screws on lower system at tips -- redrill and tap for 8.32										

Table XXVII

## WELDING OF ALUMINUM ALLOYS AND STAINLESS STEEL

Weldment Material		Input Power (kw)	Weld Time (sec)	Weld Energy (kw-sec)	Clamping Force (lb)	No. of Measurements	Tensile Strength (lb/spot)			Comments
Designation	Gage (inch)						Min	Max	Av	
PH15-7Mo Stainless Steel	0.040	2.7	.4	1.08	300	5	1250	2050	1649	
		2.7	.4	1.08	600	4	1170	2020	1662	
		4.2	.4	1.68	750	72	480	2600	1975	
Problems with tip screws -- breaking										
2024-T3 Bare Al	0.050	3.0	.4	1.2	1100	10	520	1430	992	Qualification check
		5.2	.5	2.6	1100	5	1000	1560	1188	
		5.2	.5	2.6	1500	3	1320	1580	1450	
		5.2	.4	2.08	1500	1	--	--	1070	
		5.2	.4	2.08	1100	1	--	--	1640	
Add cooling to tip of lower system										
		4.2	.4	1.68	1100	16	1070	1610	1324	
2024-T3 Bare Al	0.060	5.7	.4	2.28	1500	6	1540	2550	2017	
		5.7	.4	2.28	1800	1	--	--	1850	
		5.7	.4	2.28	1400	2	1850	2120	1985	
		6.2	.4	2.48	1500	15	1550	2310	1969	
		6.2	.25	1.55	1500	4	1270	1750	1515	
Lower system tip serrations lapped										
		5.7	.5	2.85	1500	24	1230	2350	1893	
2014-T6 Al	0.080	7.8	.5	3.9	1800	3	2610	2750	2680	
304 Stainless Steel	0.040	4.8	.4	1.92	750	20	840	1450	1043	
Lower coupler removed, reworked, and realigned										

Table XXVIII

# WELDING OF ALUMINUM ALLOYS AND STAINLESS STEEL AFTER EXTENSIVE REWORK OF LOWER COUPLER

Weldment Material		Input Power (kw)	Weld Time (sec)	Weld Energy (kw-sec)	Clamping Force (lb)	No. of Measurements	Tensile Strength (lb/spot)			Comments
Designation	Gage (inch)						Min	Max	Av	
2024-T3 Bare Al	0.040	5	.5	2.5	1100	10	950	1640	1277	Excess energy
2014-T6 Al	0.080	8	.5	4.0	1800	2	800	1480	1140	Insufficient energy Coupler joint heating
		8	.6	4.8	1800	2	800	1600	1200	
304 Stainless Steel	0.040	5.7	.8	4.6	750	3	1070	1320	1163	
Lower system reworked for larger stud size -- assembled but not brazed										
2014-T6 Al	0.080	8.8	.5-.6	4.4-5.3	1500	3	1580	2000	1760	
Rebrazed joints to complete rework										
2024-T3 Bare Al	0.050	4.2	.5	2.1	1100	7	870	1400	1207	
	0.071	8.0	.5	4.0	1800	9	2000	2600	2253	
Tip problems										

Table XXIX

## WELDING OF REFRACTORY METALS AND ALLOYS

Weldment Material		Input Power (kw)	Weld Time (sec)	Weld Energy (kw-sec)	Clamping Force (lb)	No. of Measurements	Tensile Strength (lb/spot)			Comments
Designation	Gage (inch)						Min	Max	Av	
Columbium	0.015	4.2	.2	.84	1000	1	-	-	398	Surface finish good but slightly scuffed. Tip re-dressed after each weld
		4.8	.3	1.4	800	1	-	-	185	
		4.2	.4	1.7	800	3	230	430	352	
		4.2	.5	2.1	800	1	-	-	325	
Mo-0.5Ti	0.020	4.8	.5	2.4	850	1	-	-	130	Weldments cracked; tip damage
		8.0	.2	1.6	850	7				
Tungsten	0.020	3.5-	.5-	1.75-	850	5				Weldments cracked; severe tip sticking
		7.0	1.0	3.5						
Molybdenum (TZM)	0.020	3.6	.3-.5	1.08-1.8	600-1000	8				Severe tip sticking
Mo-0.5Ti	0.040	3.6	.5	1.8	800	3	130	260	185	C-103 underlay
Rene'41	0.040	8.0	.4	3.2	1200	3	2000	2625	2325	
		8.0	.4	3.2	900	1	--	--	2175	
		10.0	.4	4.0	900	5	2450	3075	2685	
	0.060	10.0	.4	4.0	2000	2	700	1430	1065	Tip damage
2024-T3 Bare Al	0.071	8.0	.5	4.0	1800	24	1975	2850	2390	Qualification check

Table XXX

WELDING REFRACTORY METALS AND ALLOYS WITH MODIFIED WELDING TIPS  
AND WITH POWER-FORCE PROGRAMMING

Weldment Material		Max.	Weld Time (sec)	Weld Energy (kw-sec)	Clamping Force (lb)	No. of Measure- ments	Tensile Strength (lb/spot)			Comments
Designation	Gage (inch)	Input Power (kw)					Min	Max	Av	
Rene' 41	0.060	8.0	.7	4.87	1600	4	1100	2325	1931	FFP*
		8.0	.7	4.87	2000	4	1500	2500	2025	FFP
		8.0	.7	4.87	2400	1	--	--	3200	FFP
Inconel X	0.040	8.5	.5	4.83	1100	2	1490	1500	1495	FFP
Columbium (D-31)	0.060	8.5	1.0	7.4	2600	2	120	620	370	FFP*
		10.0	1.0	8.7	2600	1	--	--	40	FFP*
Mo-0.5Ti	0.040	10.0	1.0	8.7	1800-2600	11	--	--	--	Ob 0.15 under- lay on some**
		10.0	1.0	8.7	1800	1	--	--	260	
		10.0	1.0	8.7	1500-2000	1	--	--	170	*
Rene' 41 to Mo-0.5Ti	0.060- 0.040	10- 12	1.0	8.7- 10.4	1800	3	590	900	696	

\* Tip sticking and tip degradation.

## REFERENCES

1. Aeroprojects Incorporated, "Ultrasonic Welding of Selected Refractory Metals and Alloys." Research Report 63-54, Navy Contract NOW 61-0410-c, June 1963.
2. Maropis, N. and J. G. Thomas, "Ultrasonic Welding of Refractory Metals and Alloys with Power-Force Programming." Research Report 63-66, Aeroprojects Incorporated, Navy Contract NOW 63-0125-c, December 1963.
3. Gelles, S. H., "Beryllium Research and Development Program: Report for 1 April 1960 - 30 September 1961 on Metallic Materials." Report ASD-TDR-52-509, Vol. 1, Nuclear Metals, Inc., Cambridge, Mass., October 1962. (Includes section on Ultrasonic Welding of Beryllium).
4. Jones, J. B., N. Maropis, et al., "Development of Ultrasonic Welding Equipment for Refractory Metals." Report ASD TR 7-888, Vol. II, Aeroprojects Incorporated, Air Force Contract AF 33(600)-43026, December 1961.
5. Weisenberg, L. A. and R. J. Morris, "How to Fabricate Rene' 41." Metal Progress, Vol. 78, No. 5, November 1960.
6. "Columbium Alloy D-31." DuPont Technical Bulletin, E. I. du Pont de Nemours Co., Wilmington, Delaware, April 1960.
7. Tietz, T. E. and J. W. Wilson, "Mechanical, Oxidation, and Thermal Property Data For Seven Refractory Metals and Their Alloys." Final Report, Lockheed Aircraft Corporation, Missiles and Space Division, Sunnyvale, Calif., Contract NOas 60-6119-c, September 1961.
8. Platte, W. N., "Joining Refractory Metals." Scientific Paper 62-125-306-P2, AIME Refractory Metals Symposium, Chicago, Illinois, April 13, 1962.
9. Barth, V. D., "Review of Recent Developments in The Technology of Tungsten." DMIC Report 127, Defense Metals Information Center, Battelle Memorial Institute, Columbus, Ohio, September 22, 1961.
10. Stephens, J. R., "An Exploratory Investigation of Some Factors Influencing the Room-Temperature Ductility of Tungsten." NASA Technical Note D-304, National Aeronautics and Space Administration, August 1960.



# REFERENCES (Continued)

11. Barth, V. D. and G. W. P. Rengstorff, "Oxidation of Tungsten." DMIC Report 155, Defense Metals Information Center, Battelle Memorial Institute, Columbus, Ohio, July 17, 1961.
12. Houck, J. A., Battelle Memorial Institute, Columbus, Ohio, Private Communication, March 1962.
13. Hahn, G. T., A. Gilbert, and R. I. Jaffee, "The Effects of Solutes on the Ductile-to-Brittle Transition in Refractory Metals." DMIC Memorandum 155, Defense Metals Information Center, Battelle Memorial Institute, Columbus, Ohio, June 28, 1962.
14. Davis, G. L., "Recrystallization of Tungsten Wires." Metallurgia, Vol. 6, 1958, p. 177.
15. Stephens, J. R., "An Exploratory Investigation of Some Factors Influencing the Room-Temperature Ductility of Tungsten." NASA Technical Note D-304, National Aeronautics and Space Administration, August 1960.
16. Aeroprojects Incorporated, "Ultrasonic Welding Process and Equipment for Construction of Electron-Tube Mounts." Army Contract DA-36-039-SC-86741, Quarterly Progress Report for Period January 1 through March 31, 1963.
17. Levy, A. V. and S. E. Bramer, "Refractory Sheet-Metal Structures." Machine Design, Vol. 31, June 25, 1959, p. 141-145.
18. Gerken, J. M. and J. M. Faulkner, "Investigation of Welding of Commercial Columbium Alloys." Report ASD-TDR-62-292, Thompson Ramo Wooldridge Inc., Air Force Contract AF 33(616)-7796, May 1962.
19. Torgerson, R. T., "Evaluation of Forming Characteristics of Columbium Alloys." In Douglas, D. L. and F. W. Kunz, Columbium Metallurgy, Metallurgical Society Conferences, Vol. 10. Interscience Publishers, New York, 1961.
20. Bartlett, E. S., D. N. Williams, H. R. Ogden, R. I. Jaffee, and E. F. Bradley, "High-Temperature Solid-Solution-Strengthened Columbium Alloys." Transactions of the Metallurgical Society of the AIME, Vol. 227, 1963, p. 459-467.
21. Jones, J. B., N. Maropis, J. G. Thomas, and D. Bancroft, "Fundamentals of Ultrasonic Welding, Phase II." Research Report 60-91, Aeroprojects Incorporated, Navy Contract 59-6070-c, December 1960.

REFERENCES (Concluded)

22. Berlincourt, D. A., "Power Capacities of Piezoelectric Ceramics in Sonar-Type Acoustic Transducers," Report 61-19, Clevite Corporation, 1961.
23. Berlincourt, D. A. and H. H. A. Krueger, "Behavior of Piezoelectric Ceramics Under Various Environmental and Operation Conditions of Radiating Sonar Transducers." Engineering Memorandum 64-27, Clevite Corporation, 1964.
24. Van Santen, A. W., Mechanical Vibrations. MacMillan Company, New York, 1958.
25. Jones, J. B., N. Maropis, J. G. Thomas, and D. Bancroft, "Fundamentals of Ultrasonic Welding, Phase I." Research Report 59-105, Aeroprojects Incorporated, Navy Contract NOas 58-108-c, May 1959.
26. "Ultrasonic Welding," Chapter 49 in Welding Handbook, Section Three, Fifth Edition, American Welding Society, New York, N. Y., 1964.
27. Love, A Treatise on the Mathematical Theory of Elasticity, p. 192, Dover Publications, New York, 1944.
28. Timoshenko and Goodier, Theory of Elasticity, p. 372 and 379, McGraw-Hill Book Company, Inc., 1951.

DISTRIBUTION LIST

AFML (MAA - Mr. J. Teres)  
WPAFB, Ohio 45433

AFML (MAAE)  
WPAFB, Ohio 45433

AFML (MAAM - Librarian)  
WPAFB, Ohio 45433

AFML (MATF) 6 copies  
WPAFB, Ohio 45433

AFML (MAX - Dr. Lovelace)  
WPAFB, Ohio 45433

AFFDL (FDDS)  
Attn: Aerospace Dynamics Branch  
WPAFB, Ohio 45433

AFFDL (FDTS)  
Attn: Applied Mechanics Branch  
WPAFB, Ohio 45433

AFFTC (FTBAT-2)  
Edwards AFB  
Calif. 93523

AFRPL (RPC)  
Edwards AFB, Calif.

SSD (SERTH)  
AF Unit Post Office  
Los Angeles, Calif. 90045

BSD (BSOMS)  
Norton AFB, Calif.

RTD (RTTM)  
Bolling AFB  
Wash., D. C. 20332

Hq USAF (AFRSTC)  
Pentagon, Wash., D. C. 20013

Hq USAF (AFSPDT - Mr. Joe Joers)  
Wash. D. C. 20330

AFSC STLO  
AF Unit Post Office  
Los Angeles, Calif.

AFSC STLO (RTSAW)  
c/o Department of Navy  
Room 3543  
Munitions Bldg.  
Wash., D. C. 20360

AFSC STLO (RTD)  
O'Hare International Airport  
P. O. Box 8758  
Chicago, Illinois 60666

SEG (RTD)  
SEPIE  
WPAFB, Ohio 45433

FTD (TDEWP)  
WPAFB, Ohio 45433

MAAMA (MAE)  
Technical Library  
Olmsted AFB, Pa. 17057

MOAMA (MCAE)  
Technical Library  
Brookley AFB, Ala. 36615

OOAMA (OCAE)  
Technical Library  
Hill AFB, Utah 84401

OCAMA (OCAE)  
Technical Library  
Tinker AFB, Okla. 73145

ROAMA (ROAEPP-1) PDO 4045A  
Technical Library  
Griffiss AFB, NY 13440

SMAMA (SMNE)  
Technical Library  
McClellan AFB, Calif. 95652

SAAMA (SANE0)  
Technical Library  
Kelly AFB, Texas 78241

WRAMA (WRAE)  
Technical Library  
Robins AFB, Ga. 31093

Commander  
Army Research Office  
Arlington Hall Station  
Arlington, Virginia 22210

U. S. Army Engr. R&D Labs.  
Attn: Technical Document Acct.  
Fort Belvoir, Va. 22060

U. S. Army Production Equipment  
Agency  
Rock Island Arsenal  
Attn: Mfg. Technology Div.,  
AMXPE-MT  
Rock Island, Illinois

Zeus Project Office  
U. S. Army Material Command  
Attn: AMCPM-Zee  
Redstone Arsenal, Ala.

Army Materials Research Agency  
Attn: S. V. Arnold  
Watertown 72, Mass.

Frankford Arsenal  
Metallurgical Research Labs.  
Attn: cc 1321  
Bridge & Tacony Streets  
Philadelphia, Pa. 19104

Redstone Scientific Information Center  
Attn: Chief, Documentation Section  
U. S. Army Missile Command  
Redstone Arsenal, Alabama 35809

U. S. Army Materials Command  
Attn: Materials Section, Research Div.  
Wash., D. C. 20315

Chief, Bureau of Naval Weapons  
Department of the Navy  
Industrial Division  
Attn: (PID-2) Industrial Readiness Br.  
Wash., D. C. 20013

U. S. Naval Research Laboratory  
Attn: Code 6383  
Wash., D. C. 20390

Department of the Navy  
Special Projects Office  
Attn: SP 271  
Wash., D. C. 20013

ODDRE, R&E  
Attn: Mr. J. C. Barrett  
Room 3D-117, Pentagon  
Wash., D. C. 20013

Advanced Research Projects Agency  
Asst. Dir., Materials Sciences  
Attn: Chas. F. Yost, 3D-155, Pentagon  
Wash., D. C. 20013

Defense Metals Information Center  
Battelle Memorial Institute  
Attn: Library  
505 King Avenue  
Columbus, Ohio 43201

Defense Documentation Center 20 copies  
Cameron Station  
Alexandria, Virginia 22314

National Aeronautics & Space Adm.  
Marshall Space Flight Center  
Attn: Dr. W. R. Lucas, R-P & VE-M  
Huntsville, Ala. 35812

National Aeronautics & Space Adm.  
Attn: Code RRM  
Wash., D. C. 20546

NASA, Lewis Research Center  
Attn: Chief Librarian  
Cleveland, Ohio 44125

Scientific & Technical Information  
Facility  
Attn: Technical Library  
RQT-16448  
P. O. Box 5700  
Bethesda, Maryland 20014

National Academy of Sciences  
National Research Council  
Materials Advisory Board  
2101 Constitution Ave., N. W.  
Wash., D. C. 20418

Aerojet General Corp.  
333 W. First Street  
Dayton, Ohio 45402

Battelle Memorial Institute  
Attn: R. Carlson  
505 King Avenue  
Columbus, Ohio 43201

Beech Aircraft Corp.  
Attn: Technical Library  
Wichita, Kansas 67202

Bell Aerosystems Company  
Attn: Technical Library  
P. O. Box 1  
Buffalo, New York 14205

The Boeing Company  
Aerospace Division  
Attn: L. M. Crawford  
P. O. Box 3707  
Seattle, Wash. 98124

Continental Avia. & Engrg. Corp.  
Attn: Technical Library  
Detroit, Michigan 48233

Curtiss-Wright Corp.  
Wright Aeronautical Div.  
Technical Library  
Wood-Ridge, New Jersey

Douglas Aircraft Co., Inc.  
Attn: Technical Library  
2855 Lakewood Blvd.  
Long Beach, California 90801

Douglas Aircraft Co., Inc.  
Missile & Space Systems Div.  
Attn: Technical Library  
3000 Ocean Park Blvd.  
Santa Monica, Calif. 90406

General Dynamics/Ft. Worth  
Attn: Technical Library  
P. O. Box 748  
Fort Worth, Texas 76101

Grumman Aircraft Engrg. Corp.  
Attn: Technical Library  
Bethpage, L. I., New York 11101

Hughes Aircraft Division  
Attn: Technical Library  
Florence & Teale Streets  
Culver City, Calif.

IITRI Technology Center  
Attn: Technical Library  
10 W. 35th Street  
Chicago, Illinois 60616

Lockheed California Company  
Central Library Dept. 72-35  
Bldg. 63-1  
Burbank, California 91503

Lockheed Missile & Space Co.  
Technical Information Center  
3251 Hanover Street  
Palo Alto, California 94302

Lockheed Missile & Space Co.  
Attn: Technical Library  
Sunnyvale, Calif. 94088

Lockheed-Georgia Company  
Div. of Lockheed Aircraft Corp.  
Attn: Technical Library  
Marietta, Ga. 30061

LTV Aerospace Corporation  
Vought Aeronautics Division  
Attn: W. W. Wood, Chief of Mfg. R&D  
P. O. Box 5907  
Dallas, Texas 75222

McDonnell Corporation  
Attn: Howard Siegel, Chief  
Metallurgical Engineer  
P. O. Box 516  
St. Louis, Missouri 63155

The Martin-Marietta Corp.  
Attn: Technical Library  
Baltimore, Maryland 21233

North American Avia., Inc.  
Space & Information Systems  
Attn: Technical Library  
12214 Lakewood Blvd.  
Downey, California 90052

North American Avia. Inc.  
Los Angeles Division  
Attn: Technical Library  
Los Angeles, Calif. 90052

North American Avia., Inc.  
Technical Library  
Columbus, Ohio 43216

Northrop Norair  
Attn: Technical Information  
3901 W. Broadway  
Hawthorne, California 90250

Republic Aviation Div.  
Fairchild Hiller Corp.  
Attn: Mr. G. Pfanner, Chief  
Mfg. Research & Processes  
Farmingdale, L. I., N. Y. 11735

Rohr Aircraft Corp.  
Attn: Technical Library  
P. O. Box 878  
Chula Vista, California 92101

Ryan Aeronautical Co.  
Attn: Technical Library  
2701 Harbor Drive  
San Diego, Calif. 92101

Solar Division  
International Harvester Company  
Attn: Technical Library  
2200 Pacific Highway  
San Diego, California 92112

Thompson Ramo Wooldridge, Inc.  
Attn: Technical Library  
23555 Euclid Avenue  
Cleveland, Ohio 44117

DOCUMENT CONTROL DATA - R&D		
(Security classification of title, body of abstract and indexing annotation must be entered when the overall report is classified)		
1. ORIGINATING ACTIVITY (Corporate author)		2a. REPORT SECURITY CLASSIFICATION
Aeroprojects Incorporated		UNCLASSIFIED
		2b. GROUP
3. REPORT TITLE		
ULTRASONIC WELDING EQUIPMENT FOR REFRACTORY METALS		
4. DESCRIPTIVE NOTES (Type of report and inclusive dates)		
FINAL February 15, 1962 - August 31, 1966		
5. AUTHOR(S) (Last name, first name, initial)		
Maropis, Nicholas		
6. REPORT DATE	7a. TOTAL NO. OF PAGES	7b. NO. OF PAGES
November 1966	148	28
8a. CONTRACT OR GRANT NO.	9a. ORIGINATOR'S REPORT NUMBER(S)	
AF 33(600)-43926	AFML-TR-66-351	
b. PROJECT NO.		
c. 7-888	9b. OTHER REPORT NO(S) (Any other numbers that may be assigned this report)	
d.		
10. AVAILABILITY/LIMITATION NOTICES		
This document is subject to special export controls and each transmittal to foreign governments or foreign nationals may be made only with prior approval of the Manufacturing Technology Division.		
11. SUPPLEMENTARY NOTES		12. SPONSORING MILITARY ACTIVITY
		Advanced Fabrication Techniques Branch, Manufacturing Technology Div., AF Materials Lab., AF Systems Command, Wright-Patterson AFB, Ohio
13. ABSTRACT		
<p>Ultrasonic welding equipment consisting of a highly stable and precisely adjustable motor-alternator frequency converter, new cartridge-type ceramic transducers exhibiting overall efficiencies in the range of 75 to 85 percent, and heavy-duty, force-insensitive acoustic coupling systems were developed and/or designed, built, and successfully utilized with the view to spot welding such refractory metals and superalloys as Rene 41, Mo-0.5Ti alloy, columbium, PH15-7Mo stainless steel, and tungsten. The equipment provides for programming the electrical power delivered to the transducers and the clamping force applied to the weldment so that improved impedance matching and better control of the welding process can be effected. Ultrasonic spot-type welds were made with this equipment in materials and thicknesses not heretofore achievable.</p>		

14.	KEY WORDS	LINK A		LINK B		LINK C	
		ROLE	WT	ROLE	WT	ROLE	WT

## INSTRUCTIONS

1. **ORIGINATING ACTIVITY:** Enter the name and address of the contractor, subcontractor, grantee, Department of Defense activity or other organization (*corporate author*) issuing the report.

2a. **REPORT SECURITY CLASSIFICATION:** Enter the overall security classification of the report. Indicate whether "Restricted Data" is included. Marking is to be in accordance with appropriate security regulations.

2b. **GROUP:** Automatic downgrading is specified in DoD Directive 5200.10 and Armed Forces Industrial Manual. Enter the group number. Also, when applicable, show that optional markings have been used for Group 3 and Group 4 as authorized.

3. **REPORT TITLE:** Enter the complete report title in all capital letters. Titles in all cases should be unclassified. If a meaningful title cannot be selected without classification, show title classification in all capitals in parenthesis immediately following the title.

4. **DESCRIPTIVE NOTES:** If appropriate, enter the type of report, e.g., interim, progress, summary, annual, or final. Give the inclusive dates when a specific reporting period is covered.

5. **AUTHOR(S):** Enter the name(s) of author(s) as shown on or in the report. Enter last name, first name, middle initial. If military, show rank and branch of service. The name of the principal author is an absolute minimum requirement.

6. **REPORT DATE:** Enter the date of the report as day, month, year; or month, year. If more than one date appears on the report, use date of publication.

7a. **TOTAL NUMBER OF PAGES:** The total page count should follow normal pagination procedures, i.e., enter the number of pages containing information.

7b. **NUMBER OF REFERENCES:** Enter the total number of references cited in the report.

8a. **CONTRACT OR GRANT NUMBER:** If appropriate, enter the applicable number of the contract or grant under which the report was written.

8b, 8c, & 8d. **PROJECT NUMBER:** Enter the appropriate military department identification, such as project number, subproject number, system numbers, task number, etc.

9a. **ORIGINATOR'S REPORT NUMBER(S):** Enter the official report number by which the document will be identified and controlled by the originating activity. This number must be unique to this report.

9b. **OTHER REPORT NUMBER(S):** If the report has been assigned any other report numbers (*either by the originator or by the sponsor*), also enter this number(s).

10. **AVAILABILITY/LIMITATION NOTICES:** Enter any limitations on further dissemination of the report, other than those

imposed by security classification, using standard statements such as:

- (1) "Qualified requesters may obtain copies of this report from DDC."
- (2) "Foreign announcement and dissemination of this report by DDC is not authorized."
- (3) "U. S. Government agencies may obtain copies of this report directly from DDC. Other qualified DDC users shall request through \_\_\_\_\_."
- (4) "U. S. military agencies may obtain copies of this report directly from DDC. Other qualified users shall request through \_\_\_\_\_."
- (5) "All distribution of this report is controlled. Qualified DDC users shall request through \_\_\_\_\_."

If the report has been furnished to the Office of Technical Services, Department of Commerce, for sale to the public, indicate this fact and enter the price, if known.

11. **SUPPLEMENTARY NOTES:** Use for additional explanatory notes.

12. **SPONSORING MILITARY ACTIVITY:** Enter the name of the departmental project office or laboratory sponsoring (*paying for*) the research and development. Include address.

13. **ABSTRACT:** Enter an abstract giving a brief and factual summary of the document indicative of the report, even though it may also appear elsewhere in the body of the technical report. If additional space is required, a continuation sheet shall be attached.

It is highly desirable that the abstract of classified reports be unclassified. Each paragraph of the abstract shall end with an indication of the military security classification of the information in the paragraph, represented as (TS), (S), (C), or (U).

There is no limitation on the length of the abstract. However, the suggested length is from 150 to 225 words.

14. **KEY WORDS:** Key words are technically meaningful terms or short phrases that characterize a report and may be used as index entries for cataloging the report. Key words must be selected so that no security classification is required. Identifiers, such as equipment model designation, trade name, military project code name, geographic location, may be used as key words but will be followed by an indication of technical context. The assignment of links, rules, and weights is optional.